Pavel Němec

II. SMYSLOVÉ ORGÁNY

Kolik existuje smyslů? ~ 20!

- **Interoreceptory**
- **Exteroreceptory**

TABLE 2-3. A Classification of Receptors and Their Senses

Receptor Class	Sensory Modality		Receptor Type
Mechanoreceptor	Touch	Fast adapting	Meissner's corpuscles
		Slow adapting	Merkel's disks
	Tendon stretch		Tendon organs
	Skin stretch		Ruffini endings
	Joint position		Joint receptors
	Muscle length and stretch		Muscle spindles
	Muscle contraction		Golgi tendon organ
	Vibration		Pacinian corpuscles
	Hearing		Hair cells
	Vestibular (gravity, acceleration, head position)		Hair cells
	Lateral line		Hair cells
Radiant-energy receptor	Light (including UV)		Photoreceptors
	Infrared radiation (pit organ)		Pit-organ receptors
	Infrared radiation (skin warmth)		Free nerve endings
	Infrared radiation (skin cold)		Free nerve endings
Chemoreceptor	Taste		Taste buds
	Smell		Olfactory receptors
Electroreceptor	Electric fields		Ampullae
			Tuberous receptors
Nociceptor	Pain		Free nerve endings
	General chemical sensitivity		Free nerve endings
Magnetoreceptor	Magnetic fields		Photoreceptors (?) Ampullae (?) Trigeminal receptors

Fototaxe u eukariot

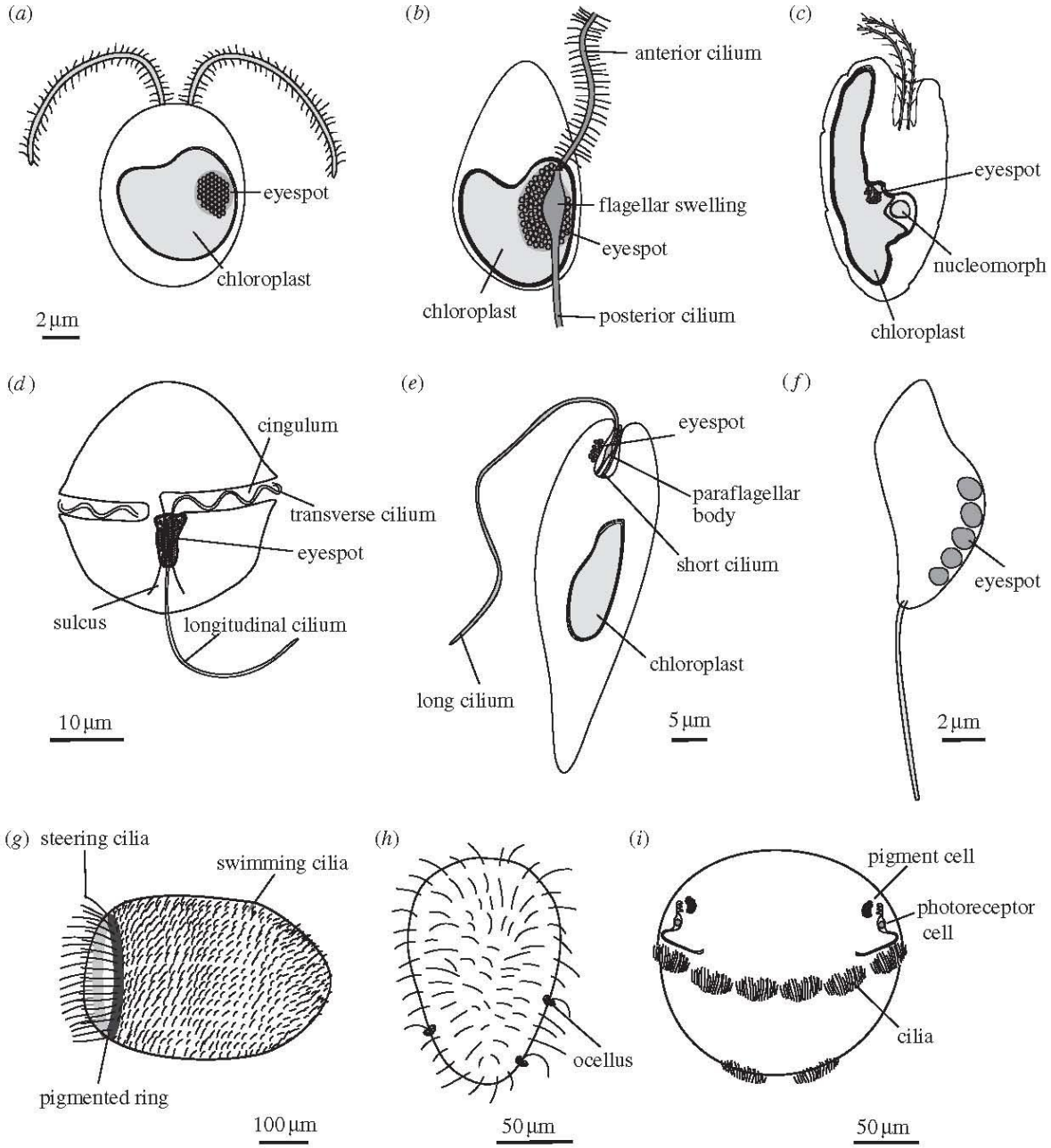

Figure 2. The diversity of phototactic eukaryotes (*a*) a green alga (scale bar, 2 µm), (*b*) a heterokont zoospore, (*c*) a cryptomonad alga, (*d*) a dinoflagellate (scale bar, 10 µm), (*e*) *Euglena* (scale bar, 5 µm), (*f*) a chytrid zoospore (scale bar, 2 µm), (*g*) a sponge larva (scale bar, 100 µm), (*h*) a cnidarian larva (scale bar, 50 µm) and (*i*) a polychaete larva (scale bar, 50 µm).

Jednoduchá fototaxe (biased random walk založený na reverzi pohybu bičíku) již u prokariot, pouze vůči strmému gradientu světla

U eukaryot fototaxe vznikla nejméně 8 x nezávisle (obvykle spojeno s přechodem od bentického k pelagickému způsobu života)

Vznik oka a evoluce jeho funkce

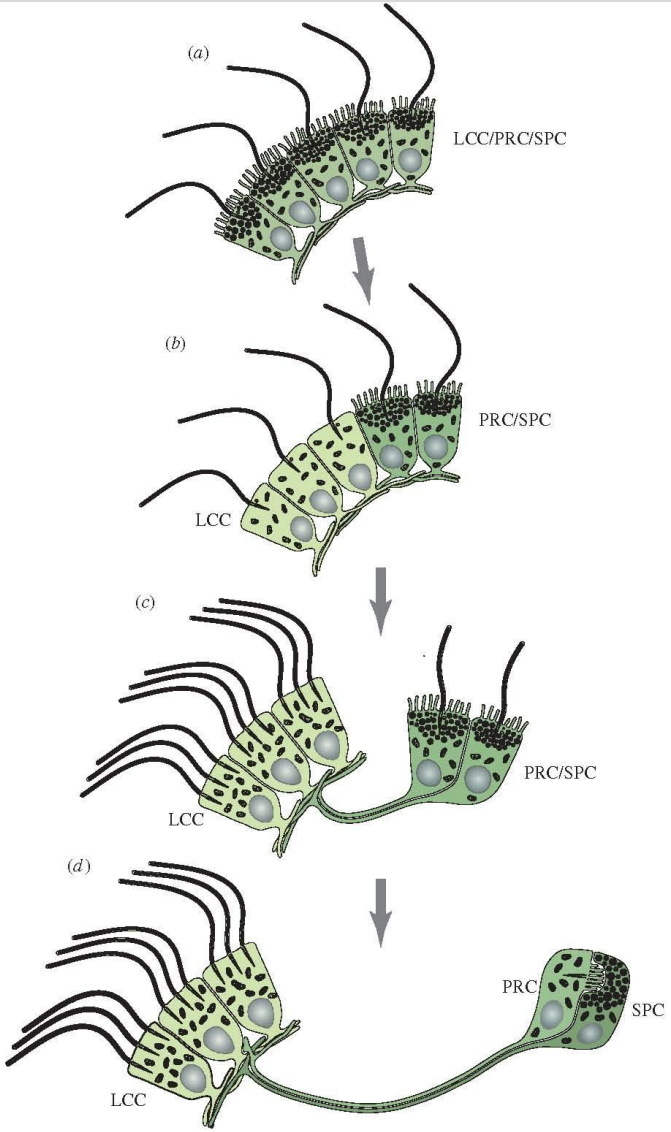

Figure 3. Evolution of two-celled rhabdomeric larval eyes mediating phototaxis, according to the division of labour m
Multi-functional locomotor-photosensory precursor cells evolve into LCCs by cell-type functional segregation. (*a*) Prec
LCC/PRC/SPC combining a locomotor cilium, photosensory rhabdomeric microvilli and shading pigment granules. (
subset of cells loses photosensitivity and shading pigment to specialize on locomotion (LCC, light green). (*c*) The L
become multiciliated. A spatially separate 'eye' comprising two combined PRC/SPC remains connected to the multicil
cells via gradually extending cellular processes that evolve into axons. (*d*) Functional segregation of PRCs (green)
SPCs (dark green). For further explanations, see text.

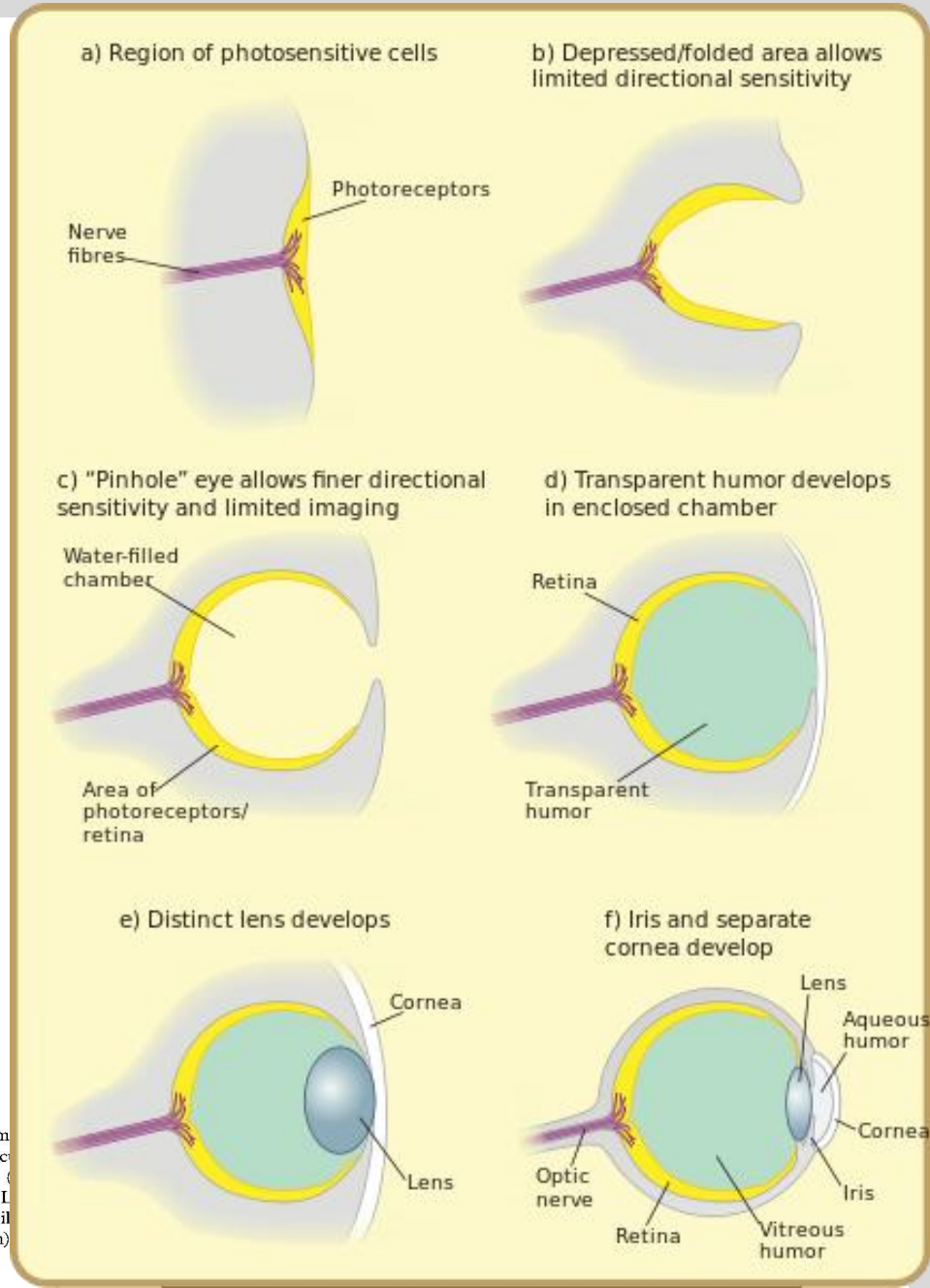

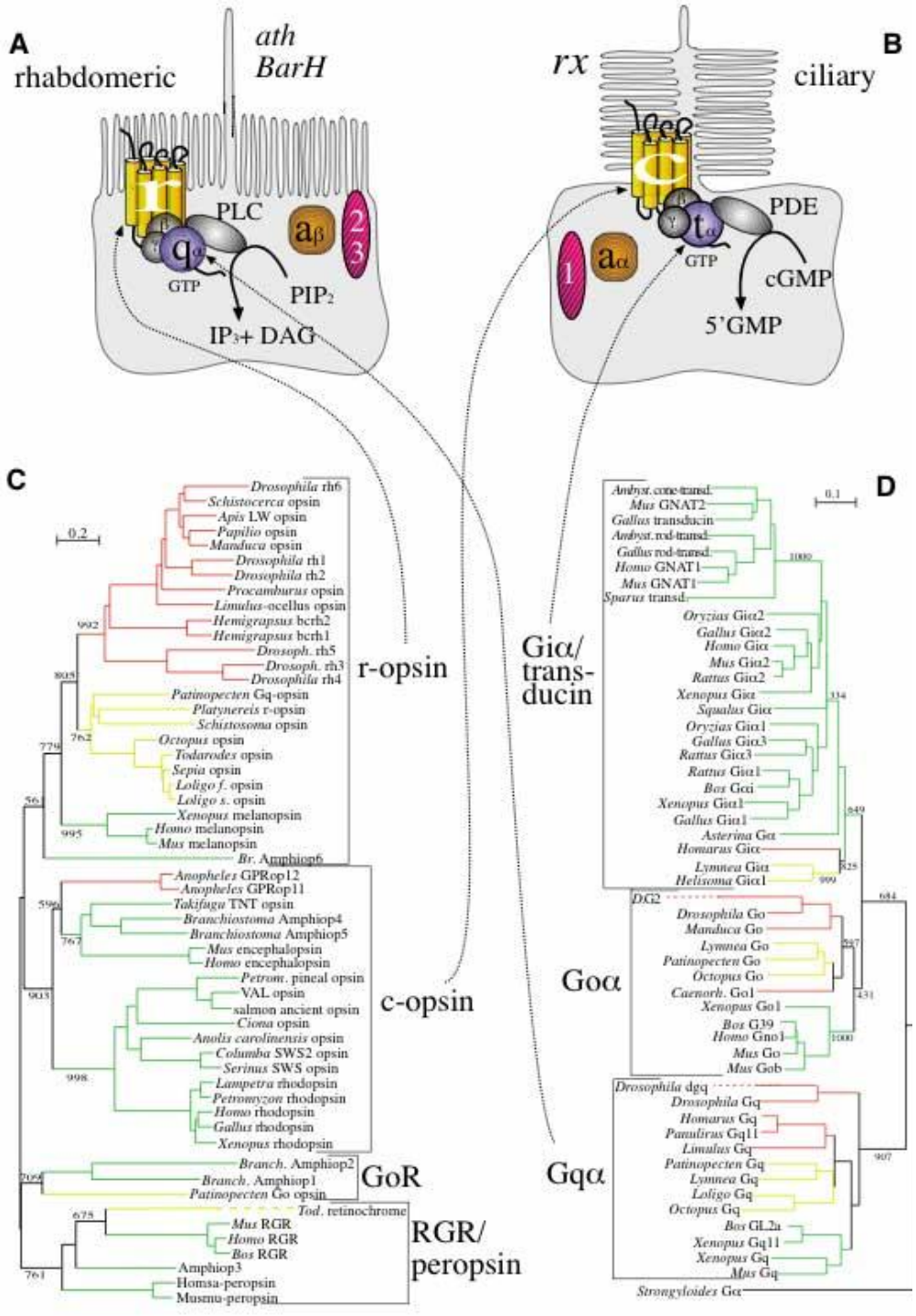

Ciliární:
Aktivace fosfodiesterázy (PDE)
a následná změna koncentrace
cyklického GMP

Rhambdomerické:
Aktivace fospholipázy C (PLC)
and the inositol fosfátu (IP3)

Příklady stavby jednoduchých očí

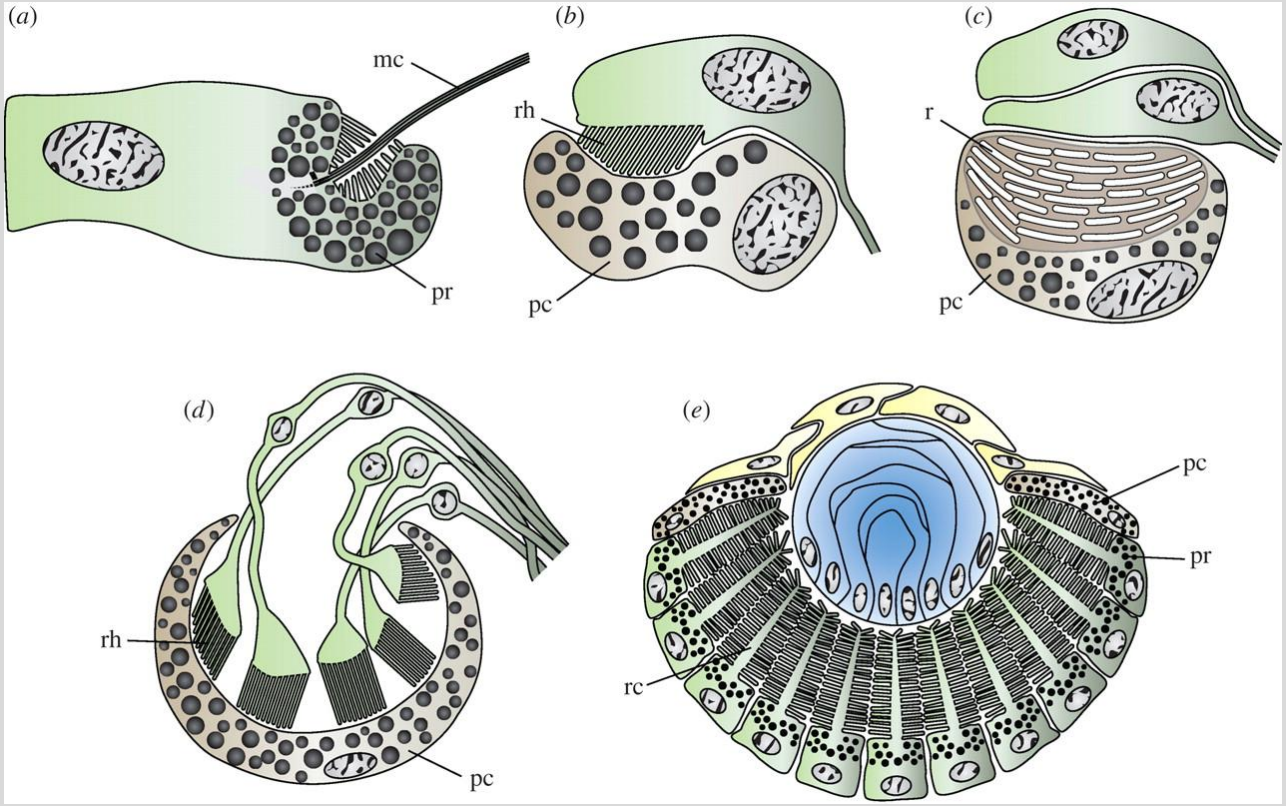

(a) ocellus larvy čtyřhranky (Cubozoa)

(b) ocellus larvy mnohoštětinatce

(c) ocellus praploštěnky (Acoela)

(d) oko ploštěnky

(e) oko čtyřhranky (Cubozoa)

Semi-schematic drawings of ocelli and simple eyes: (a) single cell ocellus of box jellyfish larva; (b) polychaete larval ocellus; (c) ocellus of acoel flatworm, with reflecting platelets in the pigment cell, but no membrane stacking in the two receptor cells; (d) inverse cup eye of planarian flatworm and (e) everse lens eye of juvenile box jellyfish. Photoreceptor cells are indicated by green shading. pr, screening pigment in receptor cell; mc, motile cilium; pc, specialized pigment cell; rh, rhabdom; r, reflective crystals; rc, receptive cilium.

Nilsson D Phil. Trans. R. Soc. B 2009;364:2833-2847

Oko se může lišit v různých ontogenetických stádiích – nereitka (Platynereis)

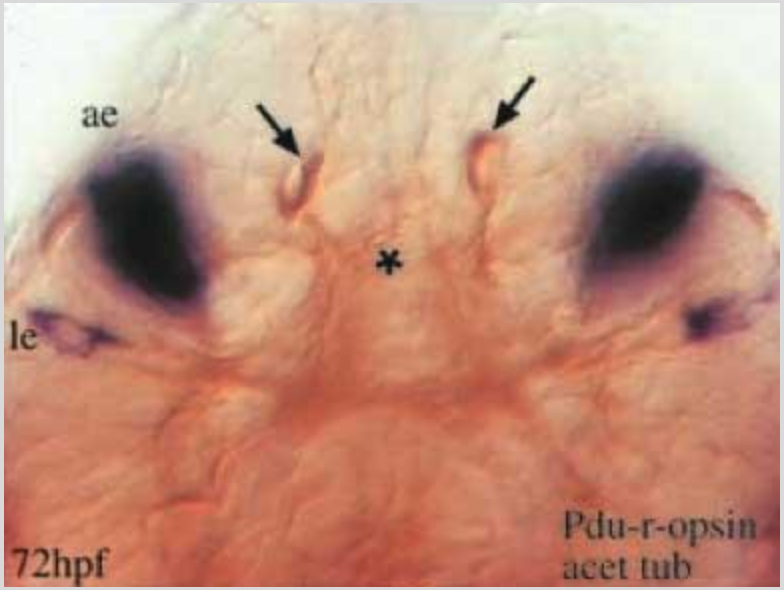

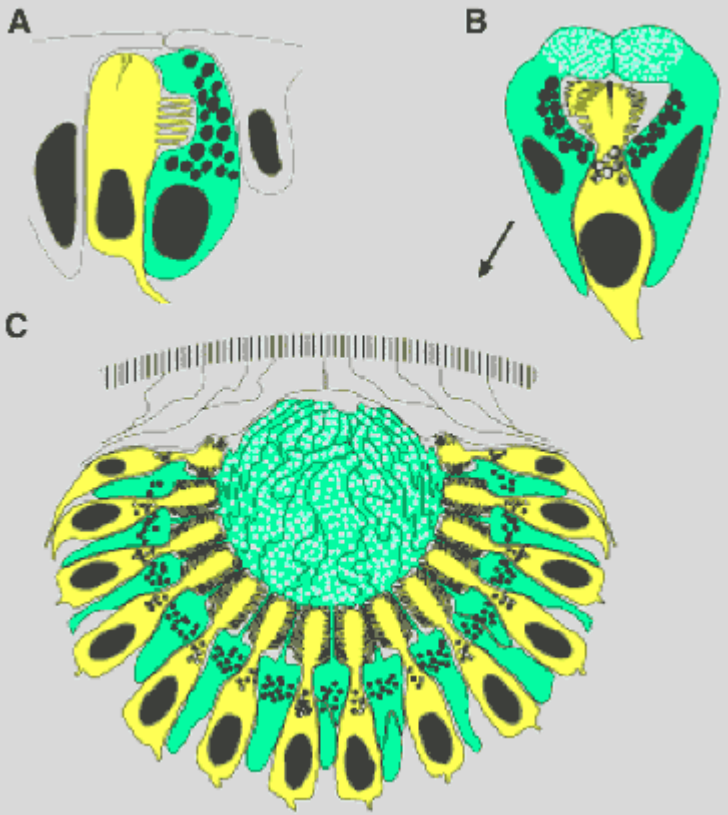

(A) oko larvy

(B) oko mladého dospělce

(C) plně vyvinuté oko

Žahavci (Cnidaria)

Čtyřhranky (Cubozoa):

- ✓ **komplexní smyslové orgány – ropalia**
- ✓ **Pax B**

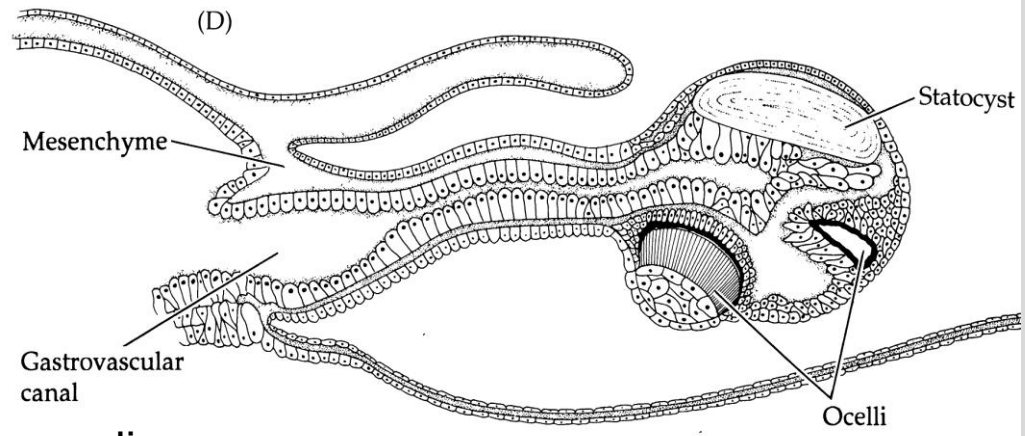

ropalium

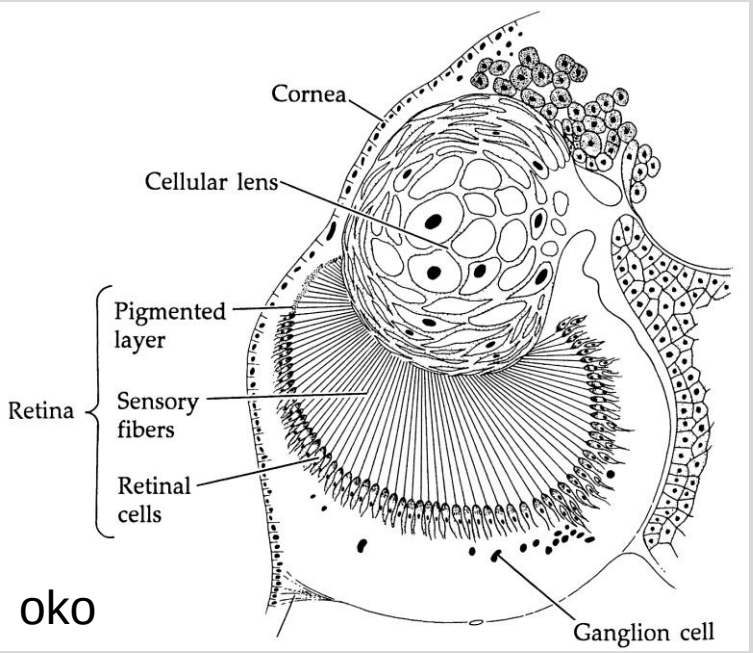

oko

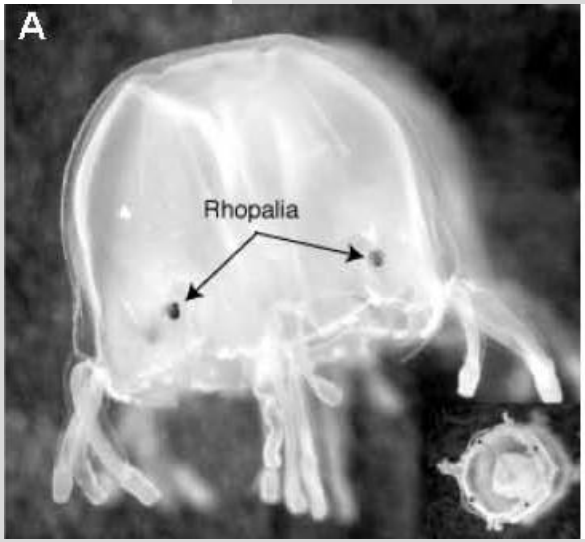

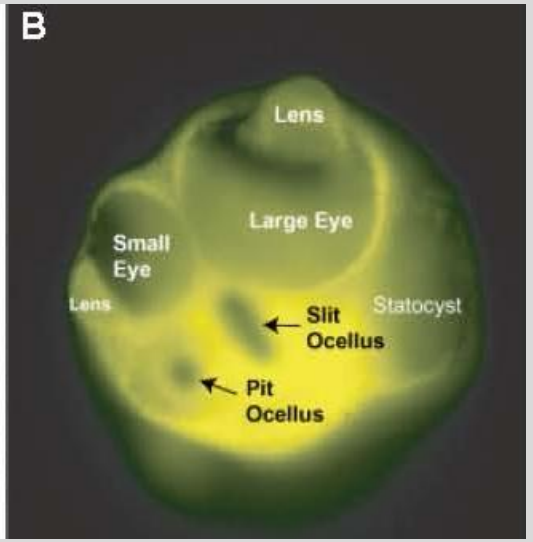

Stavební plány očí

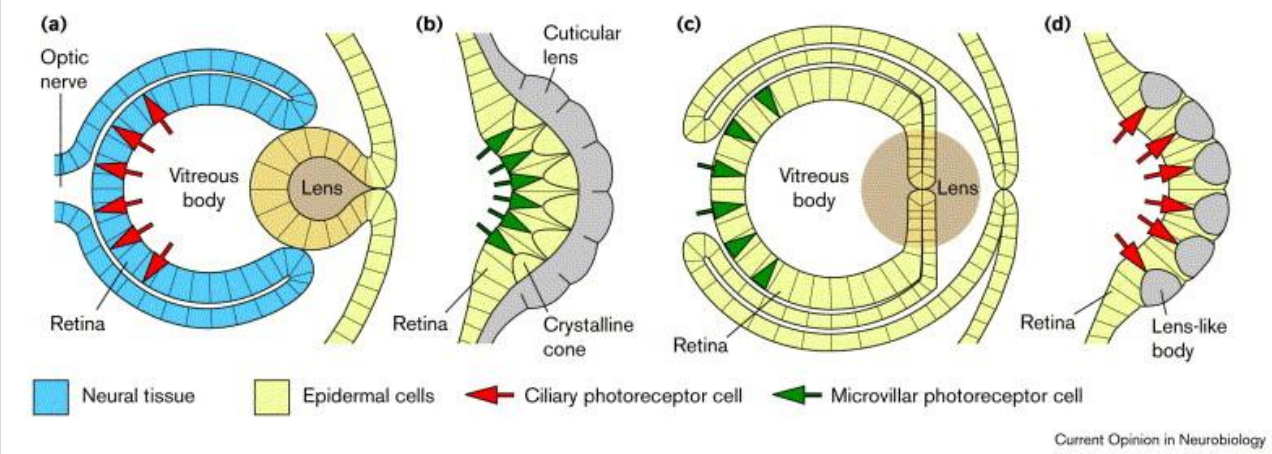

(a) komorové oko obratlovce

(b) složené oko členovce

(c) komorové oko hlavonožce

(d)Složené oko mnohoštětintce

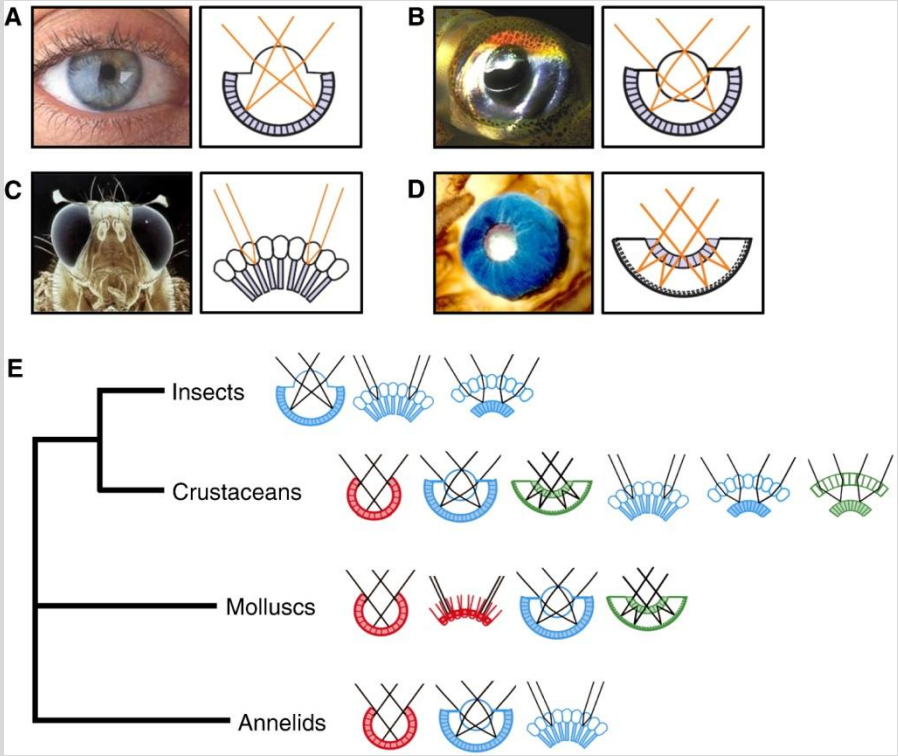

(a) komorové oko obratlovce

(b) složené oko členovce

(c) komorové oko hlavonožce

(d) Složené oko hřebenatky

(e) všimněte si, že u velkých taxonů se vynvinuly velmi různé typy očí, mezi skupinami existuje značná konvergence

Červeně – chybí optický aparát

Modře – optika založená na lomu světla (čočky, rohovky)

Zeleně – optika založená na odrazu světla

Složené oko hřebenatky (Pectinidae, Molusca).

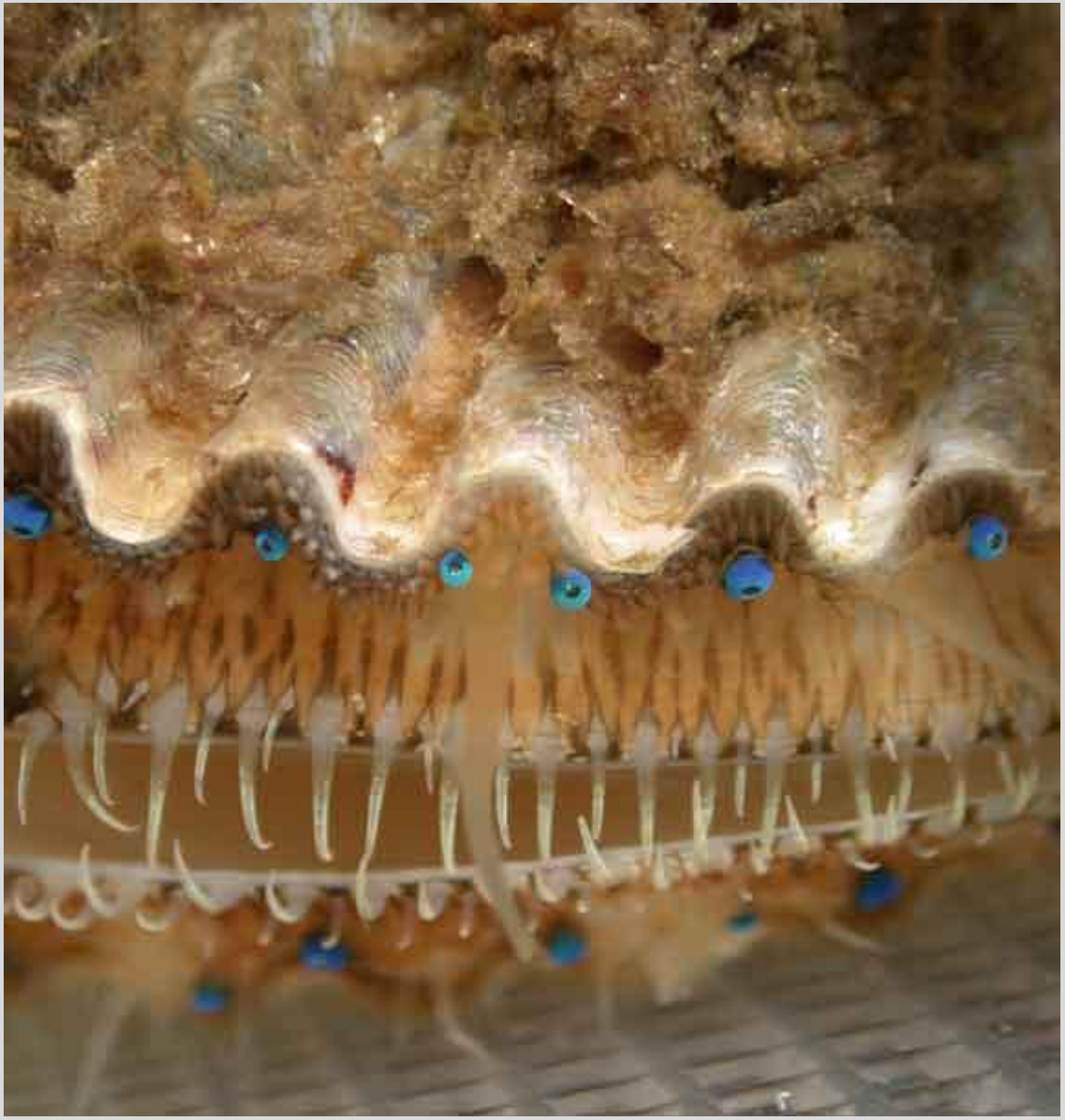

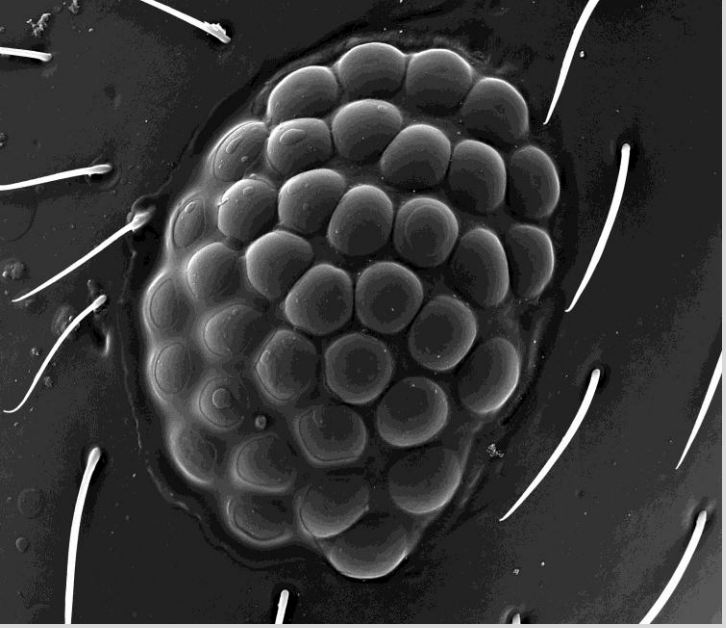

Složené oko hmyzu

Tvořeny jednoduchými očky, tzv. omatidii

Počet je druhově specifický:
(desítky u některých mravenců, více než 20 tisíc u vážek)

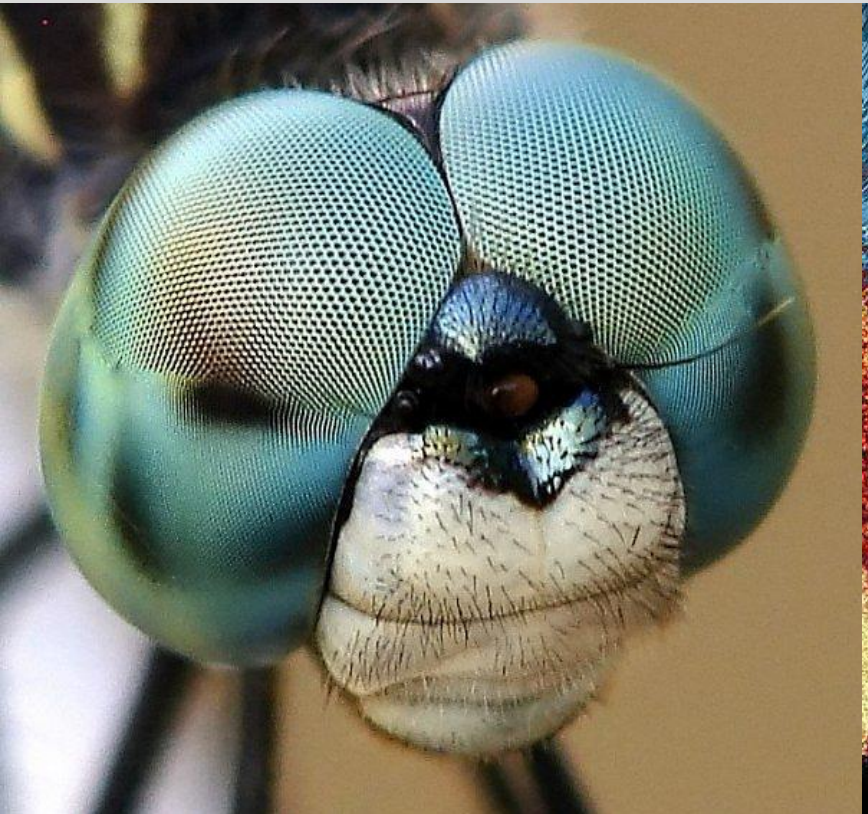

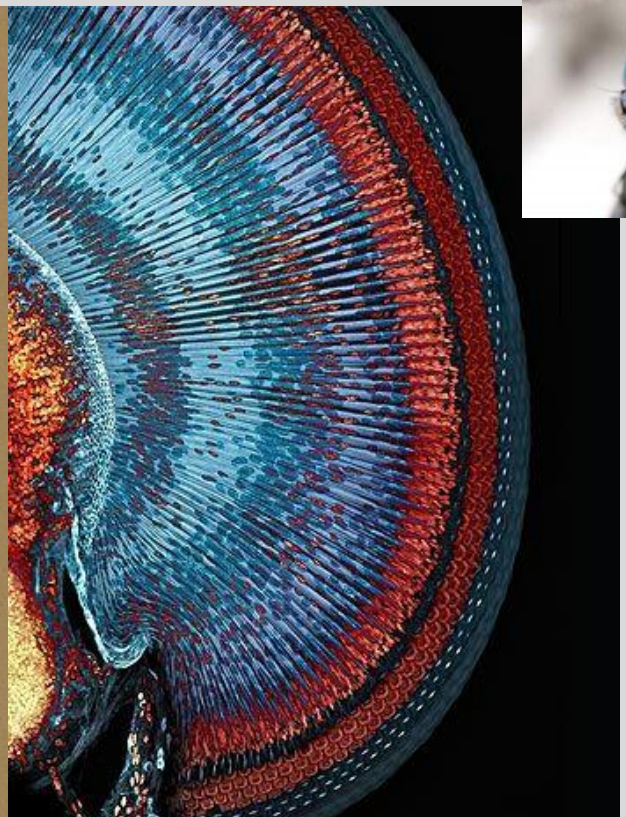

Stavba omatidia

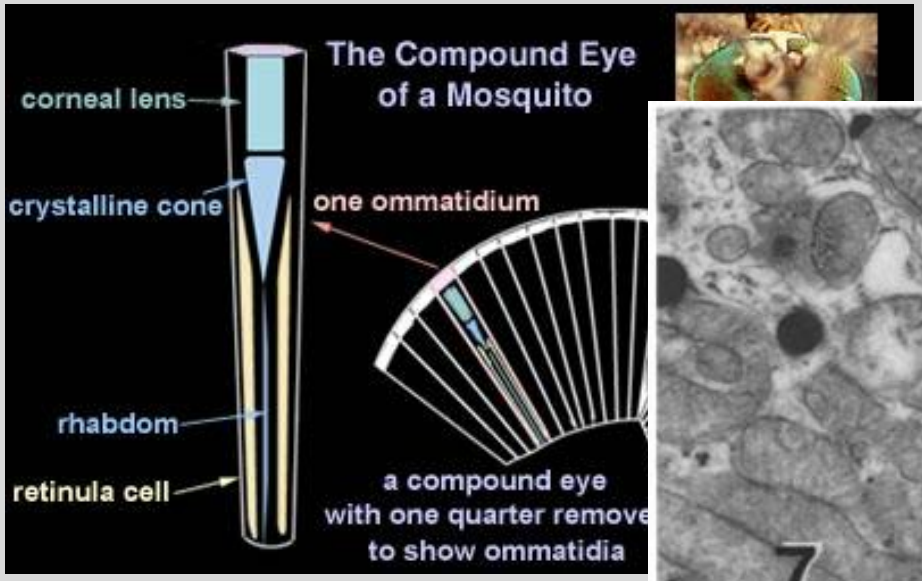

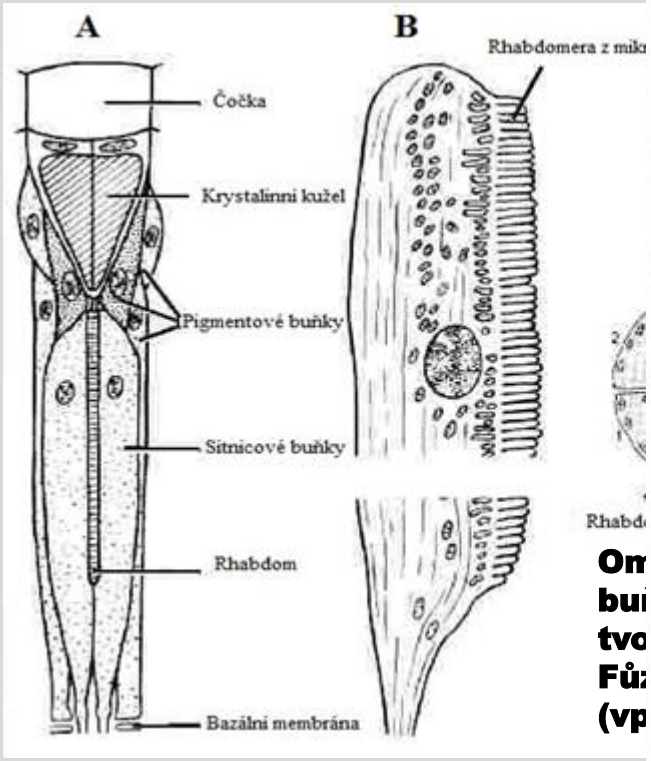

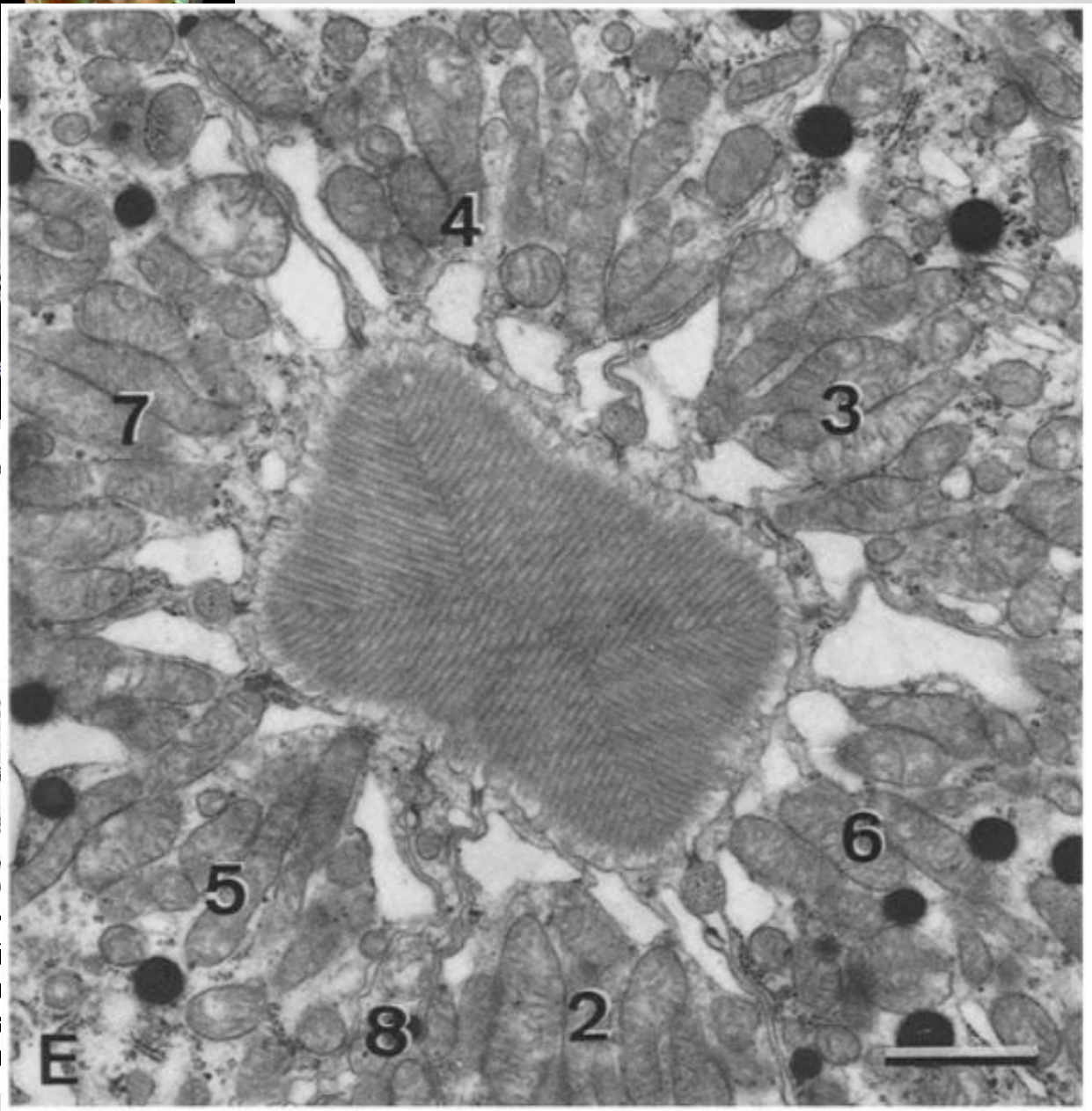

Stavba omatidia octomilky

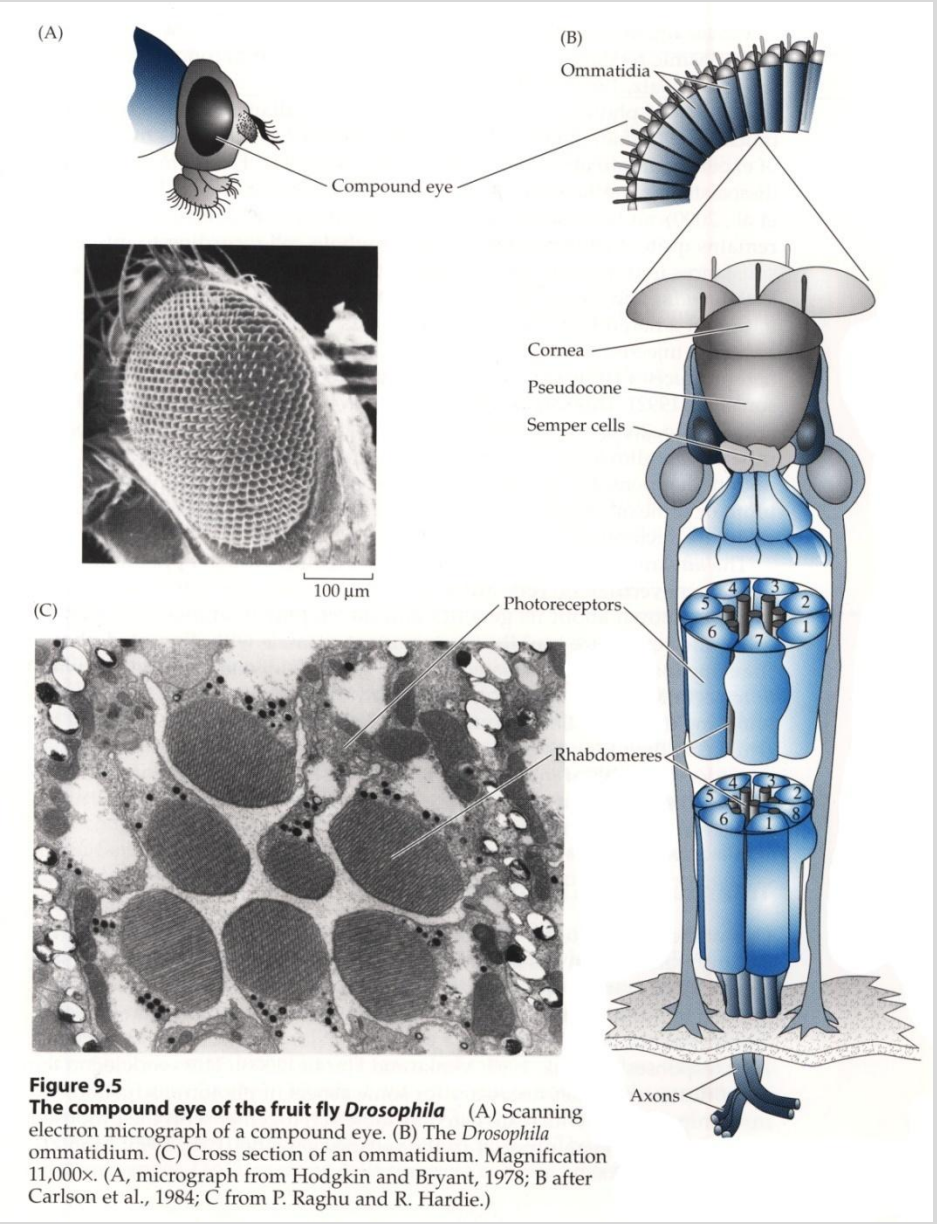

Figure 9.5
The compound eye of the fruit fly *Drosophila* (A) Scanning electron micrograph of a compound eye. (B) The *Drosophila* ommatidium. (C) Cross section of an ommatidium. Magnification 11,000×. (A, micrograph from Hodgkin and Bryant, 1978; B after Carlson et al., 1984; C from P. Raghu and R. Hardie.)

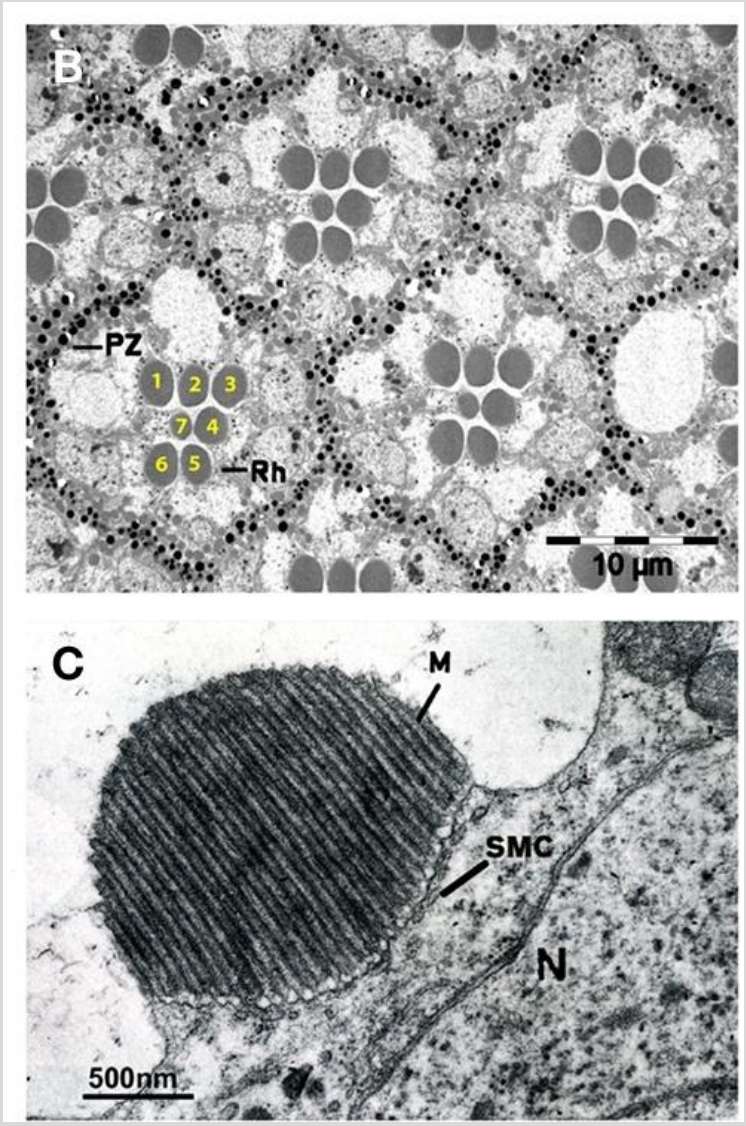

M – microvilli, SMC – submicrovillar cisternae, N – nucleus ,Rh – rhabdomere

Vnímání polarizovaného světla u hmyzu

Dorsální lem oka (DRA, dorsal rim area)
(u druhů, jejichž vývoj je závislý na vodě též ventrální část oka – detekce polarizovaného světla odraženého od vodní hladiny)

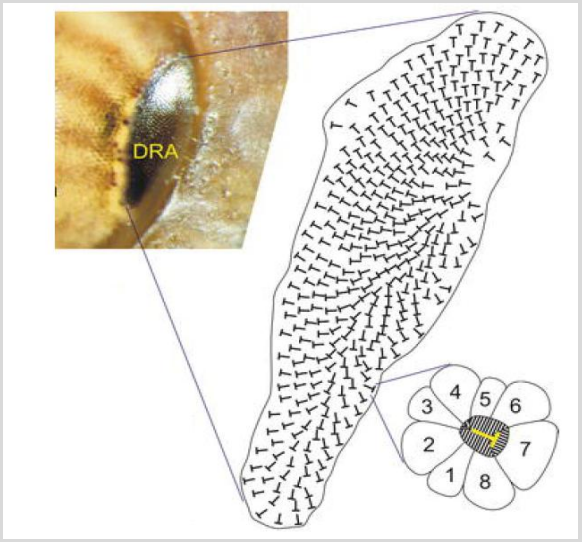

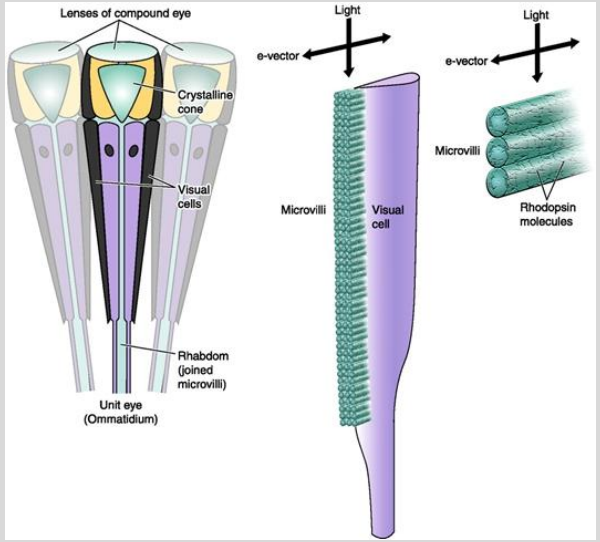

V DRA

✓**rovnoběžné uložení mikrovilů v rhabdomu**
✓**rovnoběžné uložení molekul rhodopsinu v mikrovilech**

Pokud je e-vektoru shodný se směrem uložení molekul rhodopsinu, je absorpce světla maximální, pokud je e-vektoru vůči molekulám kolmý je absorpce světla minimální.

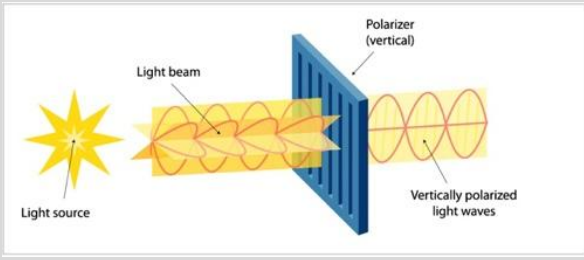

Oko chobotnice

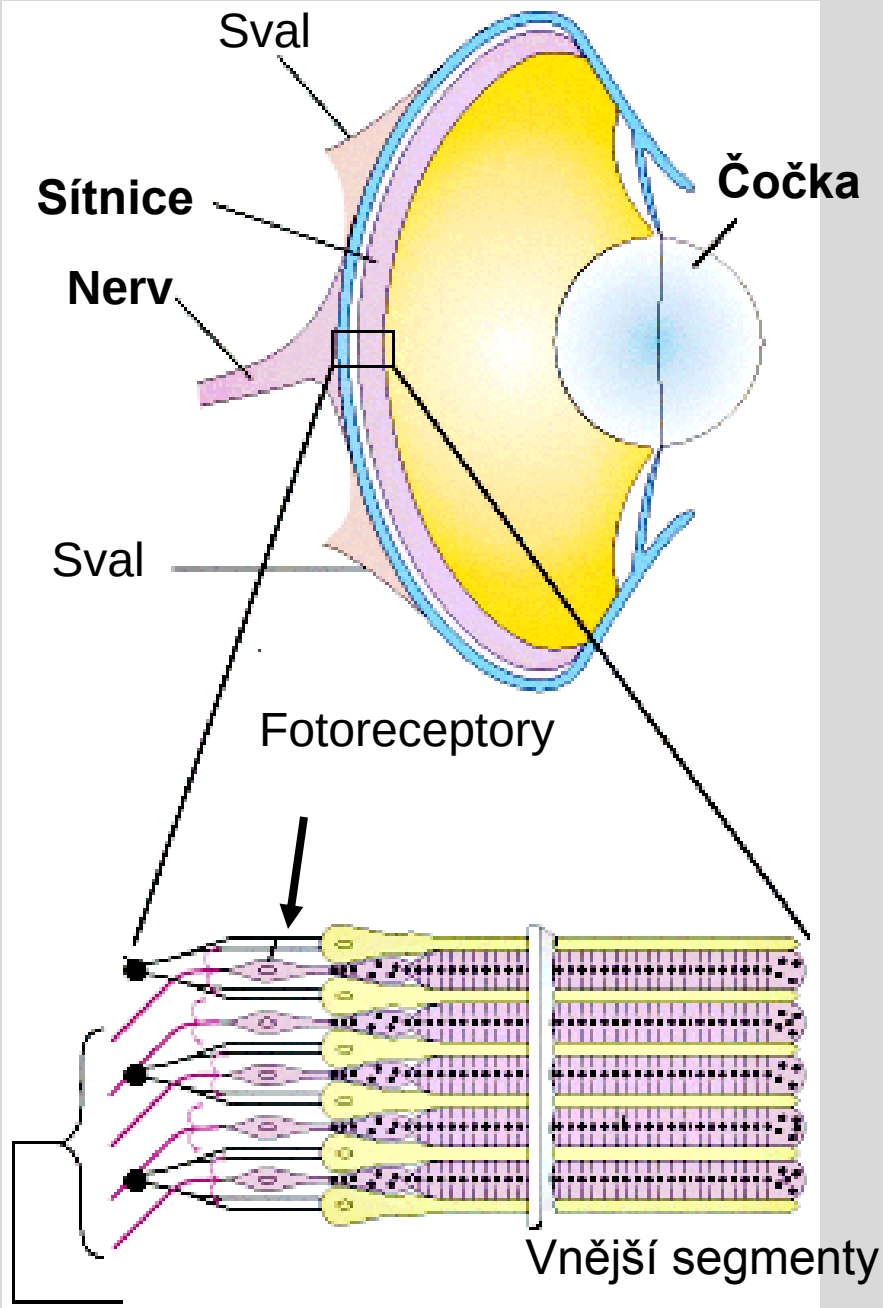

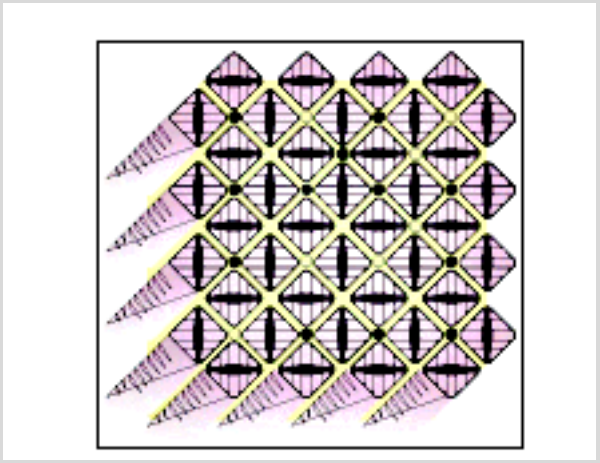

Průřez sítnicí připomíná složené oko členovců

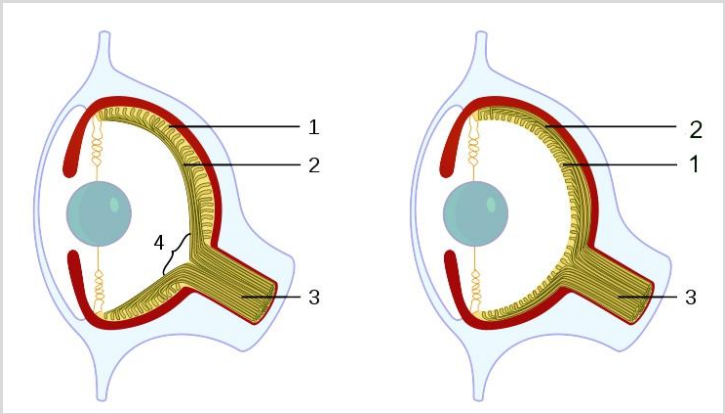

Invertované oko obratlovce

Přímé oko chobotnice

(1) fotoreceptory, (2) optická vlákna, (3) optický nerv, (4) slepá skvrna

Oko chobotnice

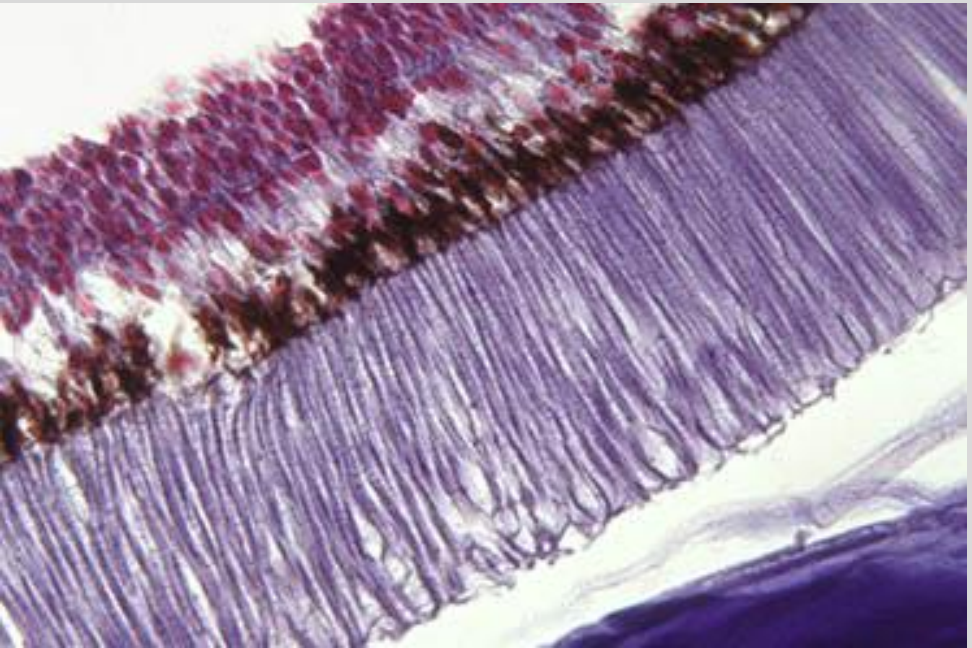

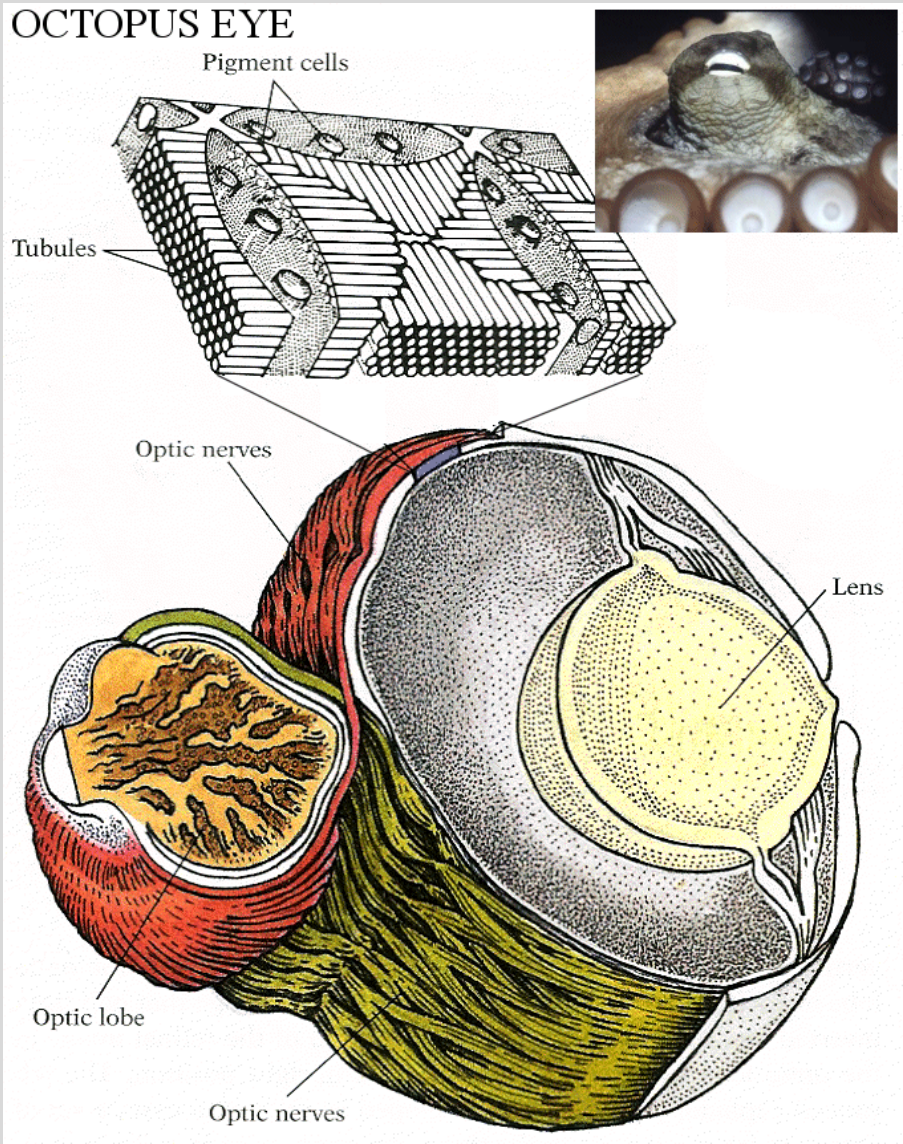

Nepárové oči

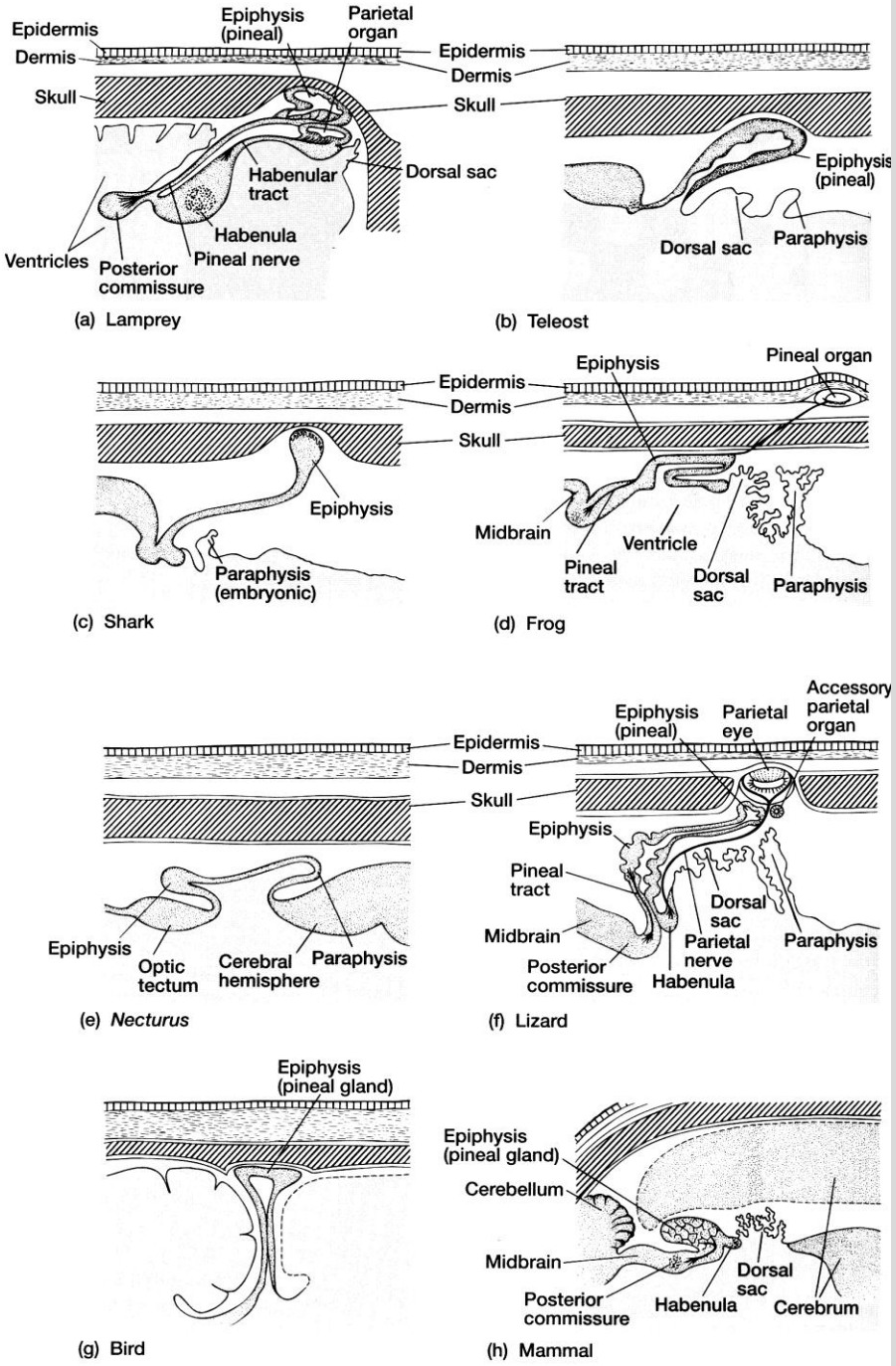

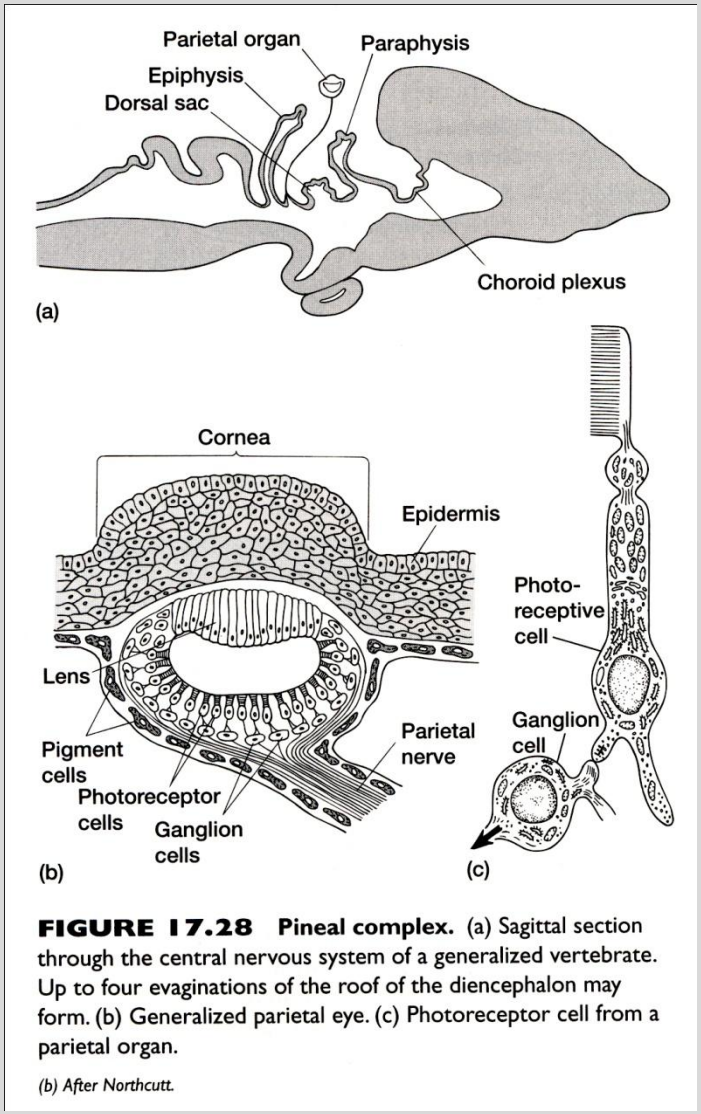

FIGURE 17.28 Pineal complex. (a) Sagittal section through the central nervous system of a generalized vertebrate. Up to four evaginations of the roof of the diencephalon may form. (b) Generalized parietal eye. (c) Photoreceptor cell from a parietal organ.

(b) After Northcutt.

oko a sítnice (retina)

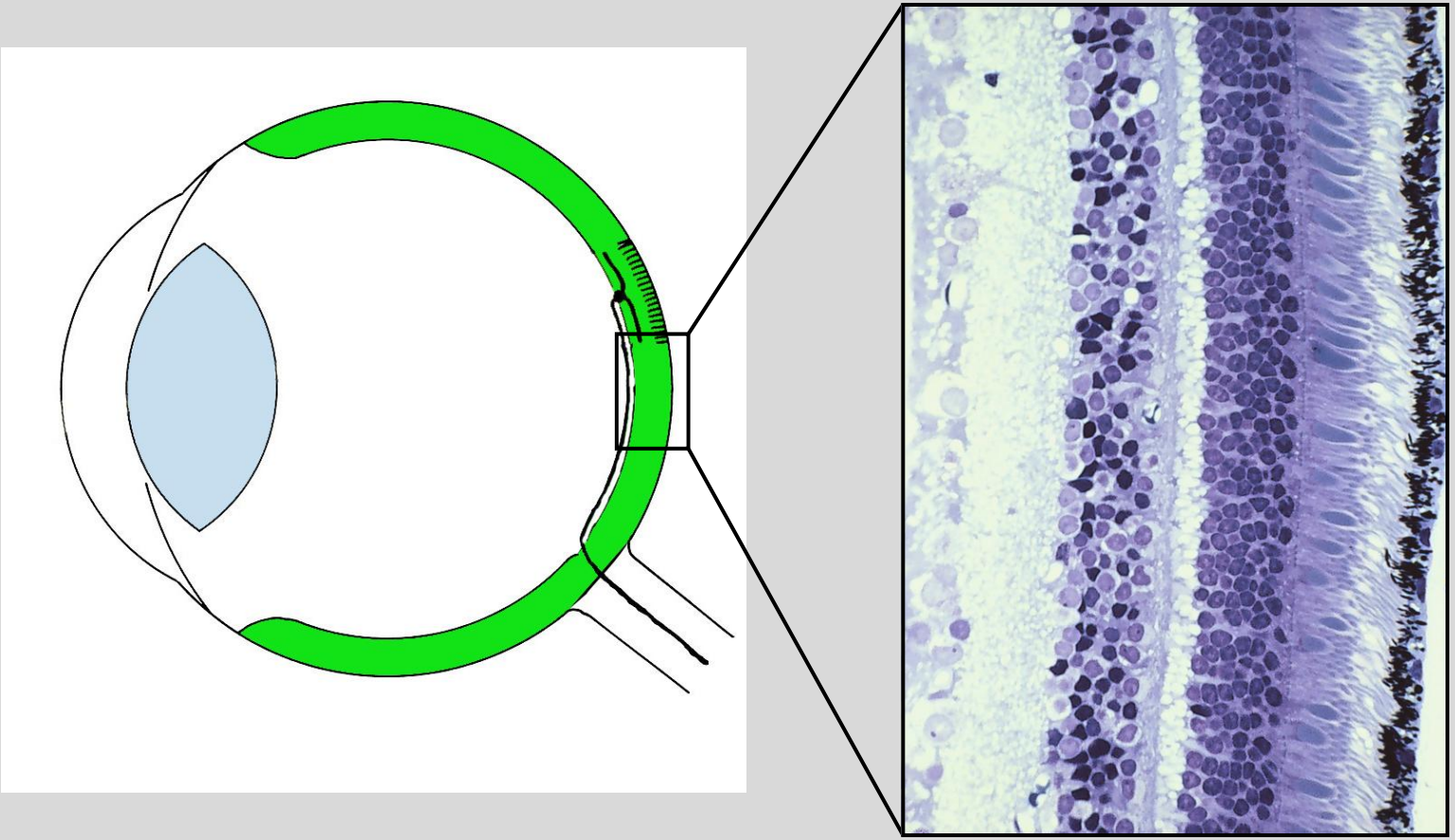

Morfologie sítnice

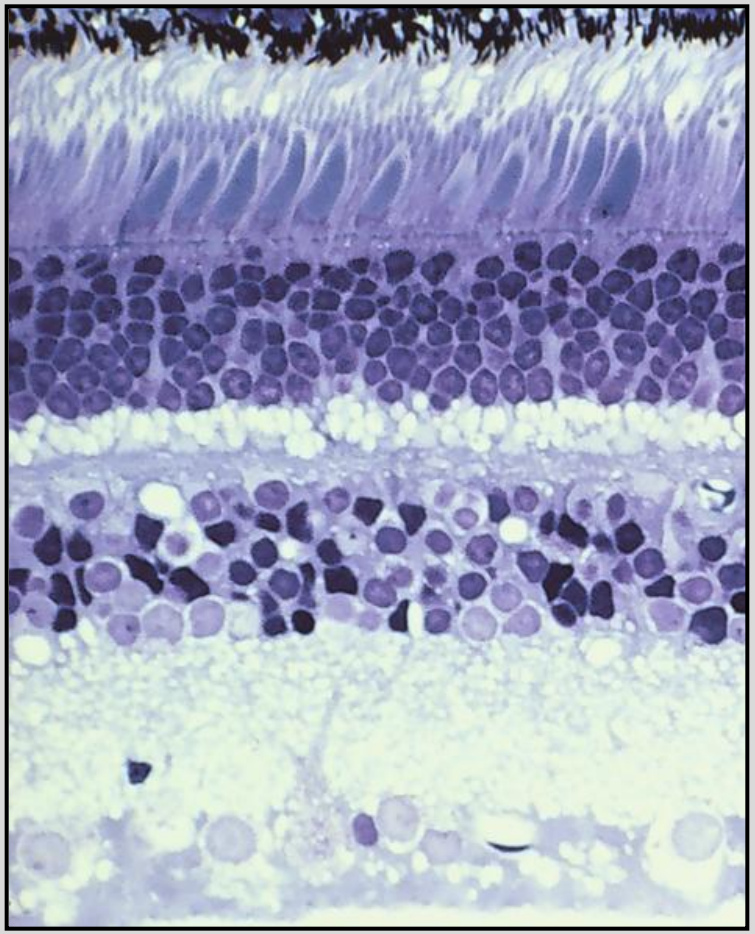

světlo

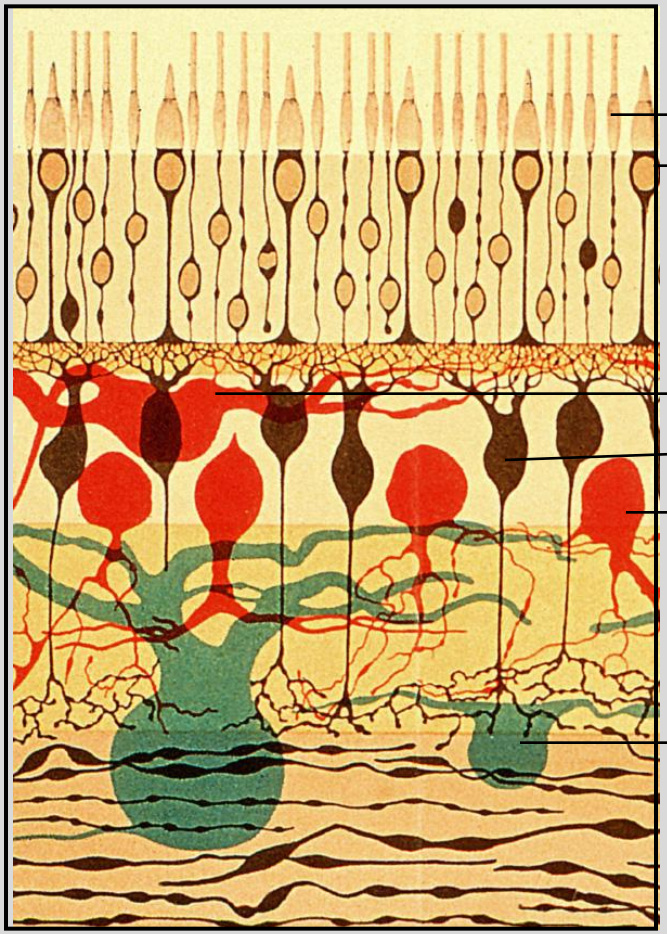

Photoreceptors:
tyčinky
čípky
Horizontal Cells
Bipolar Cells
Amacrine Cells
Ganglion Cells

Tartuferi (1887)

Přestavba buněčného jádra v tyčinkách sítnice: Adaptace savců na noční vidění

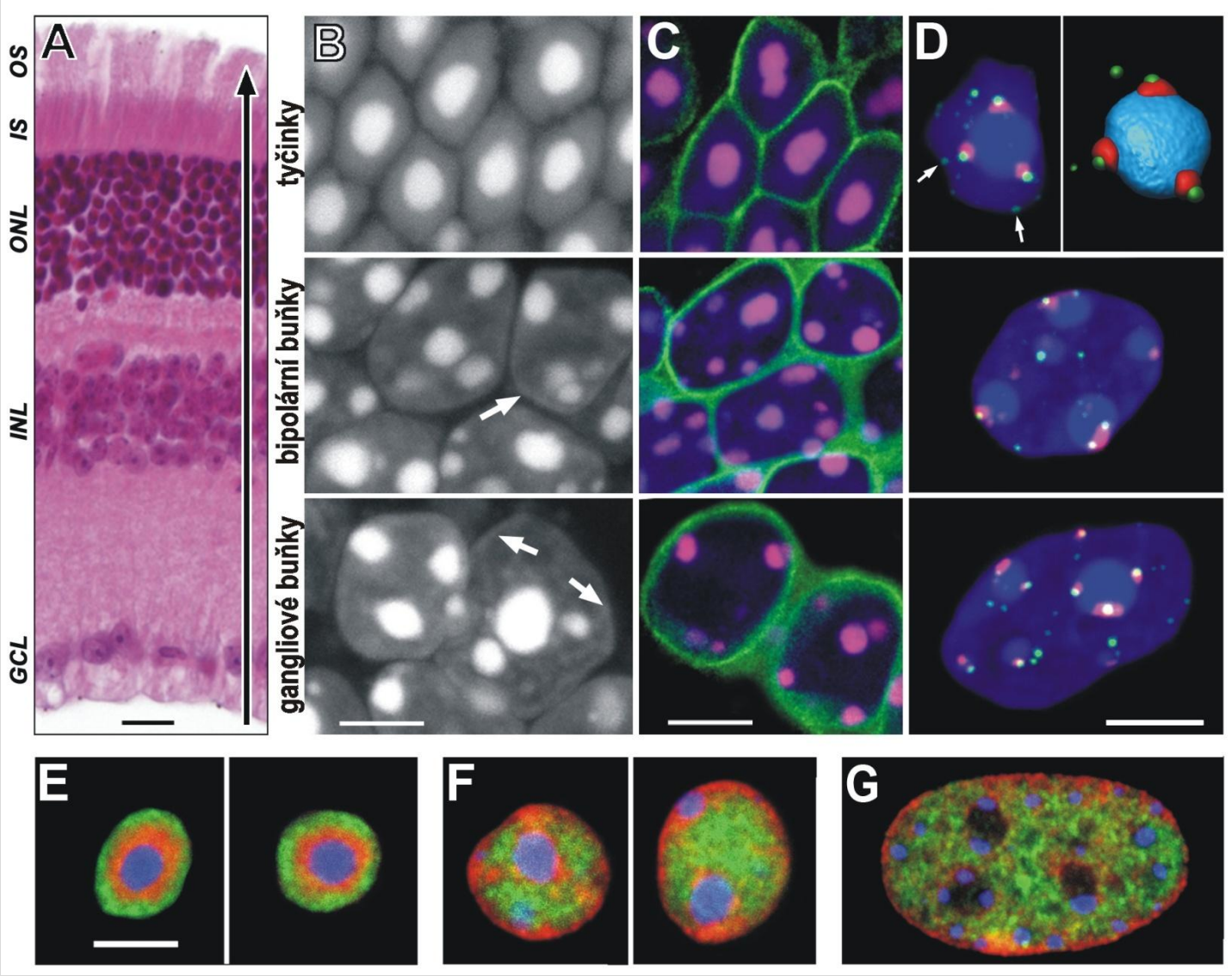

Jádra v tyčinkách fungují jako sběrné čočky

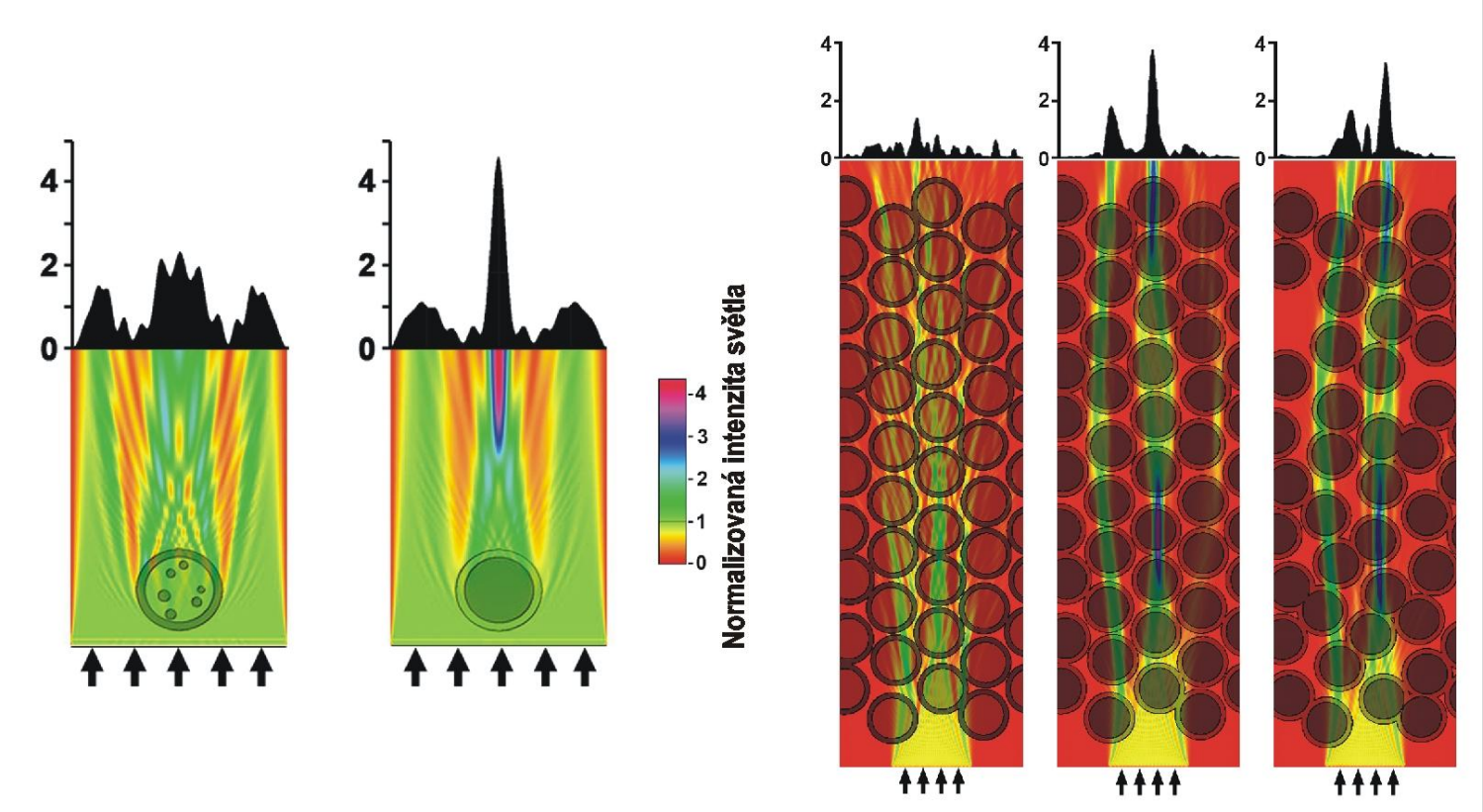

Müllerovy gliové buňky: Živé světlovody sítnice

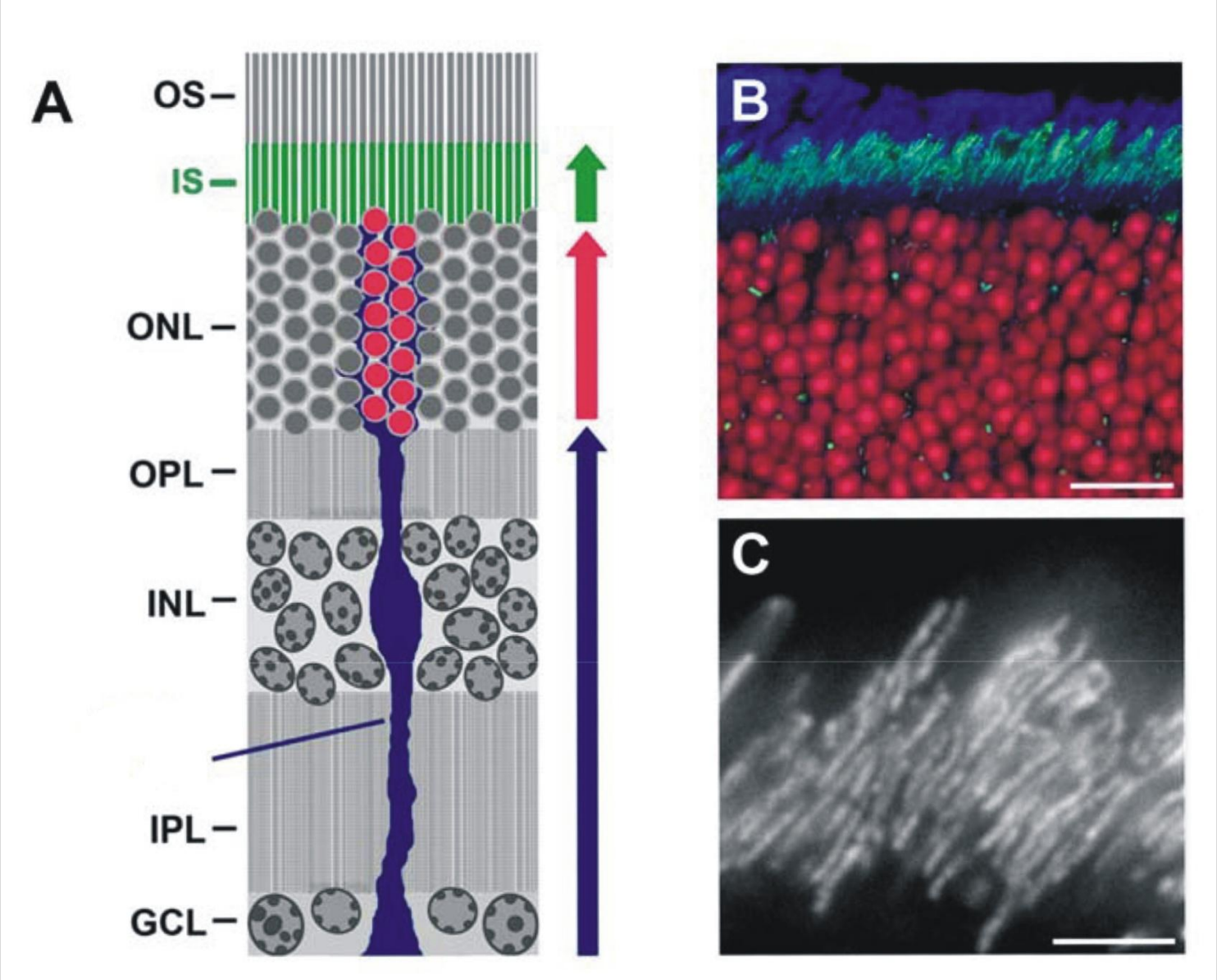

Oko obratlovců

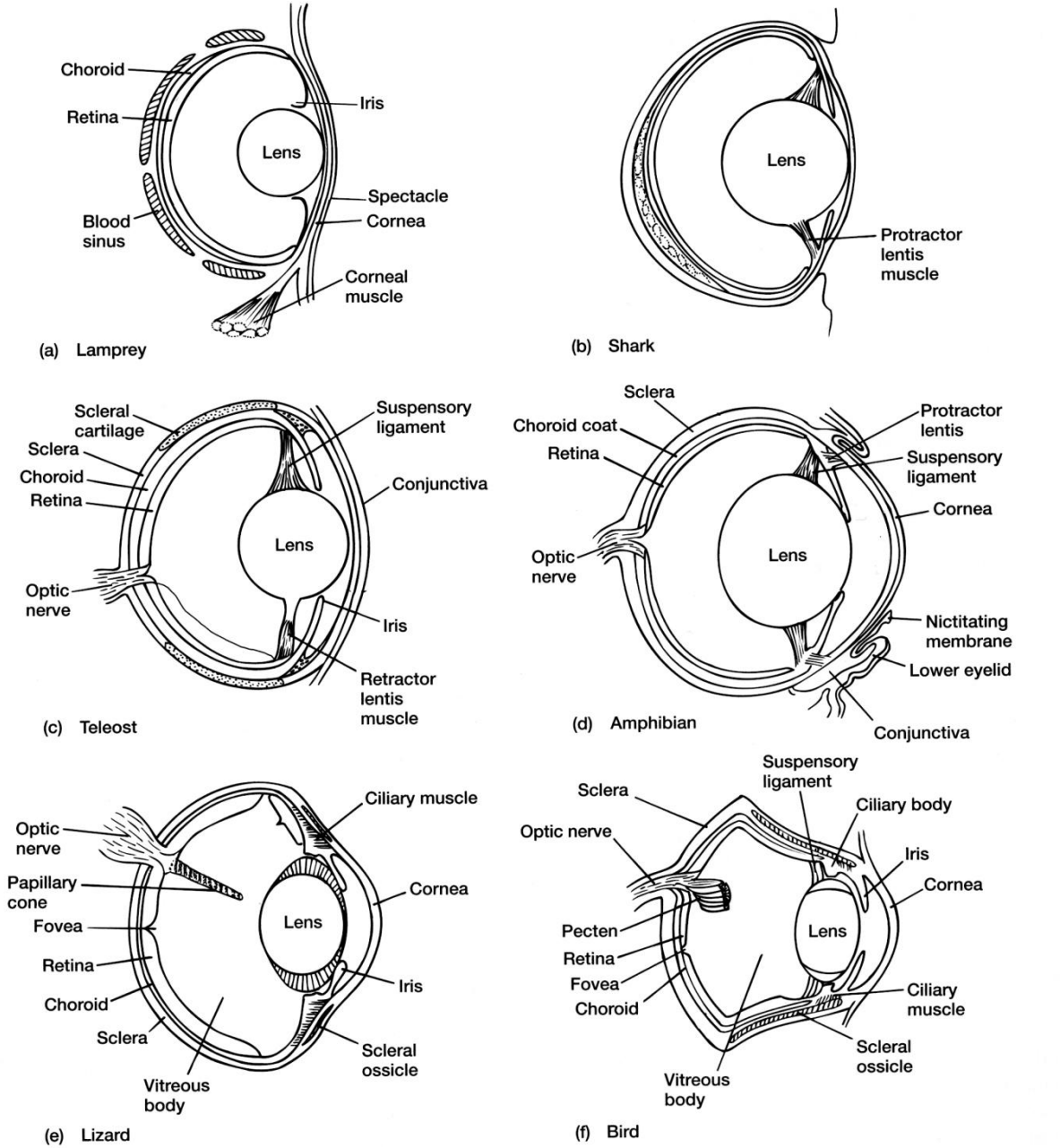

FIGURE 17.19 **Cross sections of vertebrate eyes.** (a) Lamprey. (b) Shark, *Squalus*. (c) Teleost. (d) Amphibian. (e) Lizard. (f) Bird.

After G. A. Walls.

Zaostřování obrazu na sítnici (Akomodace)

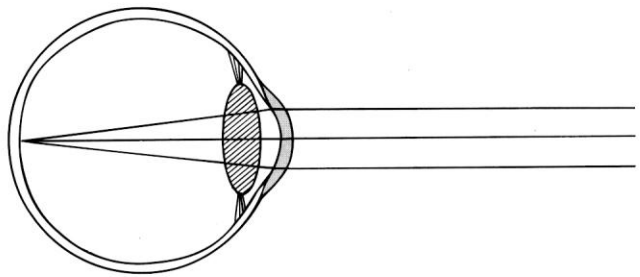

(a) Tetrapod—air

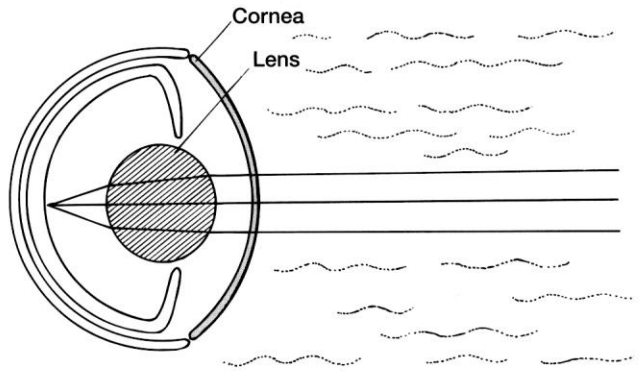

(b) Fish—water

FIGURE 17.20 Vision in air and water. (a) Light that passes through air is strongly refracted when it passes through the cornea; therefore, the cornea is primarily responsible for focusing light rays. The lens fine-tunes the focused image. (b) Because the cornea has refractive properties similar to those of water, incoming light is affected very little when it first enters the eye; therefore, the large lens bears primary responsibility for bringing light rays into focus on the retina.

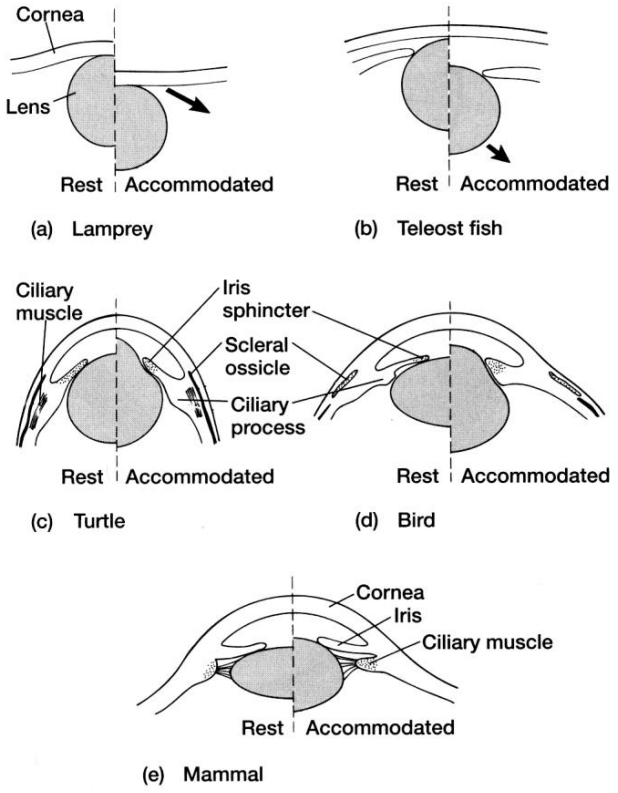

FIGURE 17.21 Accommodation in vertebrates. (a) Lamprey. Contraction of the corneal muscle pulls the cornea against the lens, forcing a change in its position and ability to focus incoming light. (b) Teleost. Accommodation in the teleost depends on a change in lens position. (c) Turtle and (d) bird. Accommodation in both involves the iris sphincter muscle squeezing the lens. (e) Mammal. Accommodation is brought about by relaxation of the suspensory ligaments of the eye.

After G. A. Walls.

Zrakový systém

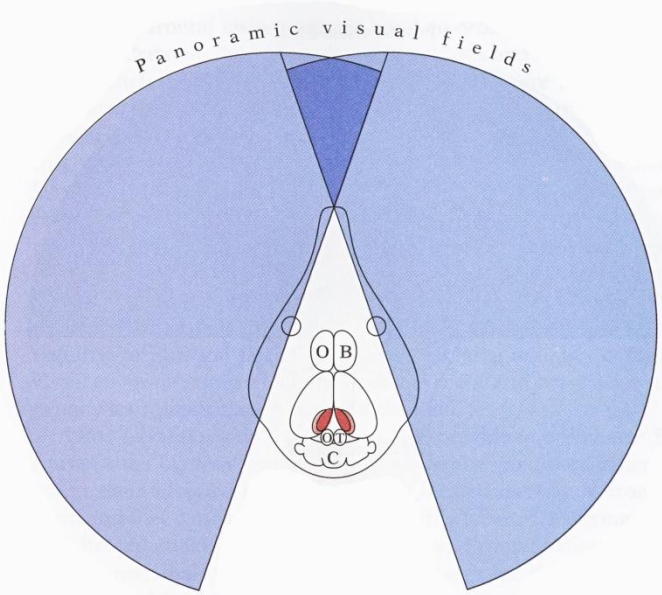

A hedgehog, *Erinaceous europaeus,* a living nocturnal insectivore that has retained many features of primitive mammals.

Život ve větvoví

Potřeba stereoskopického vidění

Frontalizace očí & specifický typ křížení zrakové dráhy

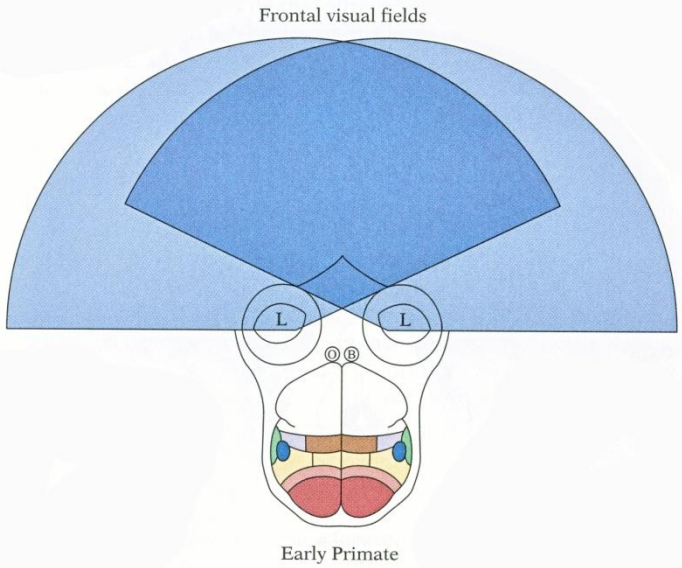

Early Primate

Foveální vidění

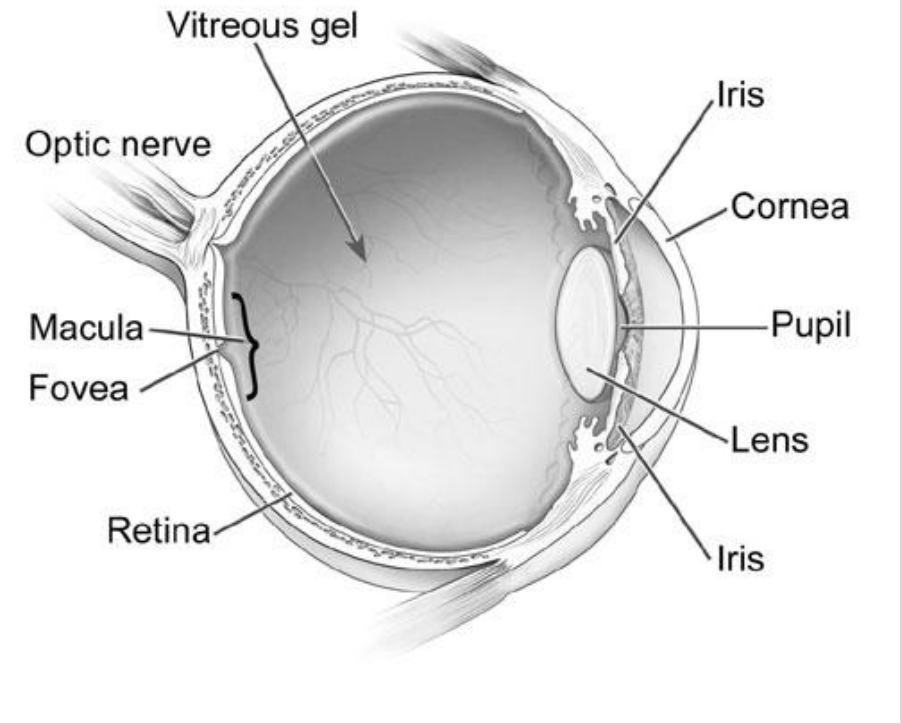

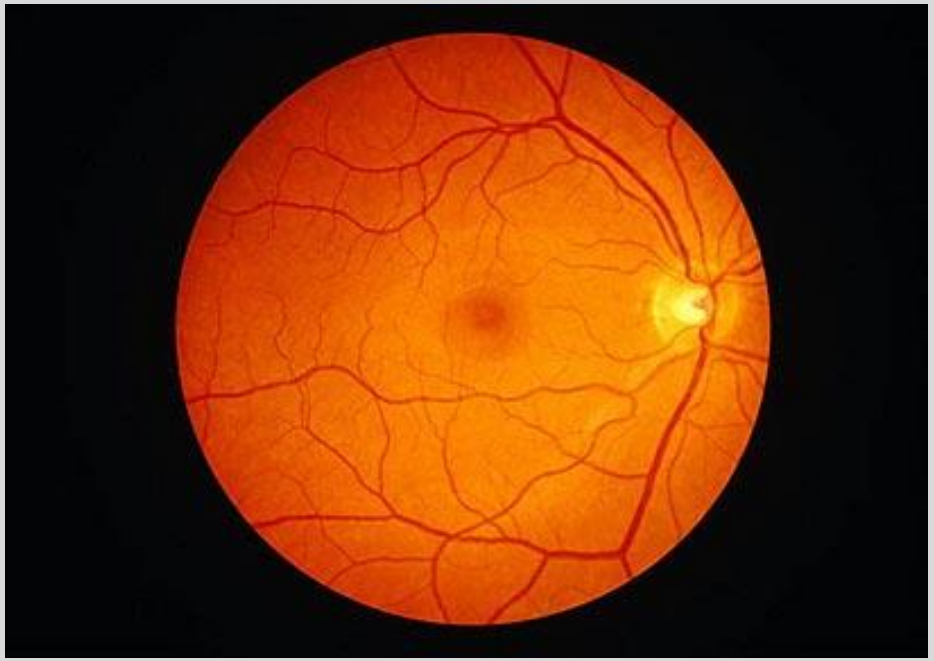

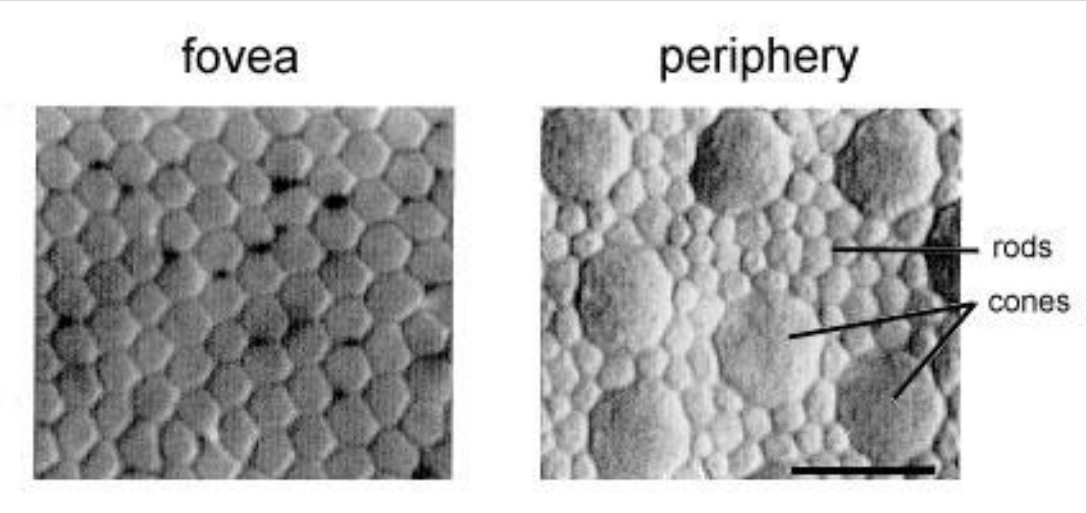

Macula (3 mm) + Fovea centralis (0,5 mm):

místo nejostřejšího vidění ~ 1-2% zrakového pole

Foveální vidění

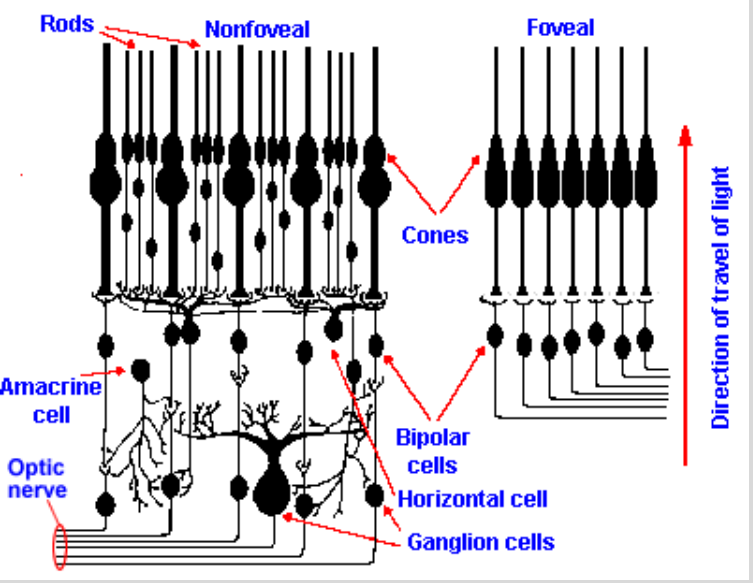

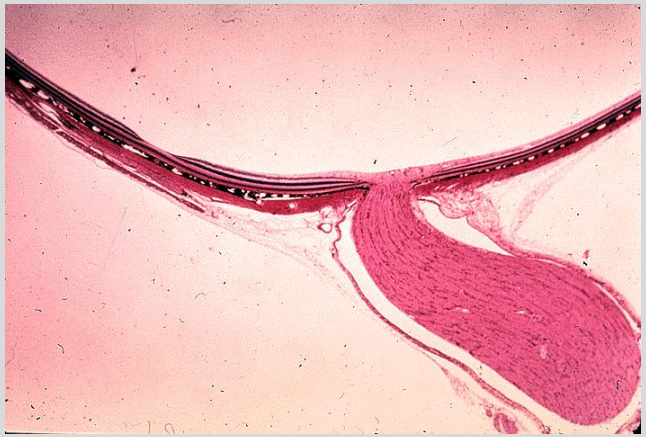

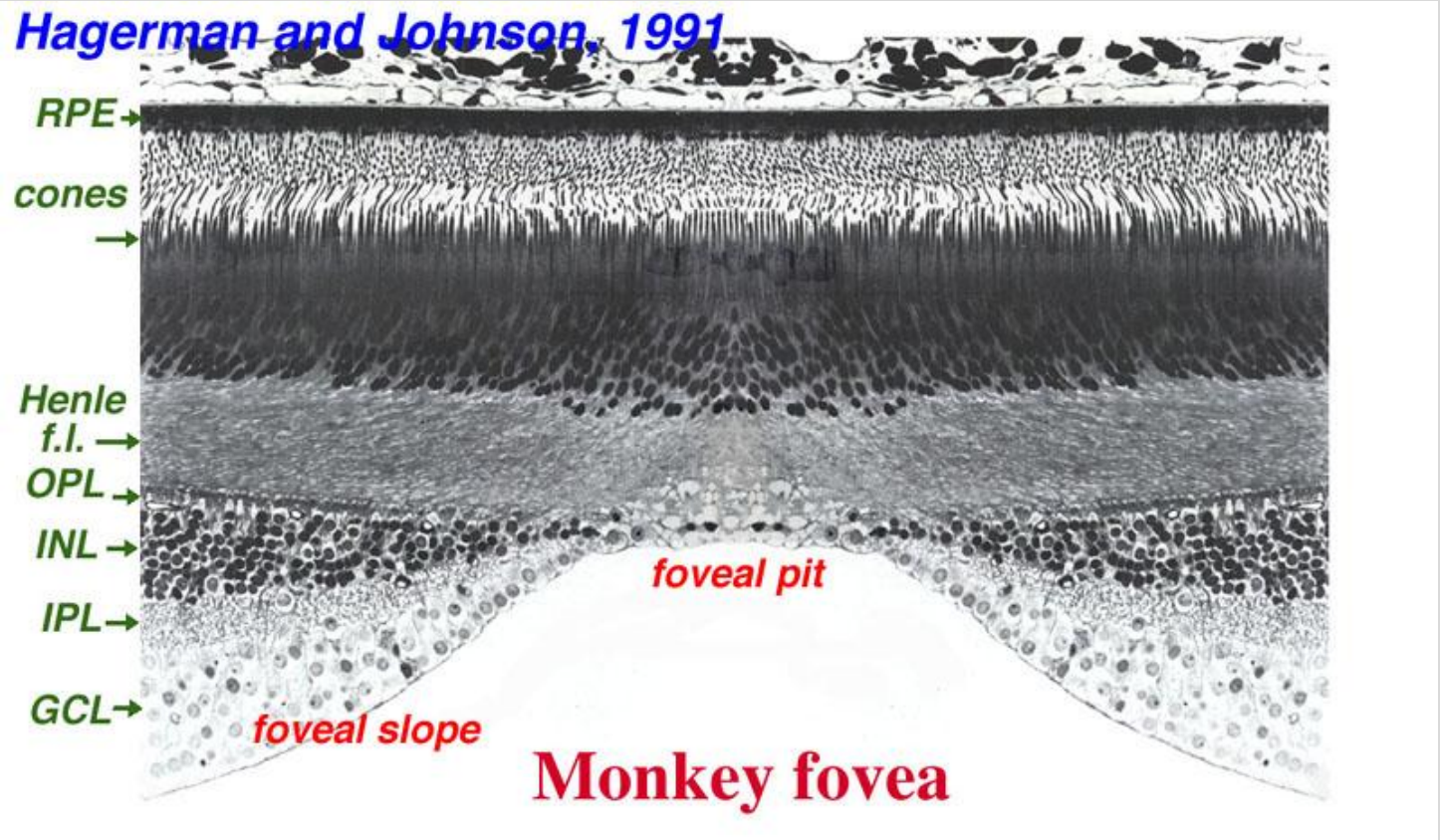

Fotoreceptory

Catarhini – opice starého světa

➢ trichromatické barevné vidění

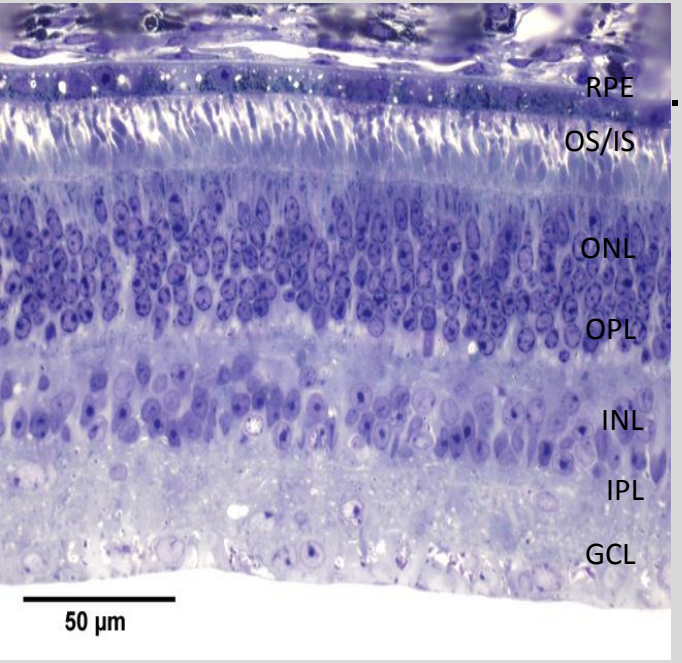

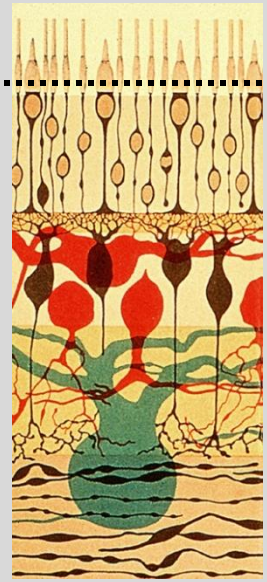

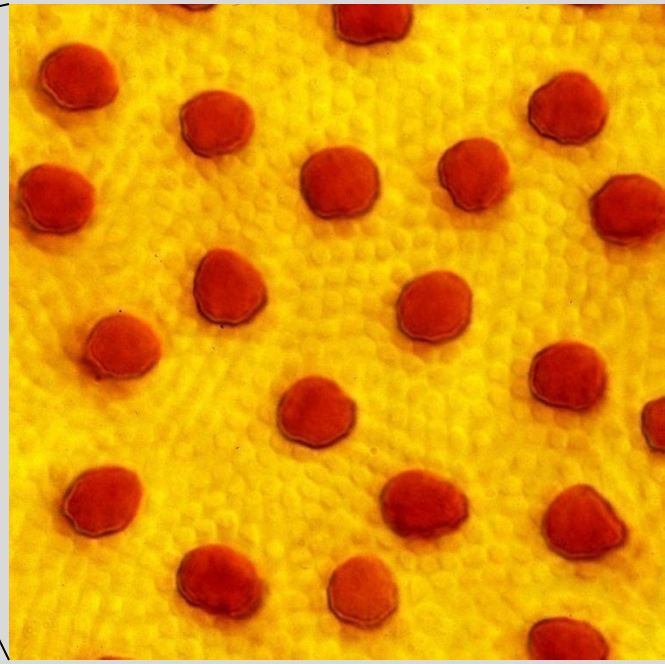

foto: H. Wässle

čípky: denní světlo, barevné vidění

tyčinky: noční, černobílé vidění

Fotopigmenty obratlovců

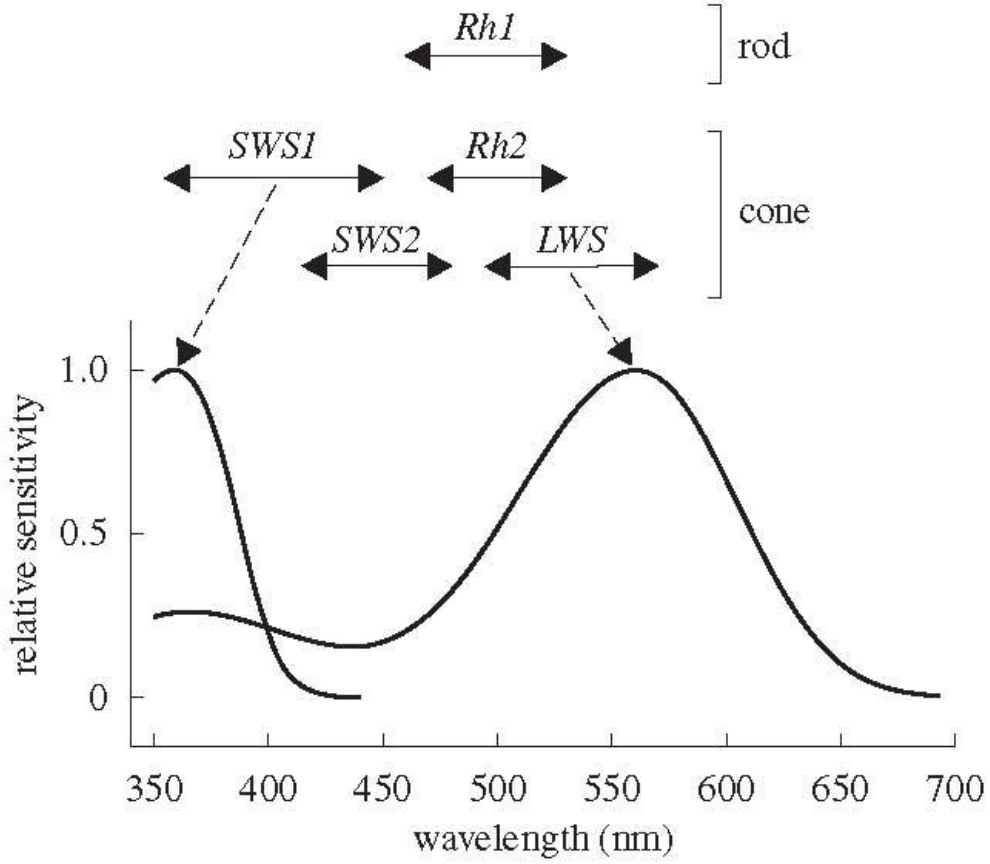

Figure 1. Vertebrate photopigment opsins are products of five opsin gene families (top). In each of these families, gene sequence variations yield photopigments whose λ_{max} values are drawn from the spectral ranges indicated by the extent of the horizontal lines. The ranges shown are those appropriate for pigments constructed using an 11-*cis*-retinal chromophore. All of the cone photopigments of eutherian mammals come from two of these gene families, *SWS1* and *LWS*. It can be inferred from gene sequence comparisons that the two types of cone photopigments found in ancestral members of this group had spectral sensitivities given by the curves at the bottom.

Phylogeny
Mammalian Visual Pigments (0psins)
Eutheria

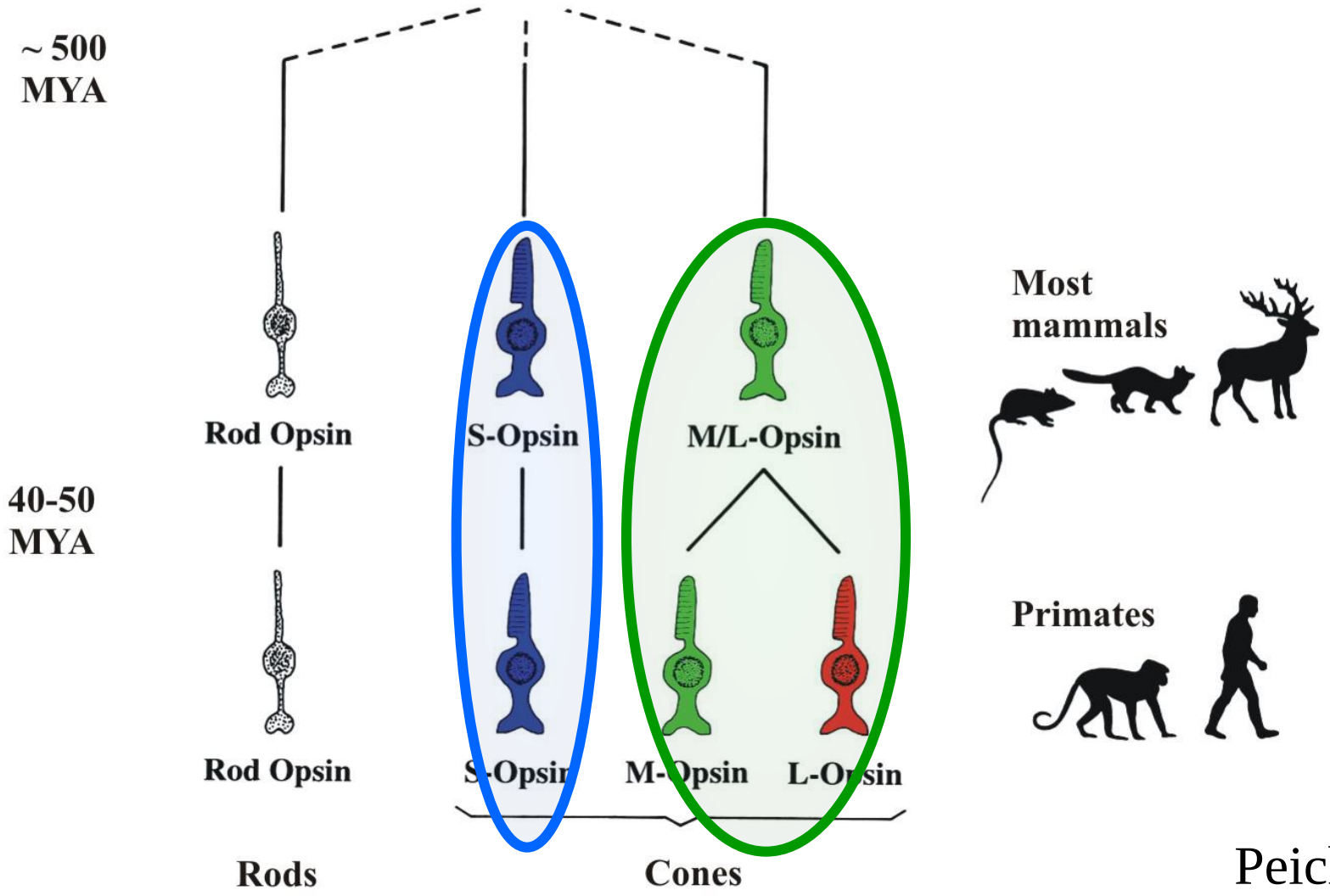

Peichl

Primate Phylogeny

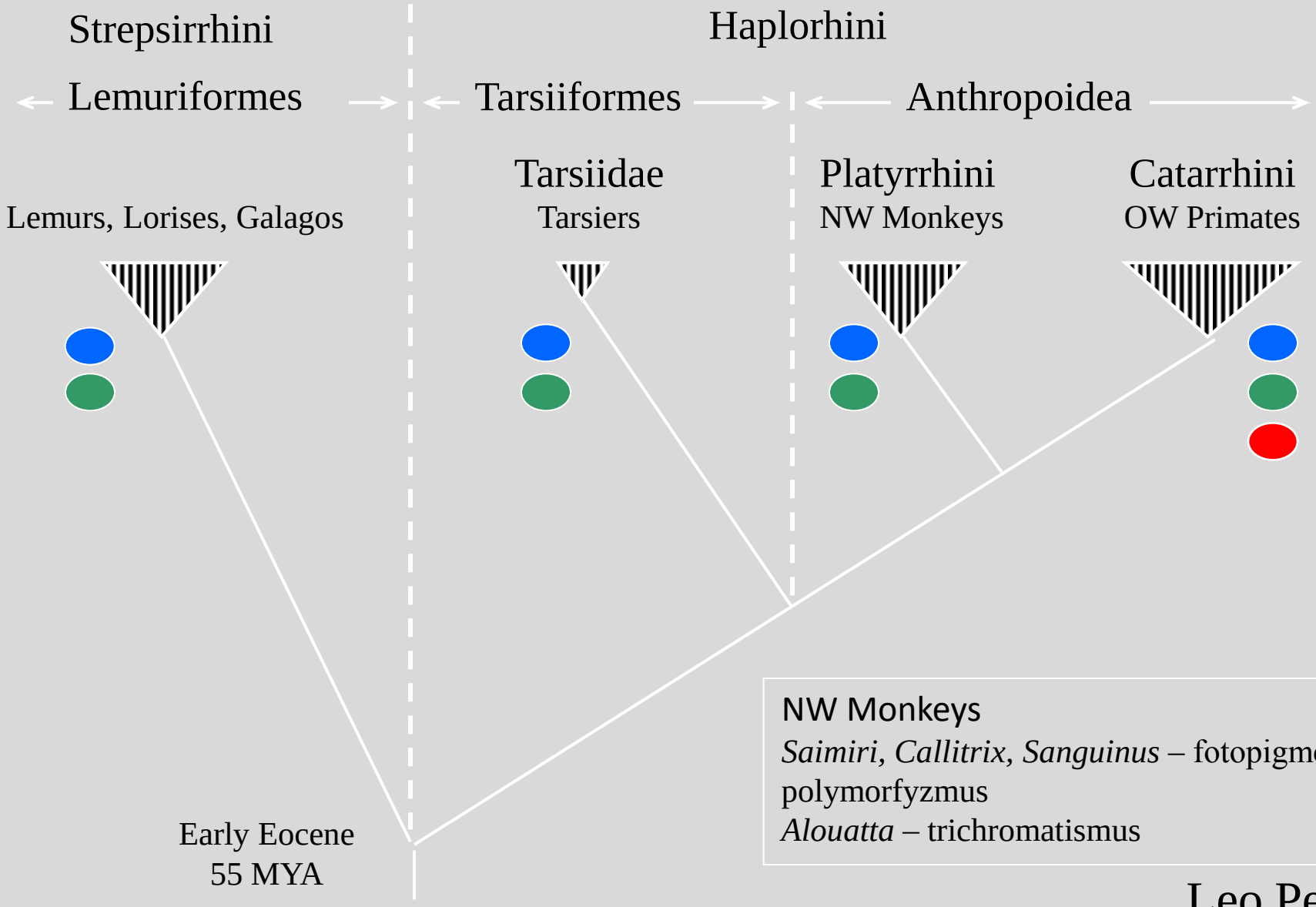

NW Monkeys

Saimiri, Callitrix, Sanguinus – fotopigmentový polymorfyzmus

Alouatta – trichromatismus

Leo Peichl

prase *(opsin double immunofluorescence)*

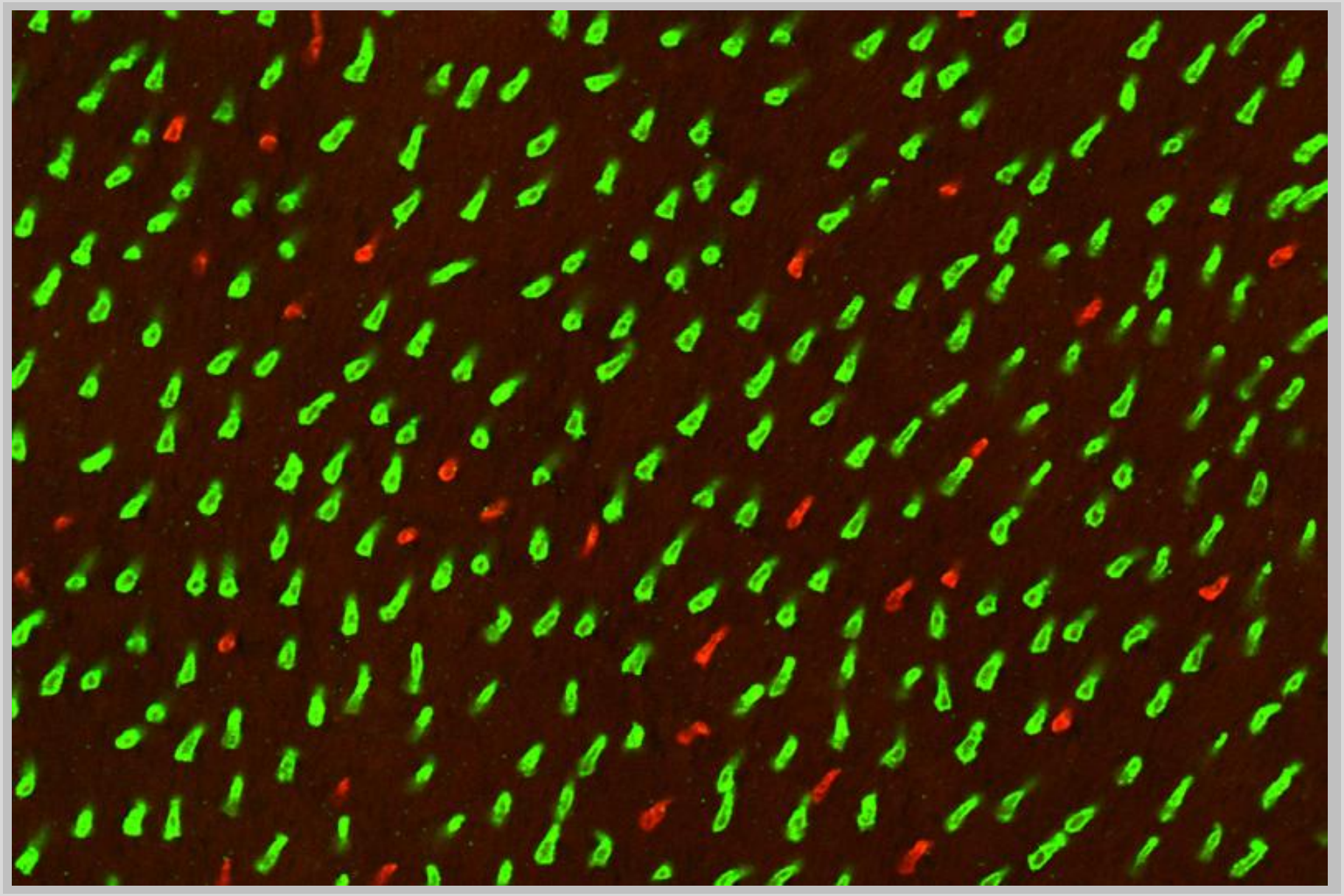

L-čípky S-čípky

Leo Peichl

Většina savců

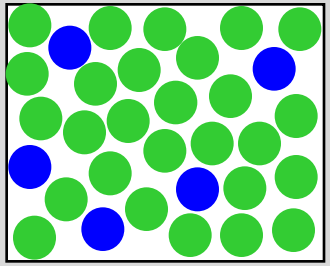

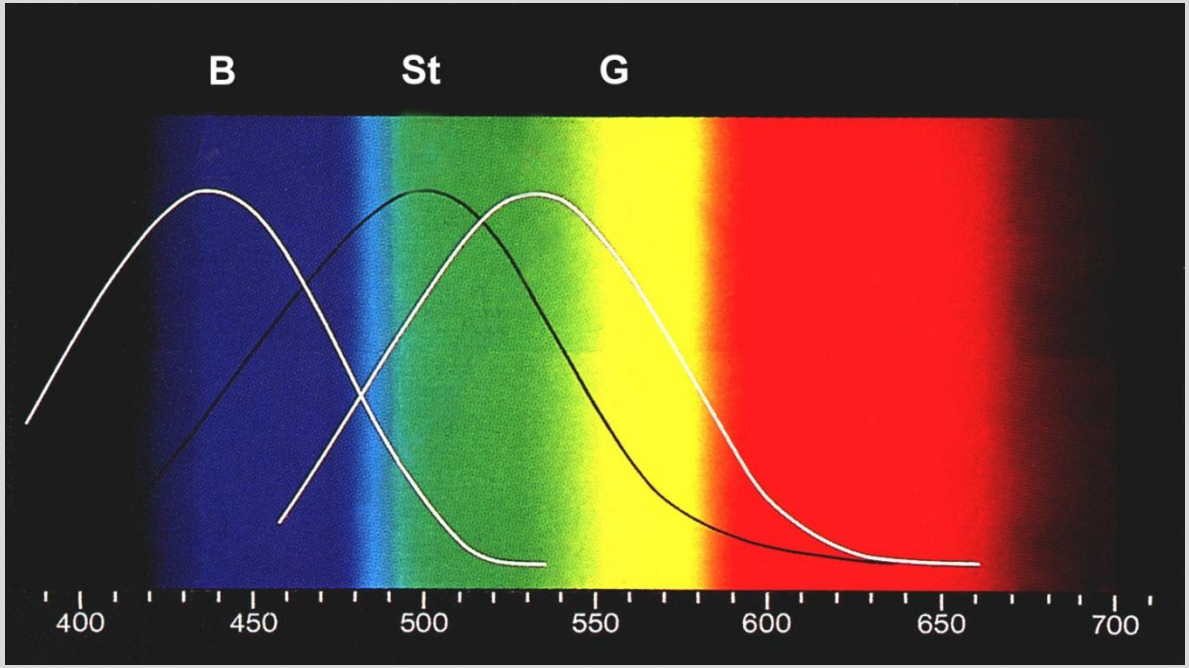

Primáti starého světa

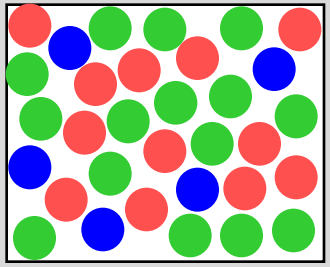

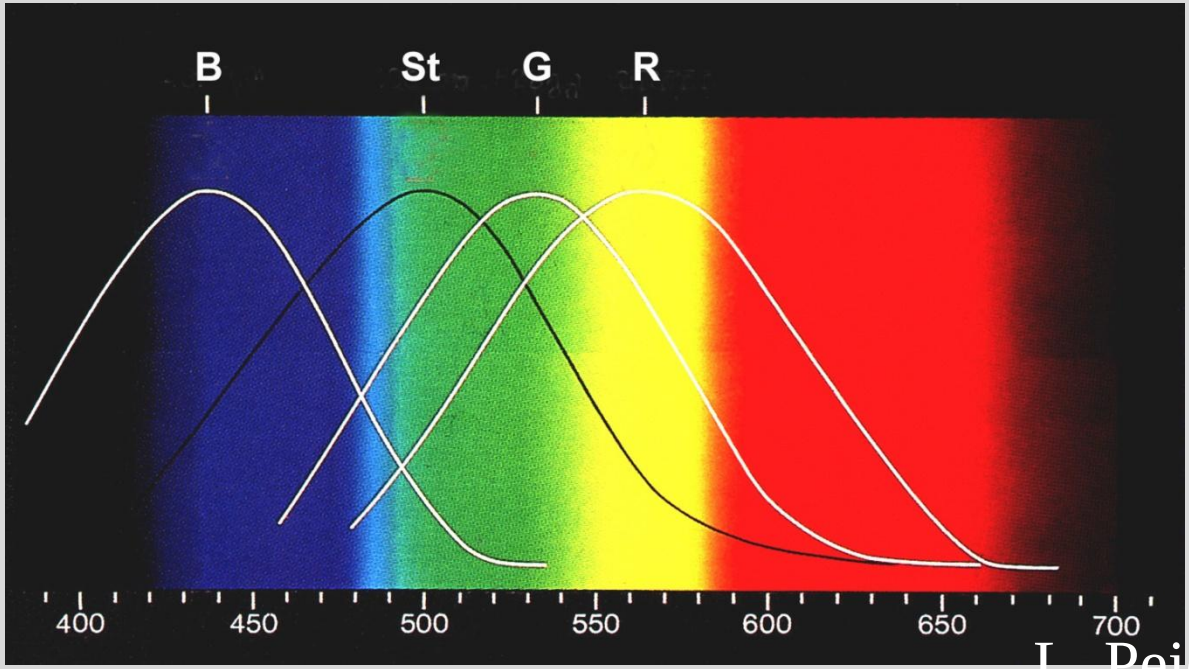

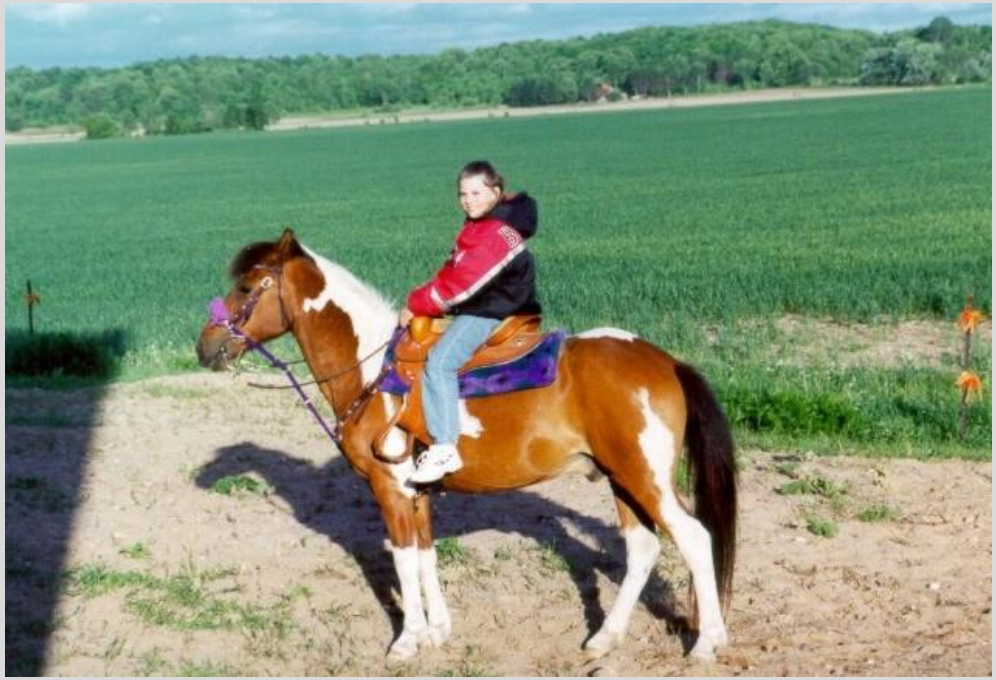

Mechanoreceptory

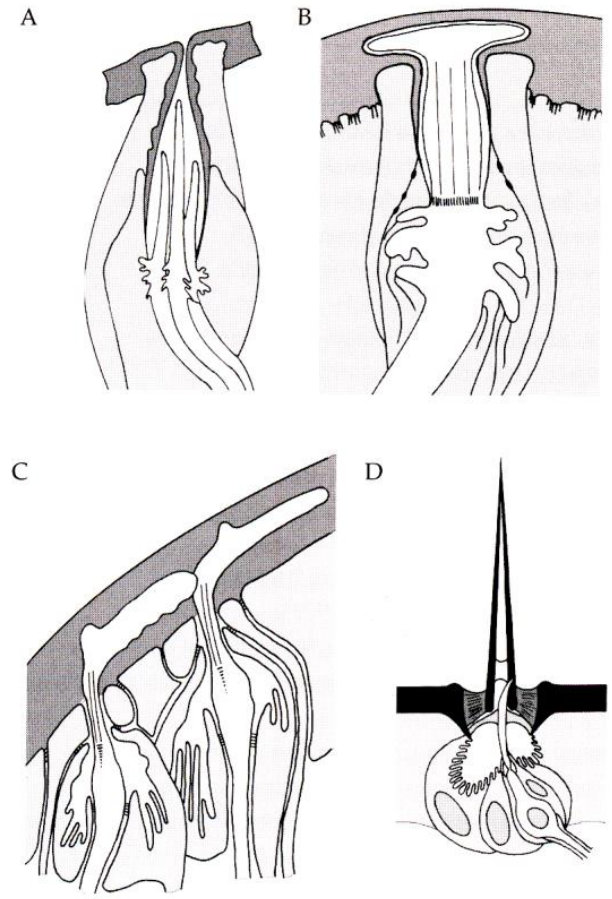

Fig. 7.3. Four different kinds of receptors associated with the cuticle in nematodes (A–C) and euarthropods (D). A. Sensory cilia project into a cavity connected to the exterior by a pore (amphid of *Dipetalonema viteae*, after McLaren 1976). B. Modified sensory cilium projects into the cuticle (head sensilla of *D. viteae*, after McLaren 1976). C. Sensory cilia project into and bend within the cuticle (head sensilla of *Caenorhabditis elegans*, after Wright 1980). D. Sensory cilium terminates in cuticle of mobile bristle (after Keil 1998).

- **Smyslové sensily**

Tíhové receptory - statocysty

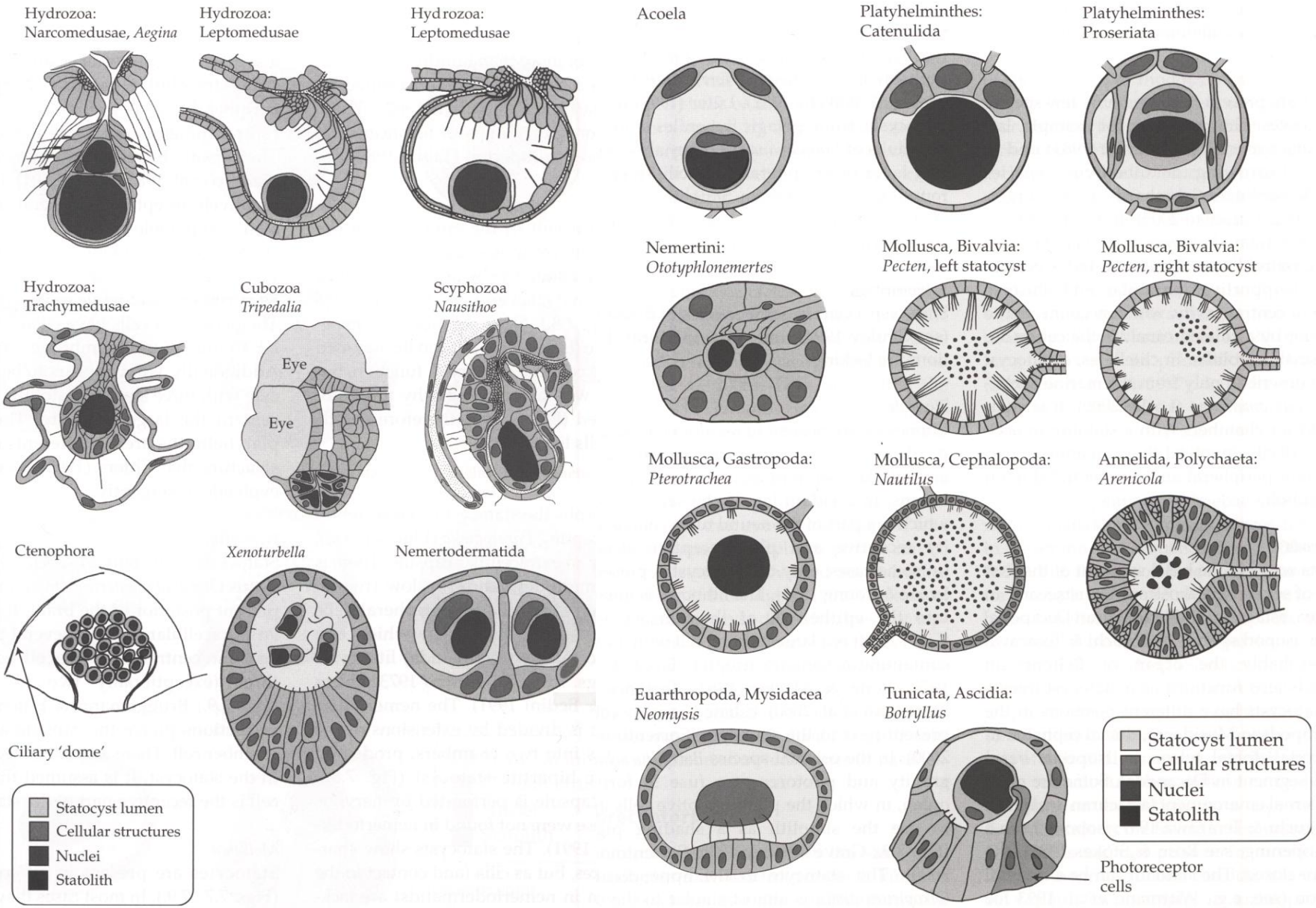

Mechanoreceptory

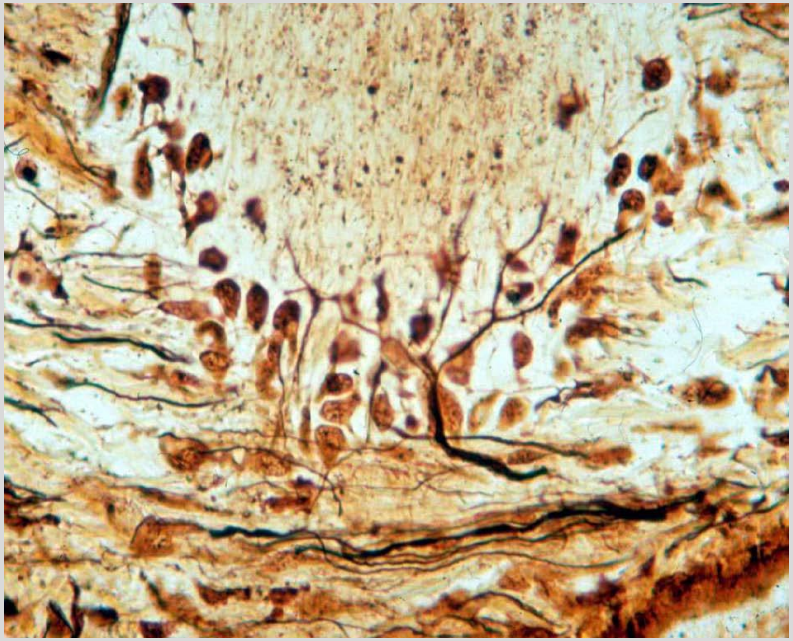

Volná nervová zakončení

Teplo, chlad, bolest

Větví se v dermis, prostupují bazální membránou a zasahují do bazálních vrstev epidermis

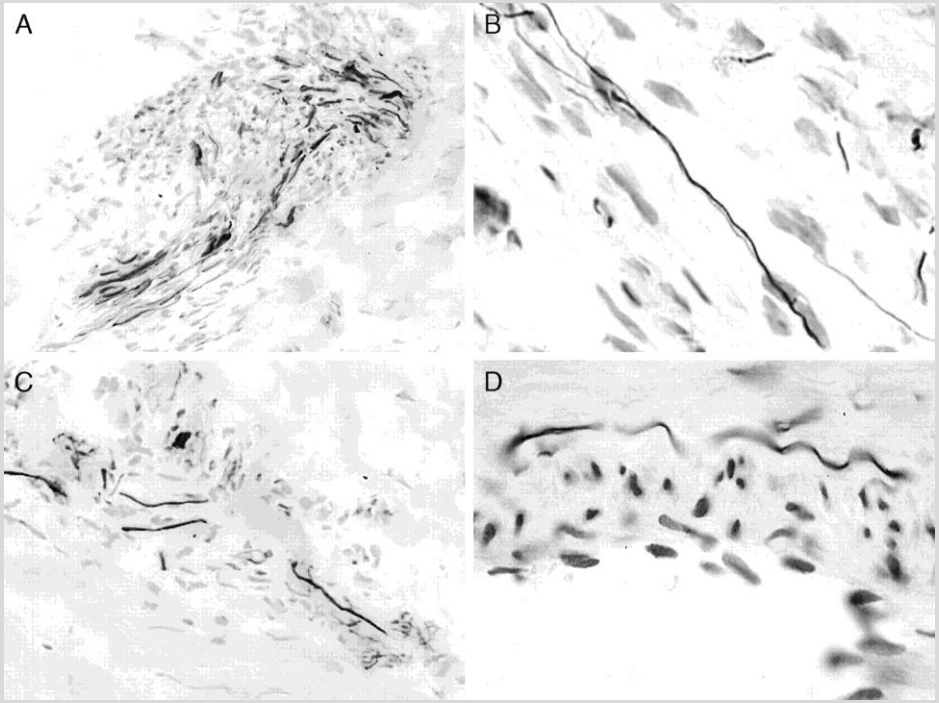

Mechanoreceptory

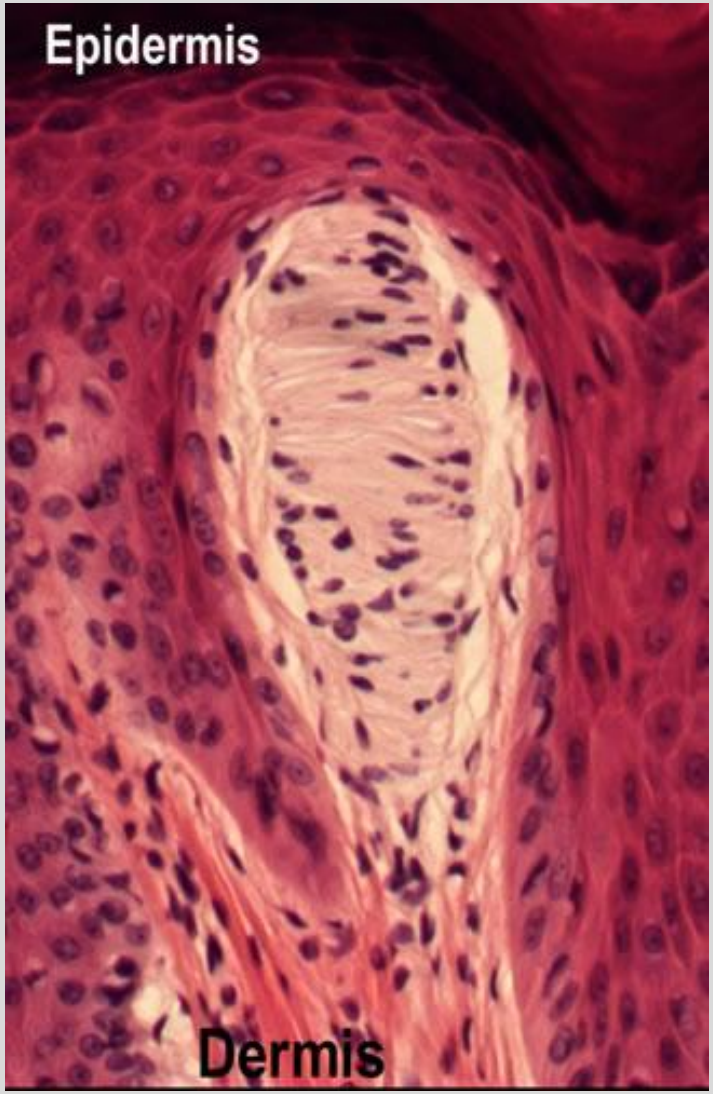

Meissnerova tělíska

dotek

Fibroblasty a silná kolagenní vlákna obklopují jádro tvořené modifikovanými Schwanovými buňkami (horizontálně vrstvené) a nervovými zakončeními

středně rychlá adaptace, malé receptivní pole

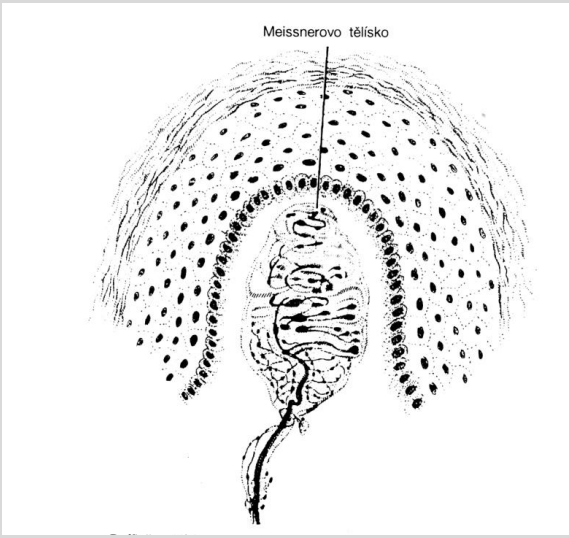

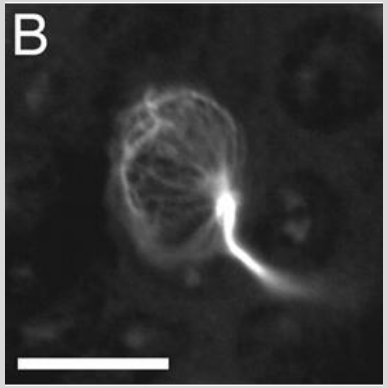

Mechanoreceptory

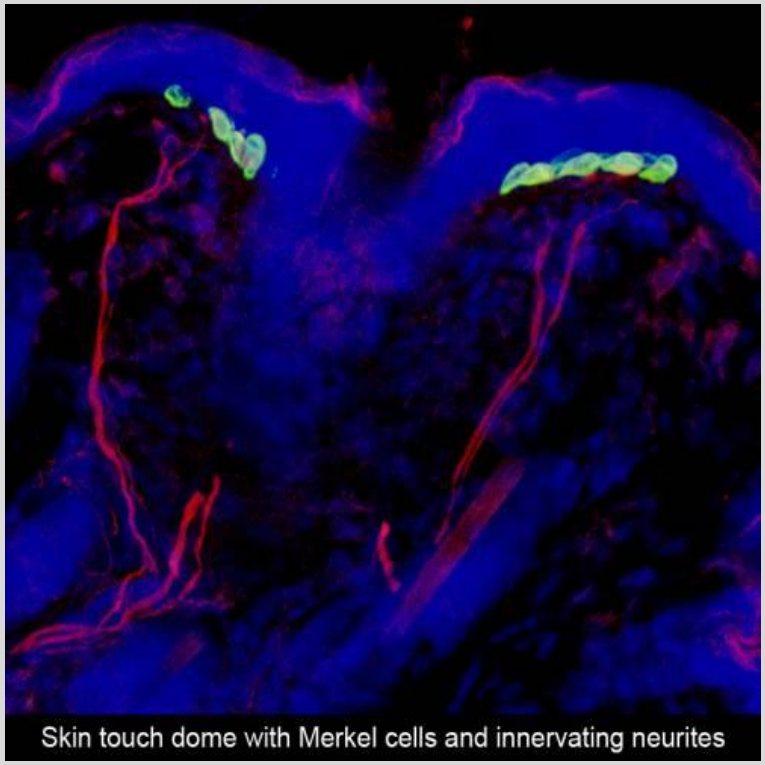
Skin touch dome with Merkel cells and innervating neurites

Merkelovy disky

Dotek, tlak

Ploténkovitě rozšířšné nervové zakončení u Merkelovy buňky

pomalá adaptace, malé receptivní pole

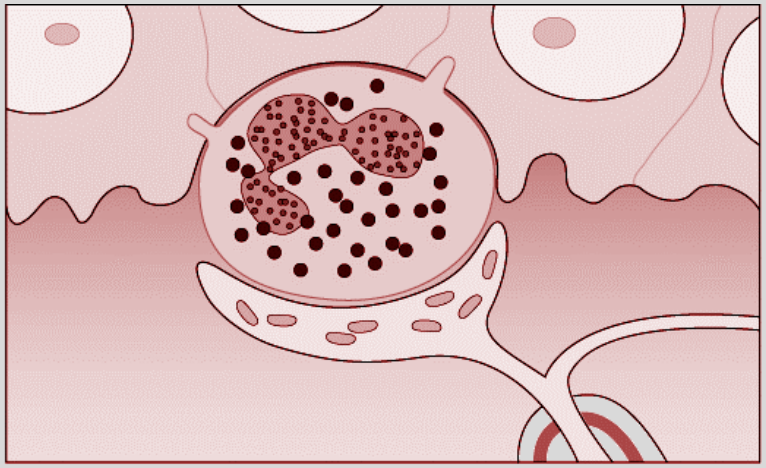

The nucleus of the cell is lobulated and the cytoplasm contains granules of unknown function similar to secretory granules. The axon terminal is filled with mitochondia and covered by a Schwann cell until it enters the Merkel cells.

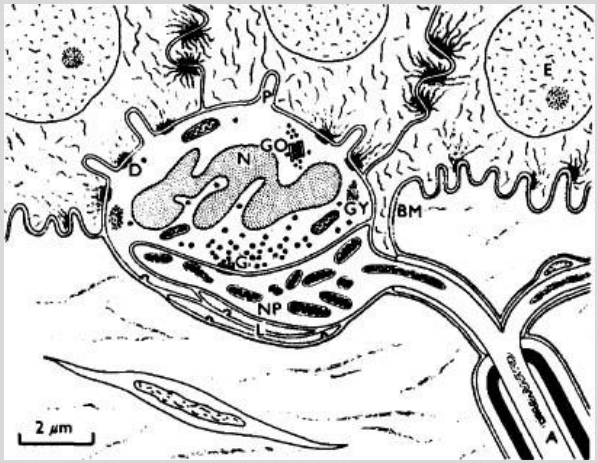

Mechanoreceptory

Ruffiniho tělíska

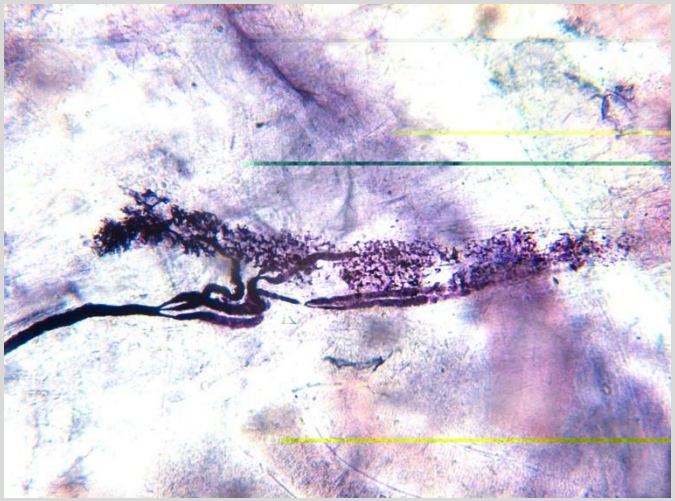

napětí kůže

Bohatě větvená nemyelinizovaná nervová zakončení protkaná kolagenními vlákny a obklopená vazivovým pouzdrem

pomalá adaptace, velké receptivní pole

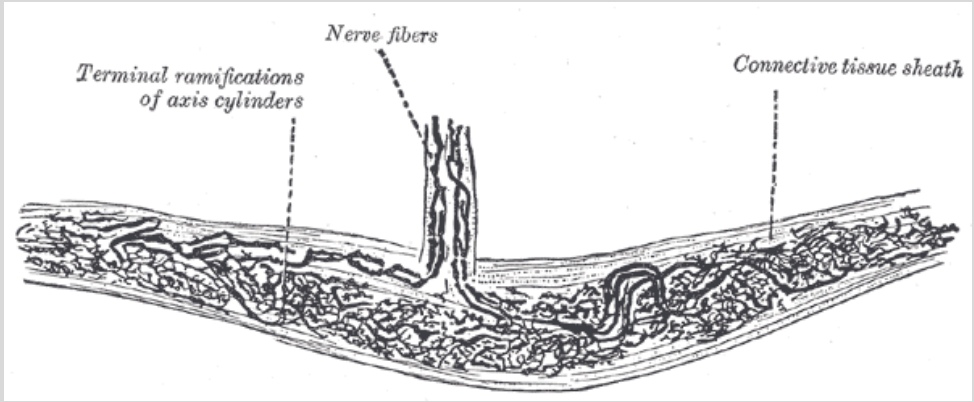

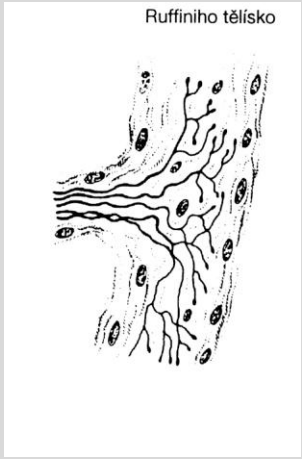

Mechanoreceptory

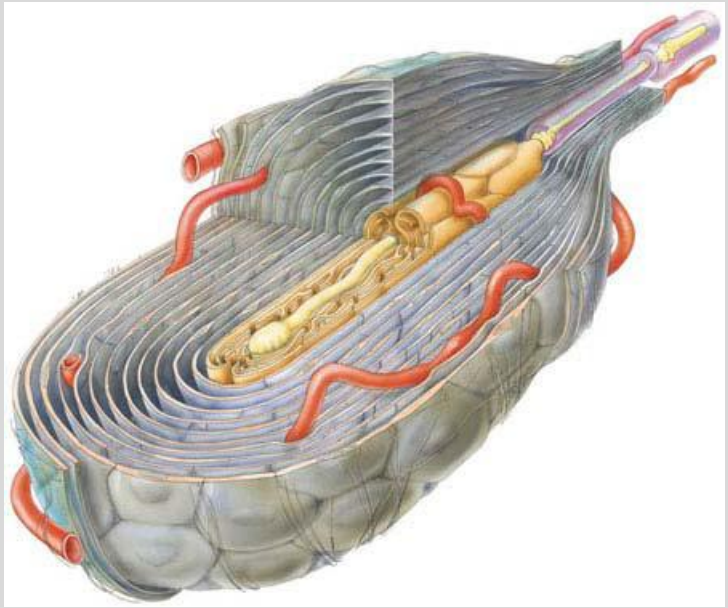

Vater-Paccinioho tělísko:

Vibrace

20-70 vrstev fibroblastů se střídá s tenkými kolagenními vlákny
vnitřní sloupec- Schwanovy buňky a nemyelinizované nervové zakončení (po výstupu z tělíska myelinizováno)

velké recepční pole

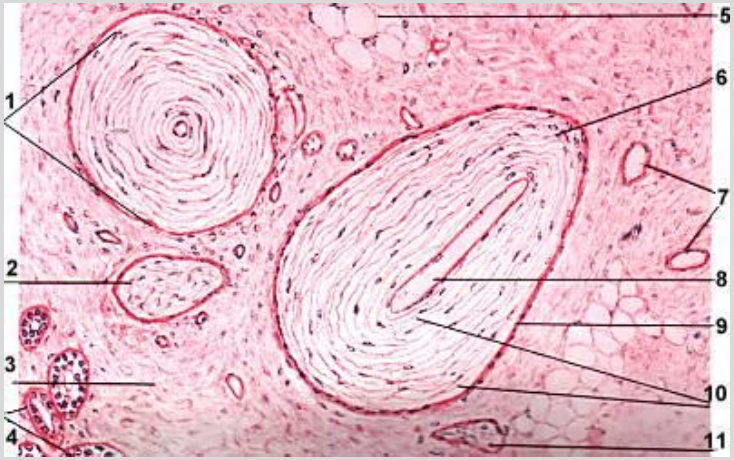

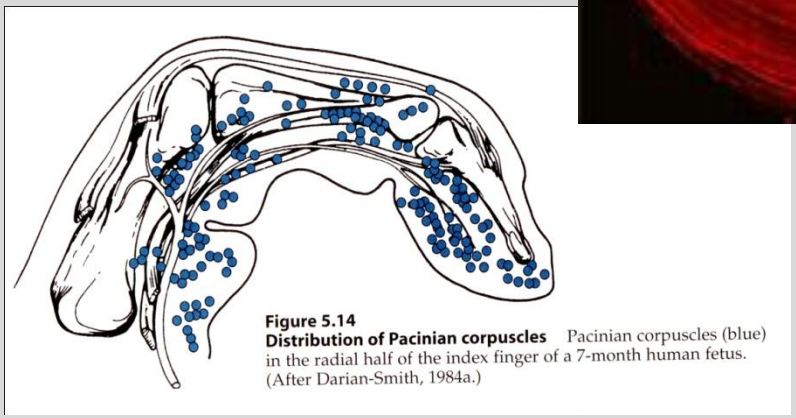

Figure 5.14
Distribution of Pacinian corpuscles Pacinian corpuscles (blue) in the radial half of the index finger of a 7-month human fetus. (After Darian-Smith, 1984a.)

Mechanoreceptory

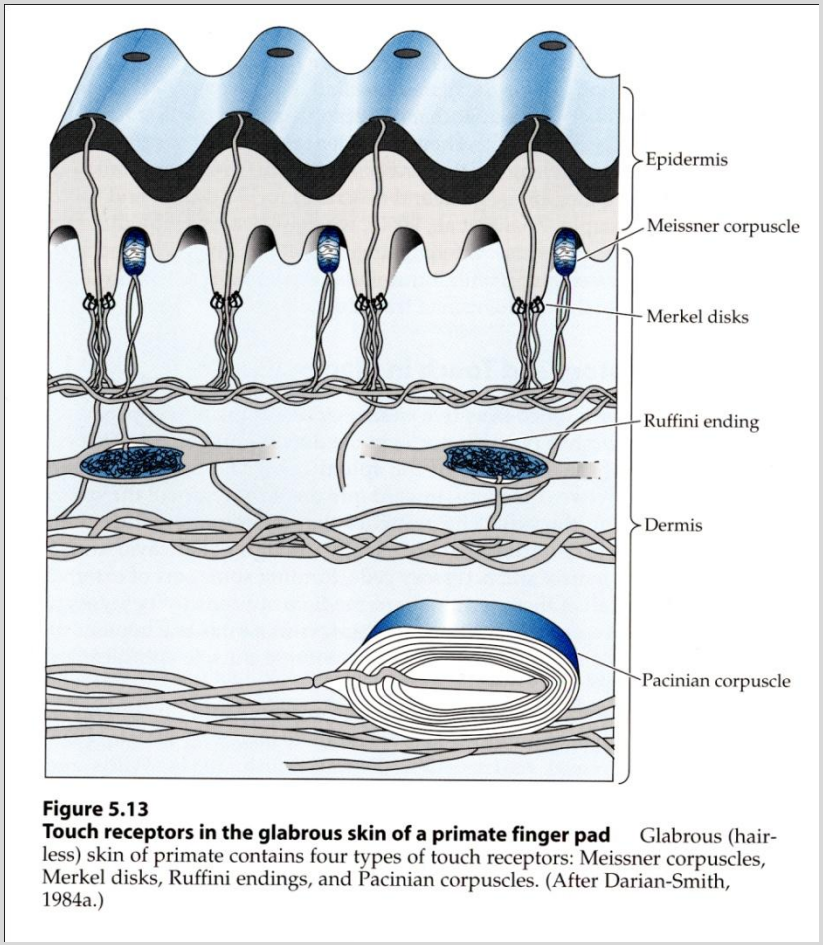

Figure 5.13
Touch receptors in the glabrous skin of a primate finger pad Glabrous (hairless) skin of primate contains four types of touch receptors: Meissner corpuscles, Merkel disks, Ruffini endings, and Pacinian corpuscles. (After Darian-Smith, 1984a.)

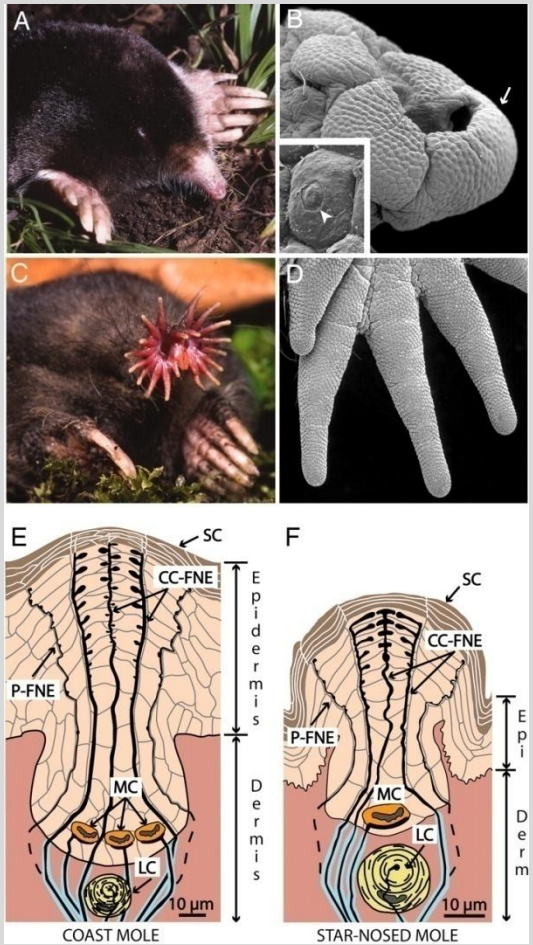

The coast mole (Scapanus orarius) and the star-nosed mole (Condylura cristata) showing adaptations to a fossorial lifestyle. (A) The coast mole has large claws and tiny eyes and lacks an external pinna. (B) A scanning electron micrograph of the coast mole's snout covered with Eimer's organs. An arrow marks organs worn by soil abrasion (see Discussion). (Inset) An Eimer's organ showing the circular disk at the top of the central cell column (arrowhead). (C) The star-nosed mole showing the rhinarium composed of 22 appendages. (D) A scanning electron micrograph of appendages covered with Eimer's organs from the right lower quadrant of the star. (E) Schematic representation of Eimer's organ in the coast mole. The epidermis contains a central epithelial cell column associated with intraepidermal free nerve endings (CC-FNE) that course to the stratum corneum (SC). A ring of smaller peripheral free nerve endings surrounds the central column free nerve endings (P-FNE). Merkel cell–neurite complexes (MC) and lamellated corpuscles (LC) reside at the base of each organ. (F) Schematic representation of the smaller Eimer's organ in the star-nosed mole with only one Merkel cell and a smaller central column

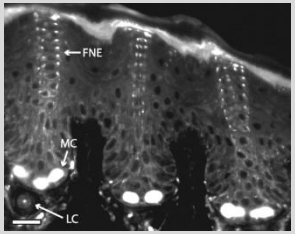

Centrální reprezentace nekoreluje s plochou tělesného povrchu

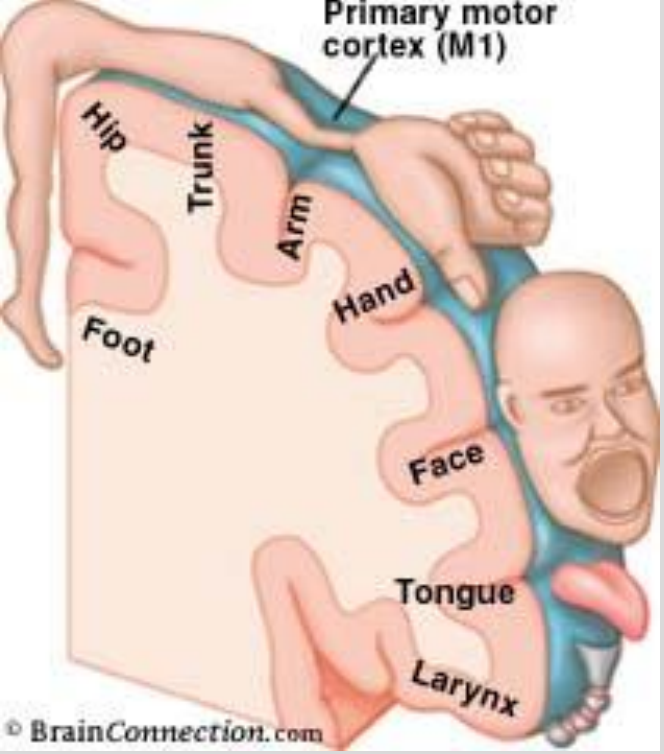

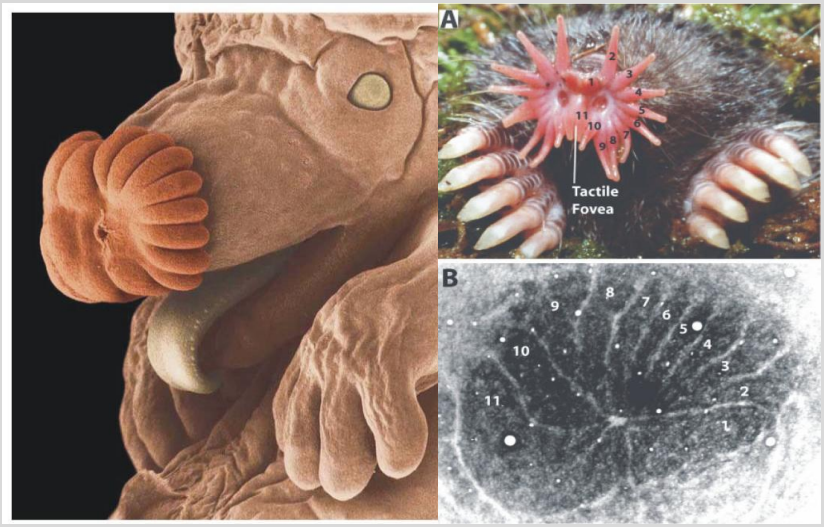

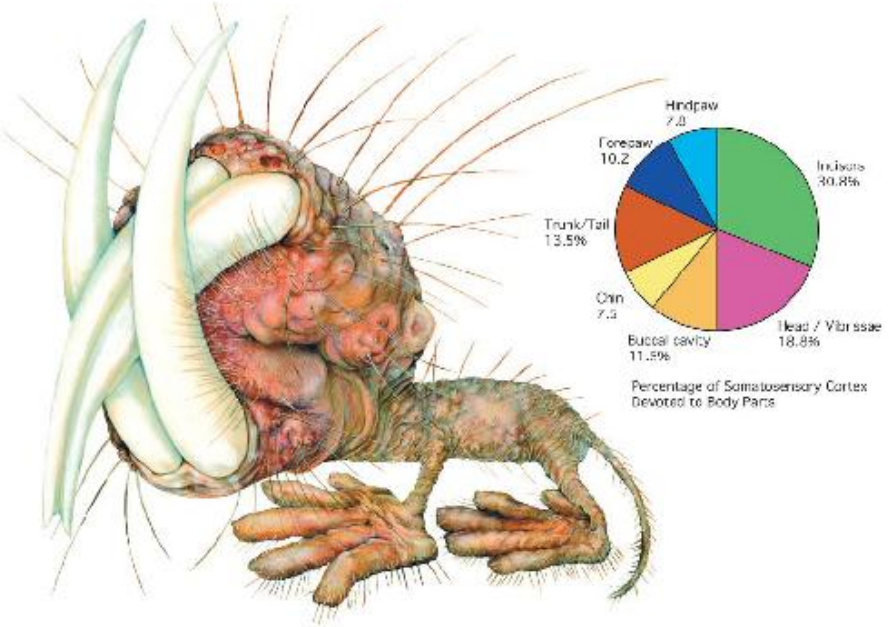

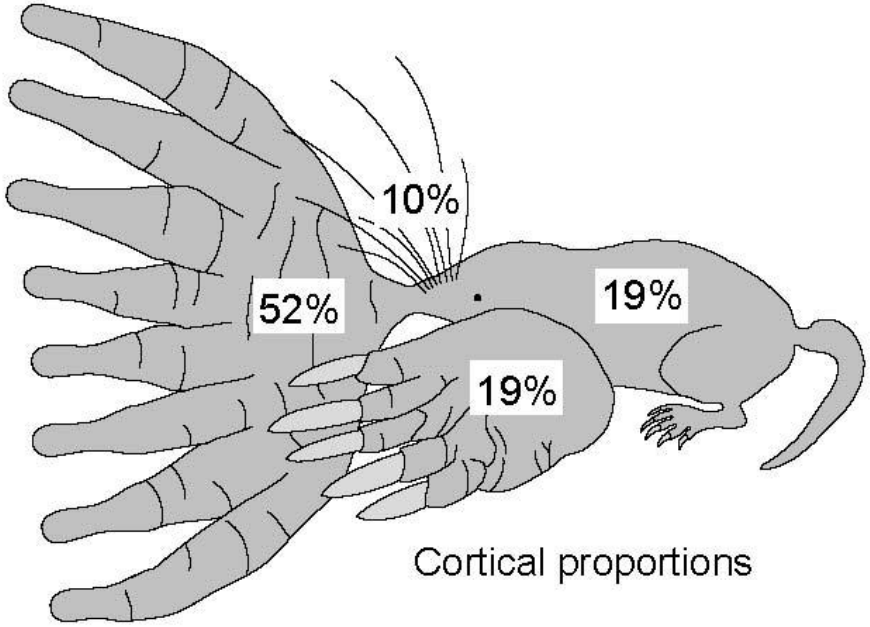

Mechanoreceptory

Figure 5.15
Touch receptors in hair follicles
Follicles of simple hairs are innervated by a few DRG axons that lose their myelin, split into several branches, and form elongate lanciform or palisade endings that surround the hair. Only one axon terminal is shown. (After Halata, 1975; Garcia-Anoveros et al., 2001.)

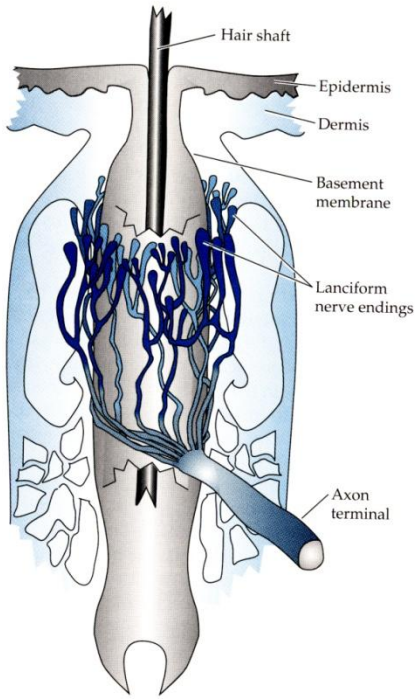

Vibrisy – sinusové chlupy

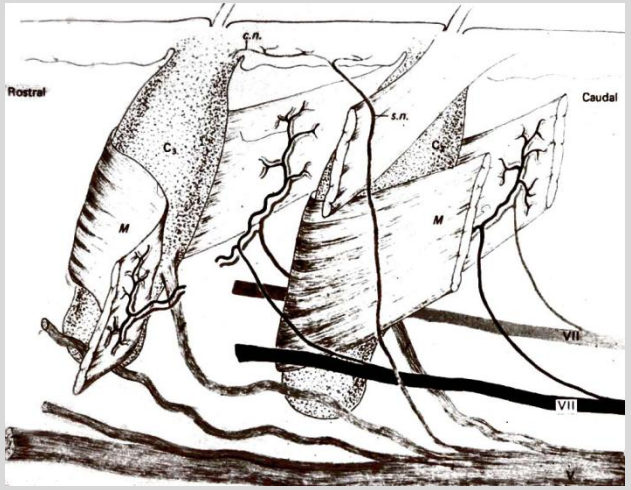

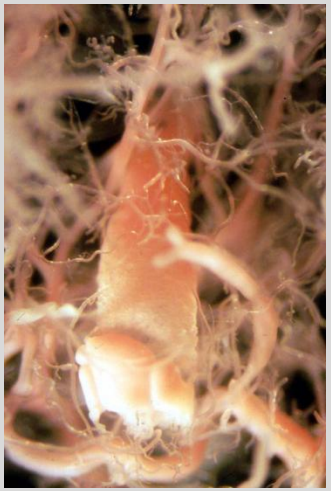

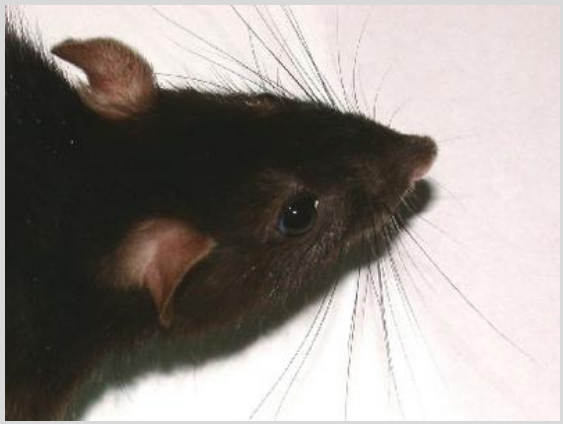

Mechanoreceptory

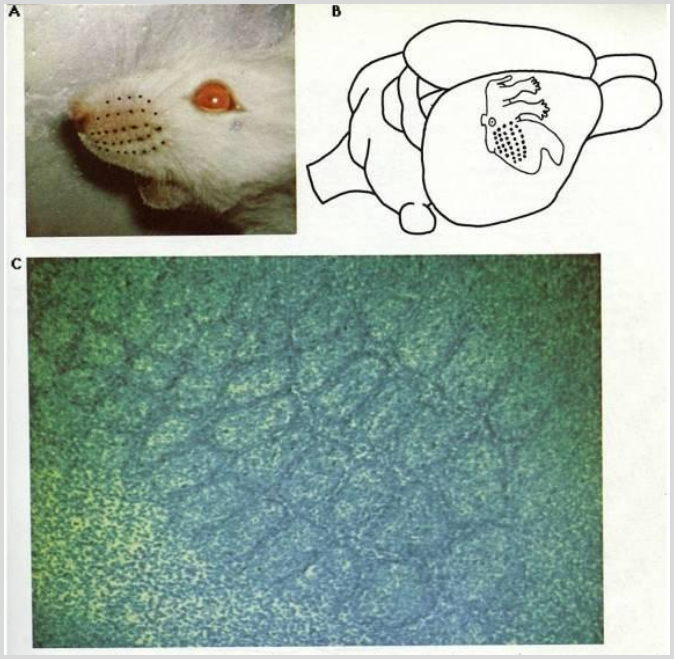

Vibrisy – sinusové chlupy – centrální reprezentace

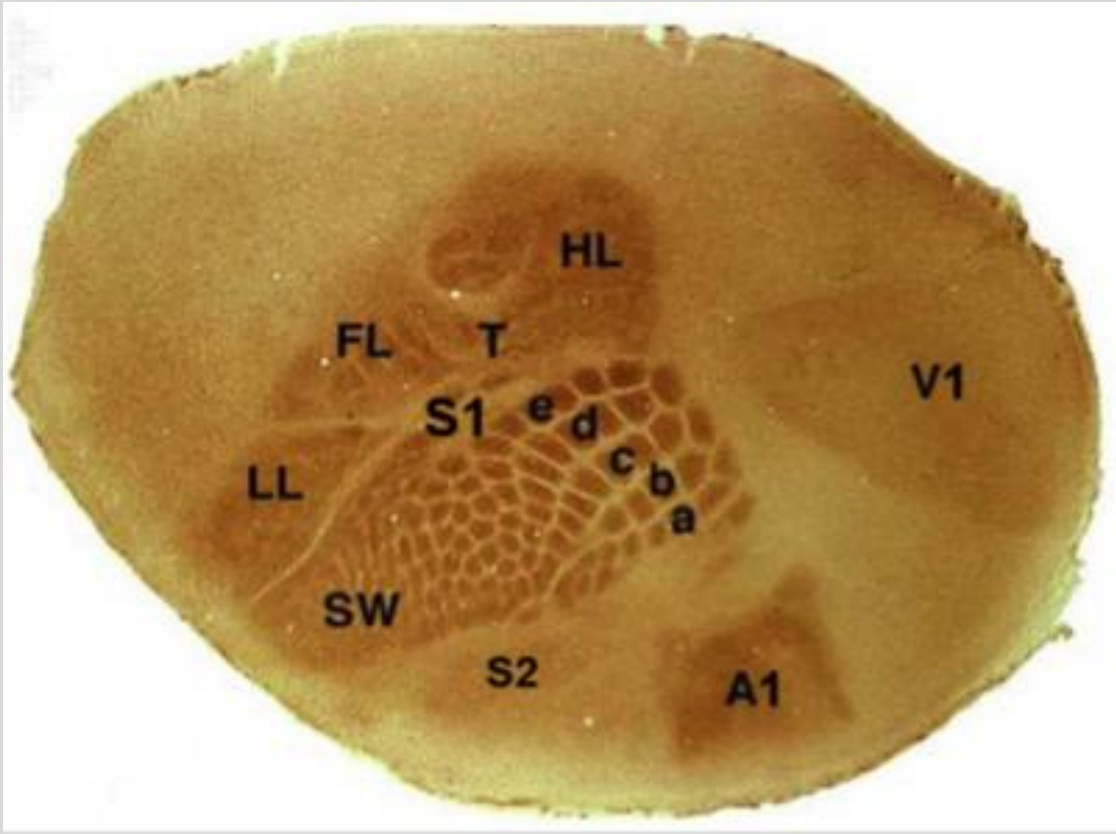

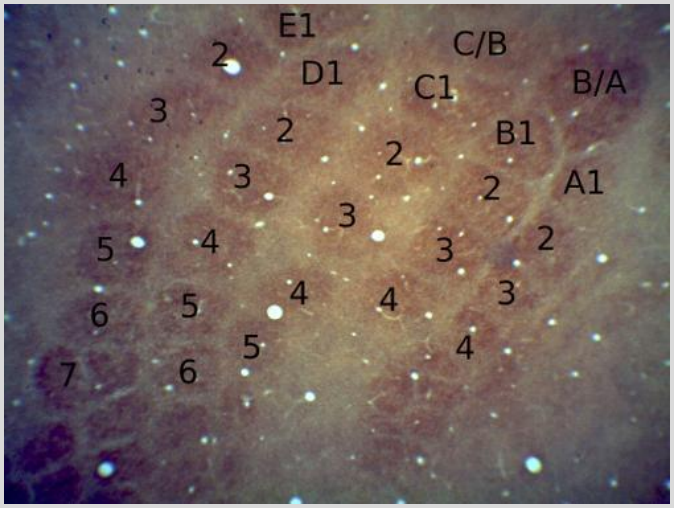

Tlakové receptory krokodýlů

✓ **detekce tlakových vln vyvolaných rozčeřením hladiny**

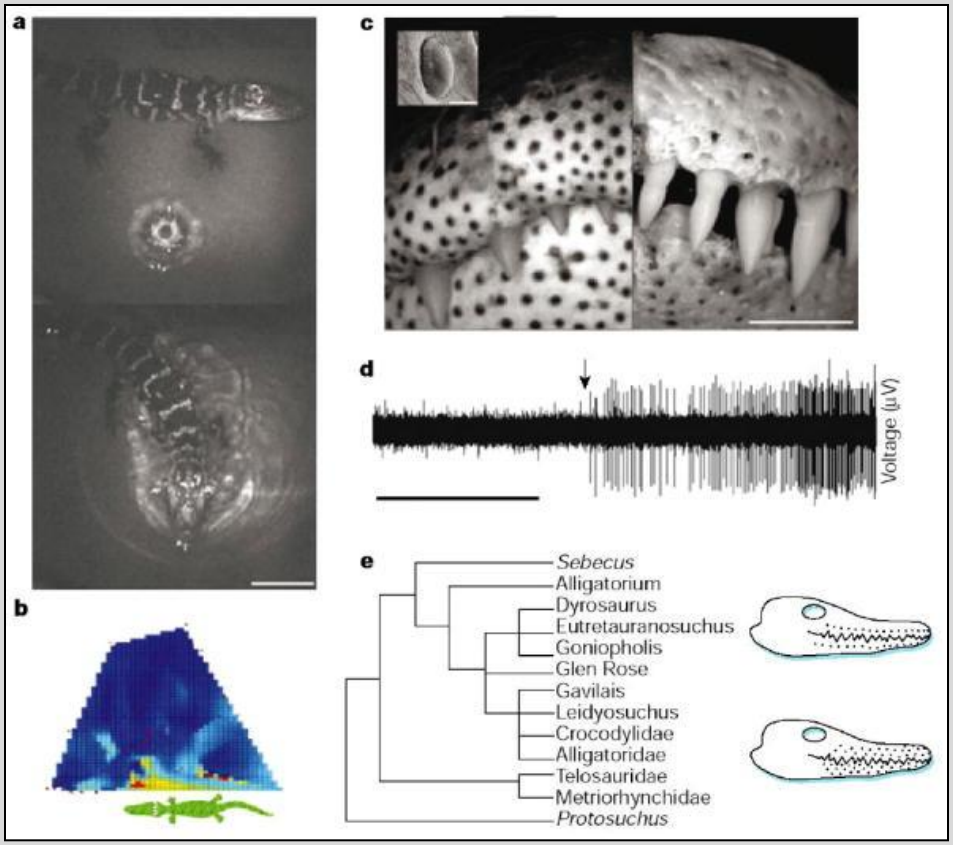

Figure 1 Dome pressure receptors (DPRs) in crocodilians. a, Infrared images of the responses of an alligator to water droplets. Scale bar, 10 cm. b, Summary of the responses of one alligator. Cartoon represents the position of the animal; colour represents an error index as follows: blue, c, Left, DPRs can be seen as black dots; right, corresponding foramina. Scale bar, 3 cm. Inset, scanning electron micrograph of an individual DPR; scale bar, 100 [mu]m. d, Physiological trace from a trigeminal ganglion showing the responses of DPRs to increases in water pressure (left to right). Arrow indicates the threshold of the response. Scale bar, 10 s. e, Cladogram of crocodyliforms 5,6 showing the presence and absence of foramina. Forms in which the pattern of foramina is absent (top drawing) are shown in italics.

Figure 2 Stubble means trouble: an alligator's face, showing the distribution of the blue dome pressure receptors.

Neurology: An ancient sensory organ in crocodilians.
Soares, Daphne

Nature. 417(6886):241-242, May 16, 2002.

Proprioreceptory

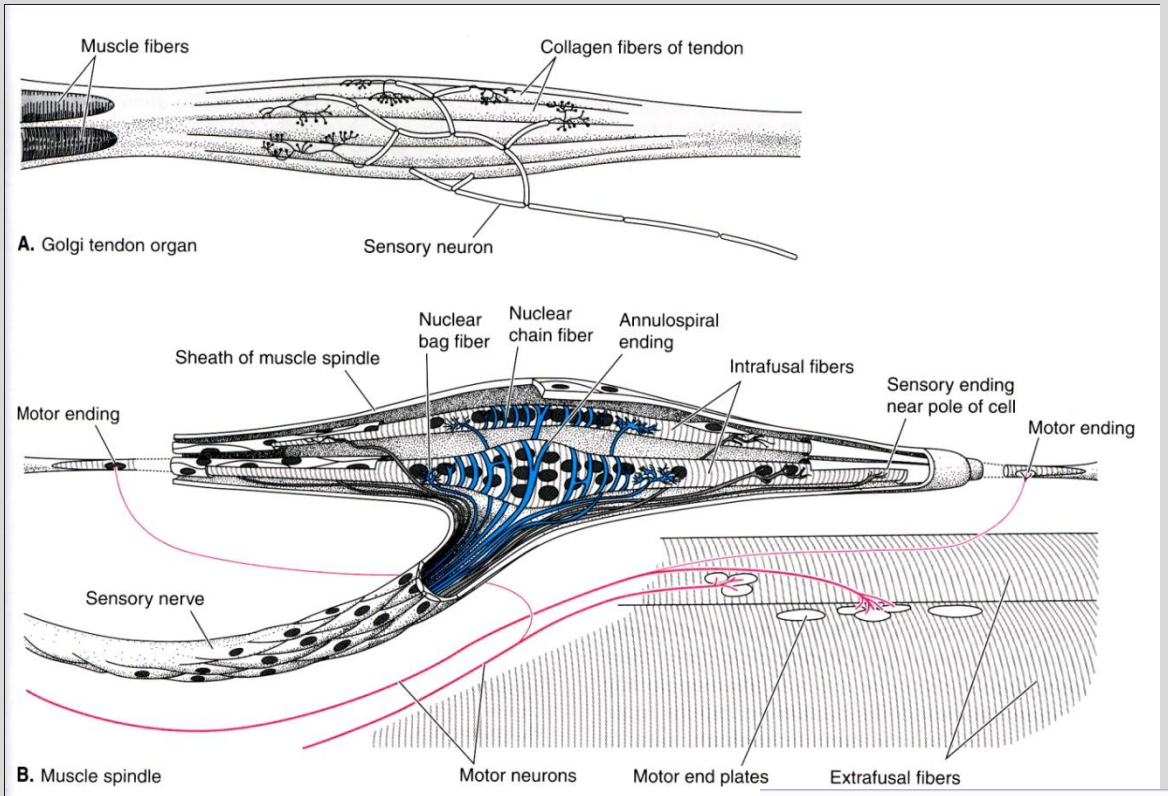

FIGURE 12-7
Proprioreceptors. *A*, Tendon organ. *B*, A muscle spindle. *(After Williams et al.)*

Golgiho šlachový orgán

napětí uvnitř šlach

Svalové vřeténko

svalové napětí

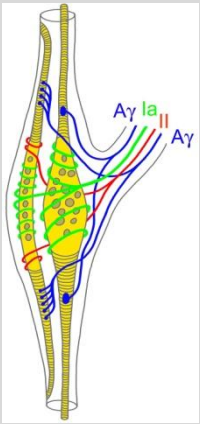

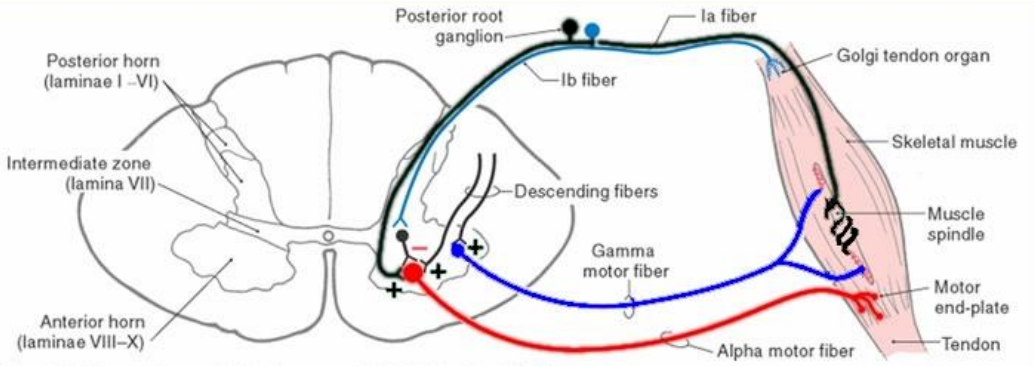

Mechanoreceptory laterální čáry – neuromasty

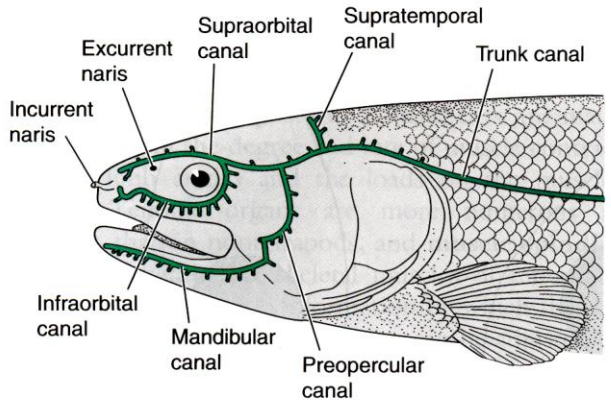

FIGURE 12-10
The distribution of lateral line canals on the head of the bowfin, *Amia*. *(After Jarvik.)*

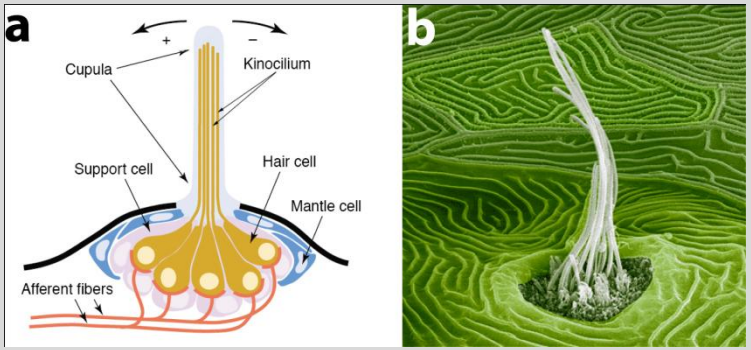

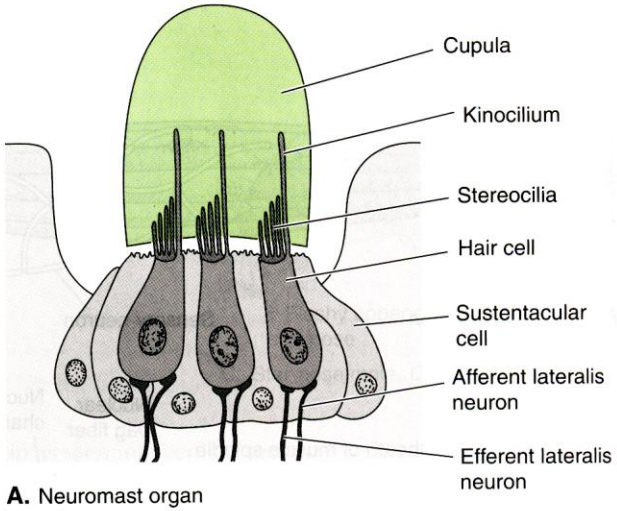

A. Neuromast organ

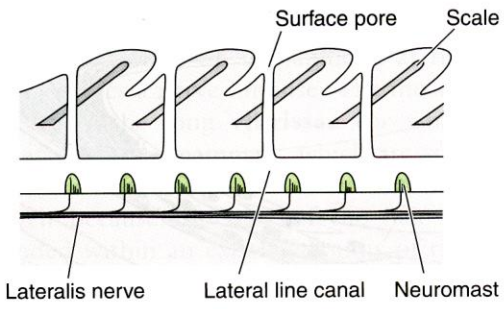

B. Neuromasts in lateral line canal

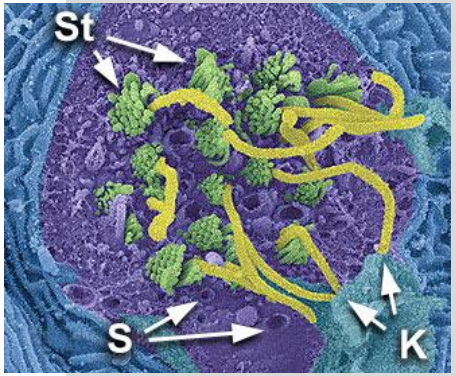

FIGURE 12-8
Neuromast and lateral line canal of a representative teleost. *A*, A neuromast. *B*, A vertical section through the skin and lateral line canal.

Mechanoreceptory – vláskové buňky

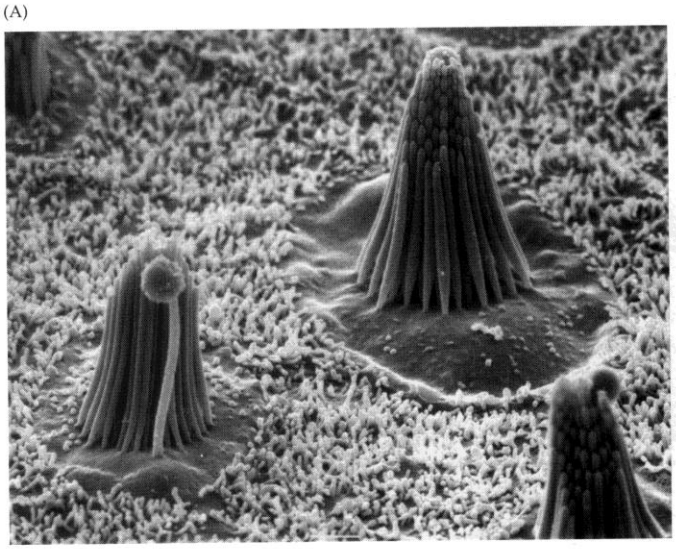

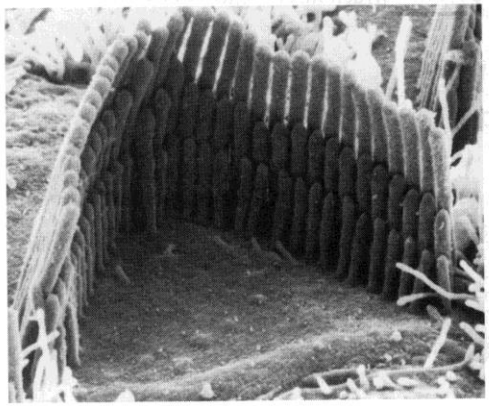

Figure 6.1
Scanning electron micrographs of hair bundles (A) Bullfrog sacculus. The otolithic membrane has been removed. Note the prominent kinocilium with the ball at the top. (B) Hair bundle of an outer hair cell from a mammalian cochlea. (A courtesy of J. A. Assad and D. P. Corey; B from Hackney and Furness, 1995.)

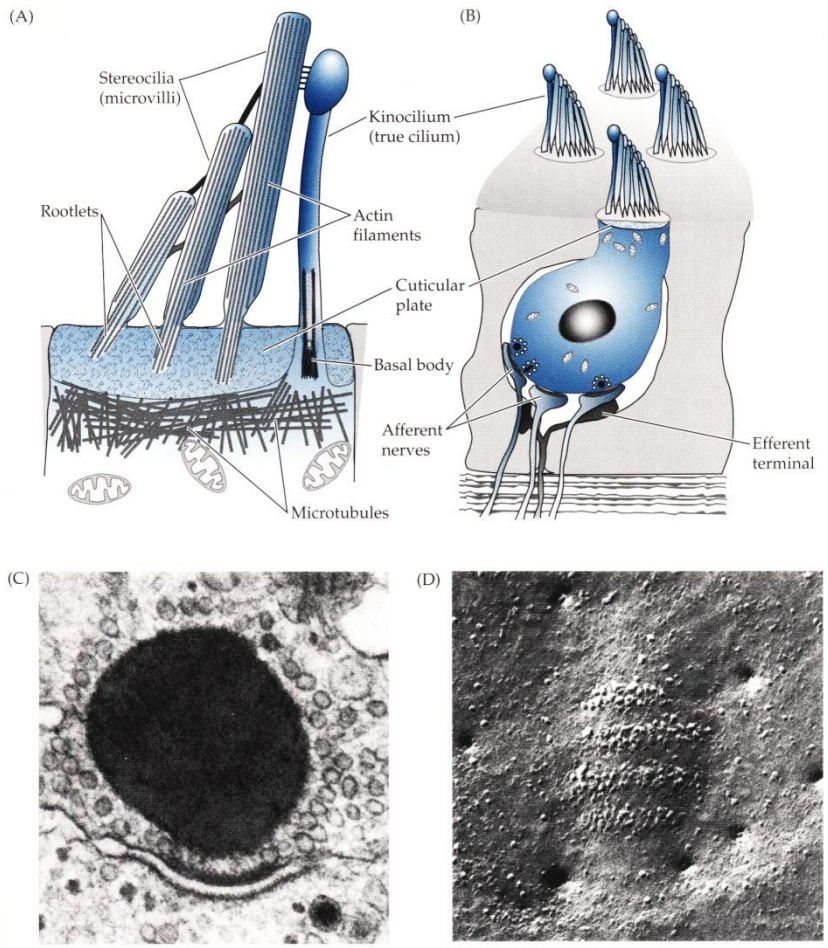

Figure 6.2
Anatomy of hair cell (A) Top of a frog hair cell, showing cuticular plate, stereocilia, and kinocilium. (B) Frog hair cell showing synapses onto afferent nerves and from efferent nerves. (C) Electron micrograph of a hair cell synapse from a frog sacculus. (D) Freeze-fracture micrograph of presynaptic membrane from a frog saccular hair cell. Magnification for C and D 90,000×. (A, B after Pickles 1988; C, D from Roberts et al., 1990.)

Mechanoreceptory – vláskové buňky

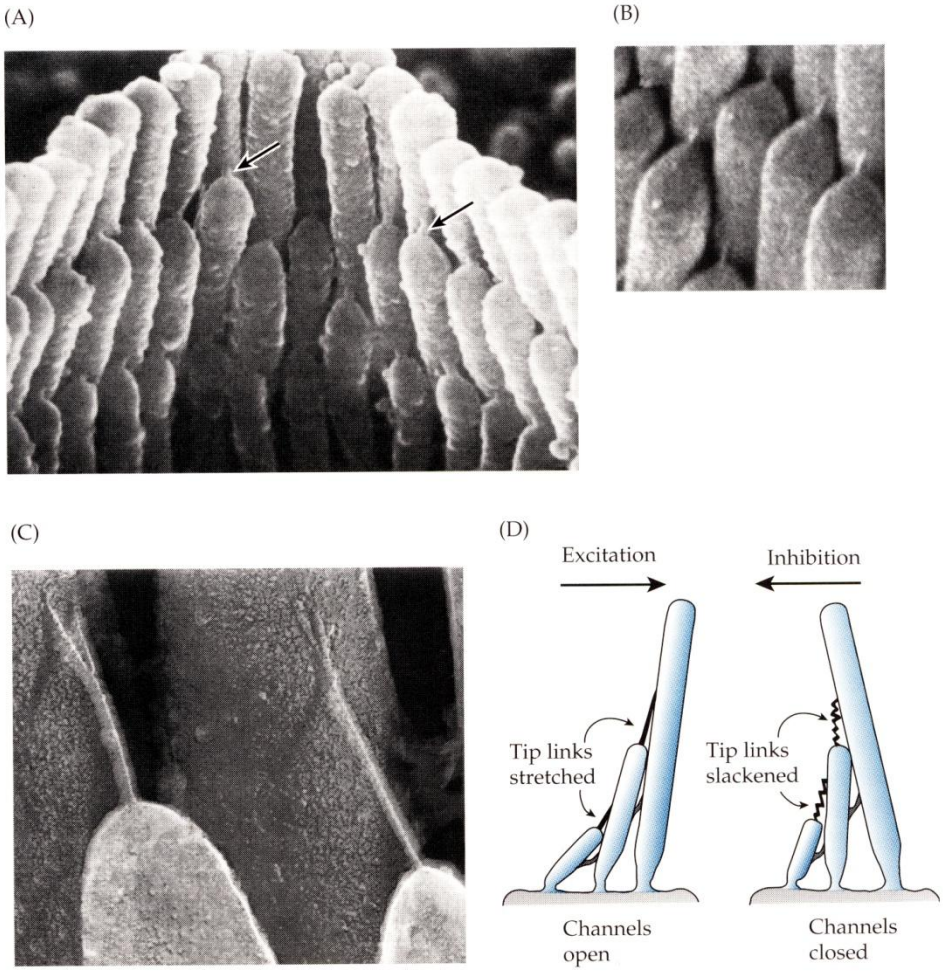

Figure 6.4
Tip links (A) Scanning electron micrograph showing tip links (arrows) from an outer hair cell of guinea pig cochlea. Magnification 24,000×. (B) Field emission scanning electron micrograph of a chicken auditory receptor. Magnification 27,500×. (C) Freeze-etch image of upper insertions of tip links of hair cells from guinea pig cochlea. Magnification 99,000×. (D) Proposed role of tip links in channel gating. (A from Pickles, 1988; B, C from Kachar et al., 2000; D after Pickles, 1984.)

Parts of the ear

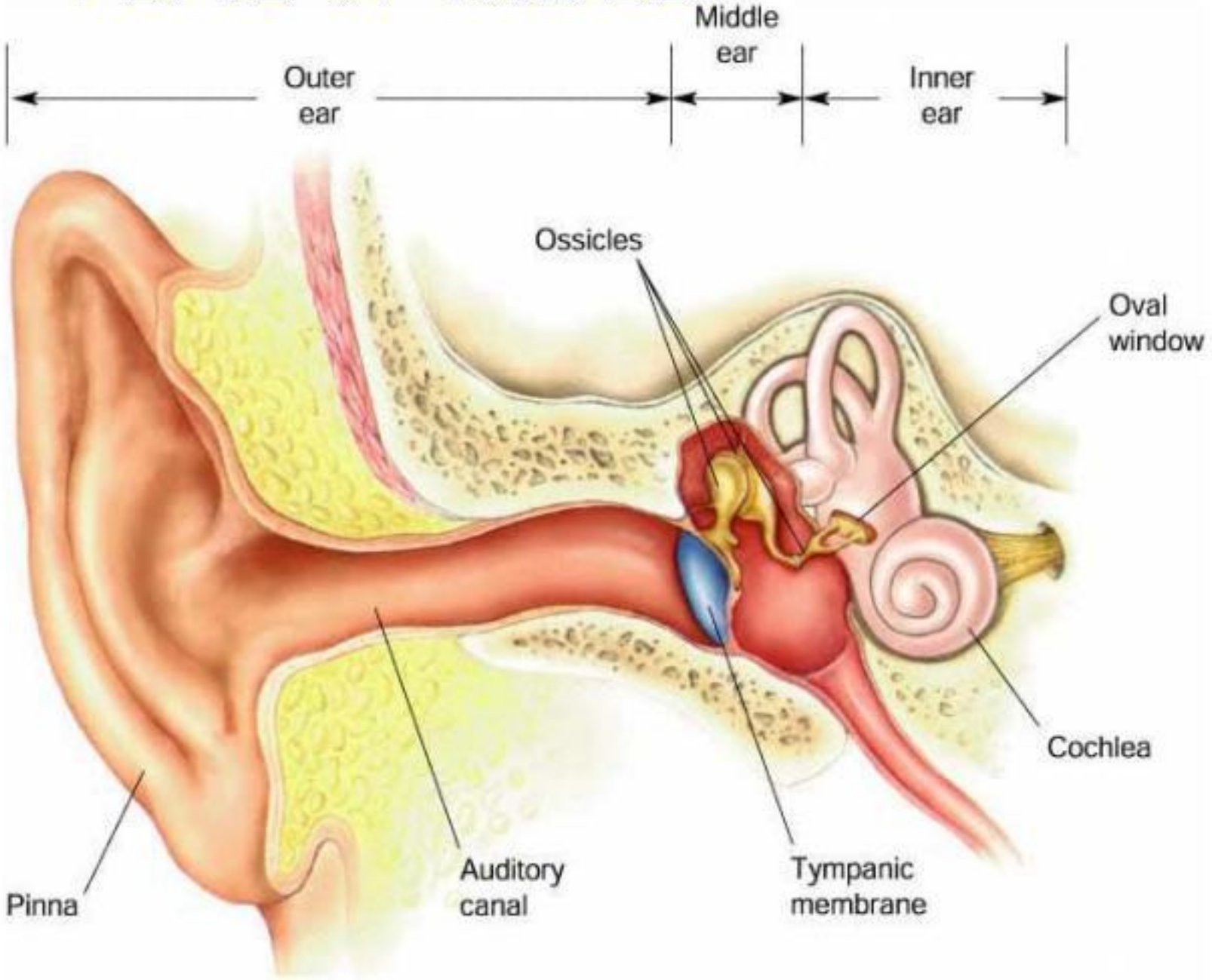

Senzorická výbava raných savců

Vision (cone diversity)	High	High	High	Low
Olfaction (receptor diversity)	Low	Low	?	High
Hearing (high frequency limit)	~1 kHz	~10 kHz	~1 kHz	>10 kHz

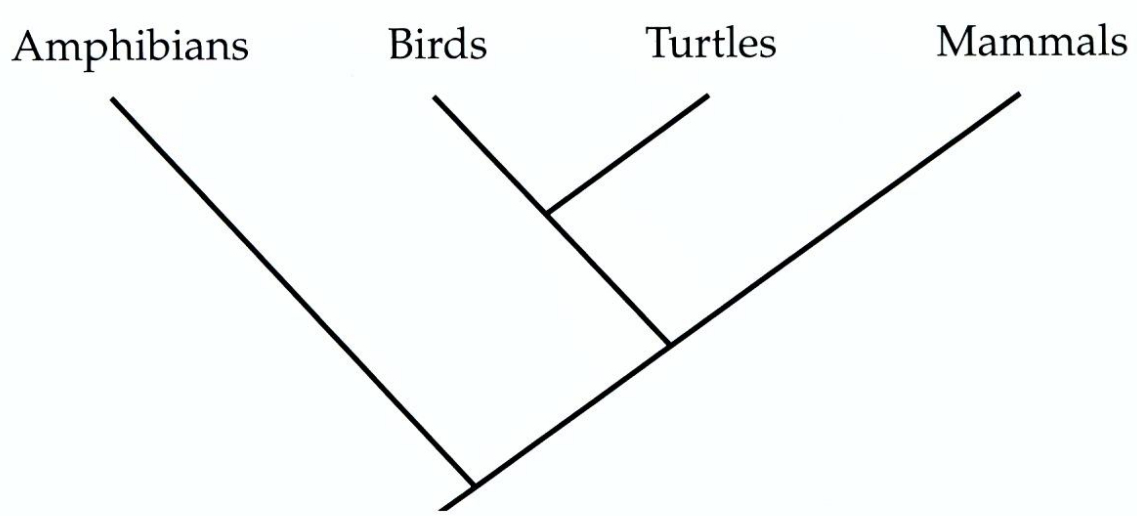

Převodní aparát nižších obratlovců

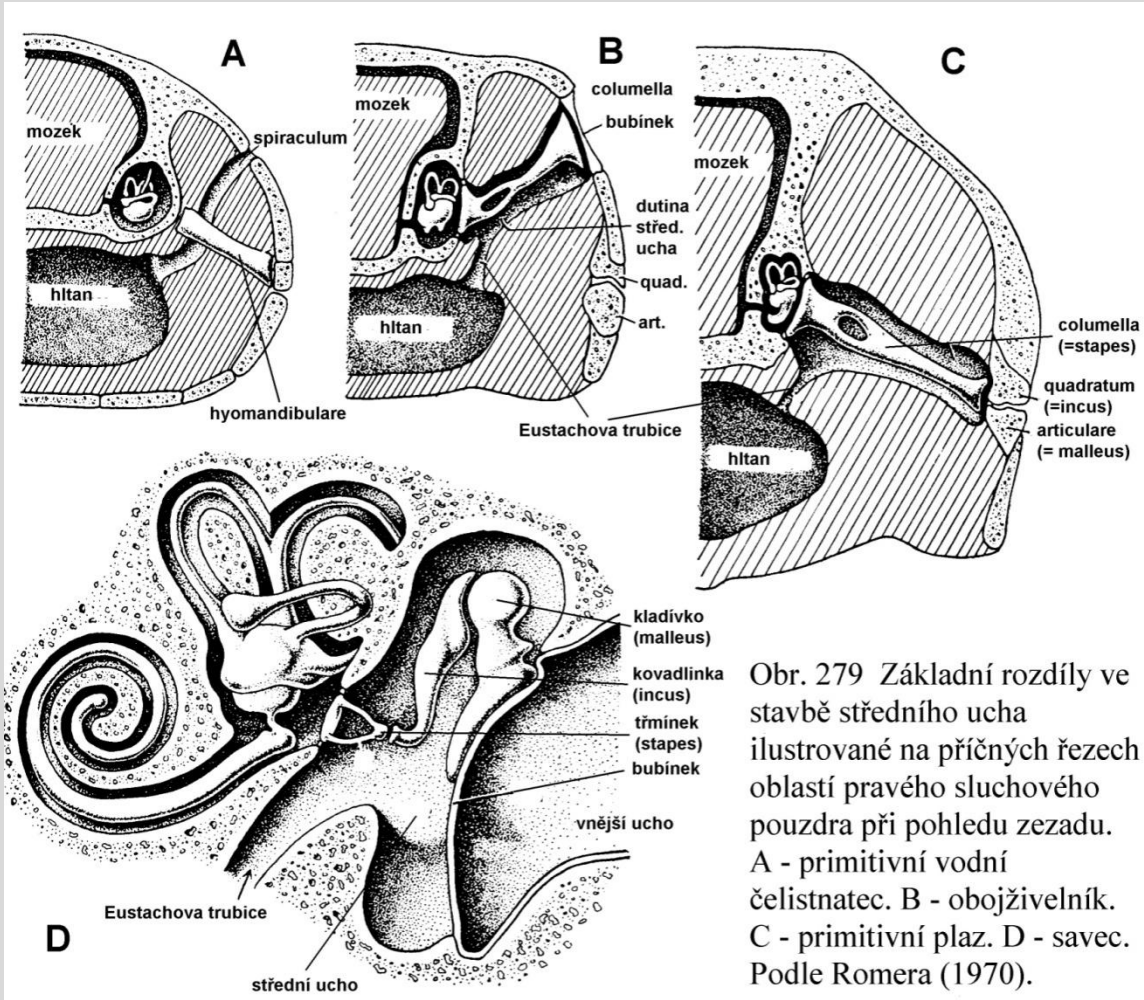

Obr. 279 Základní rozdíly ve stavbě středního ucha ilustrované na příčných řezech oblastí pravého sluchového pouzdra při pohledu zezadu. A - primitivní vodní čelistnatec. B - obojživelník. C - primitivní plaz. D - savec. Podle Romera (1970).

Převodní aparát nižších obratlovců

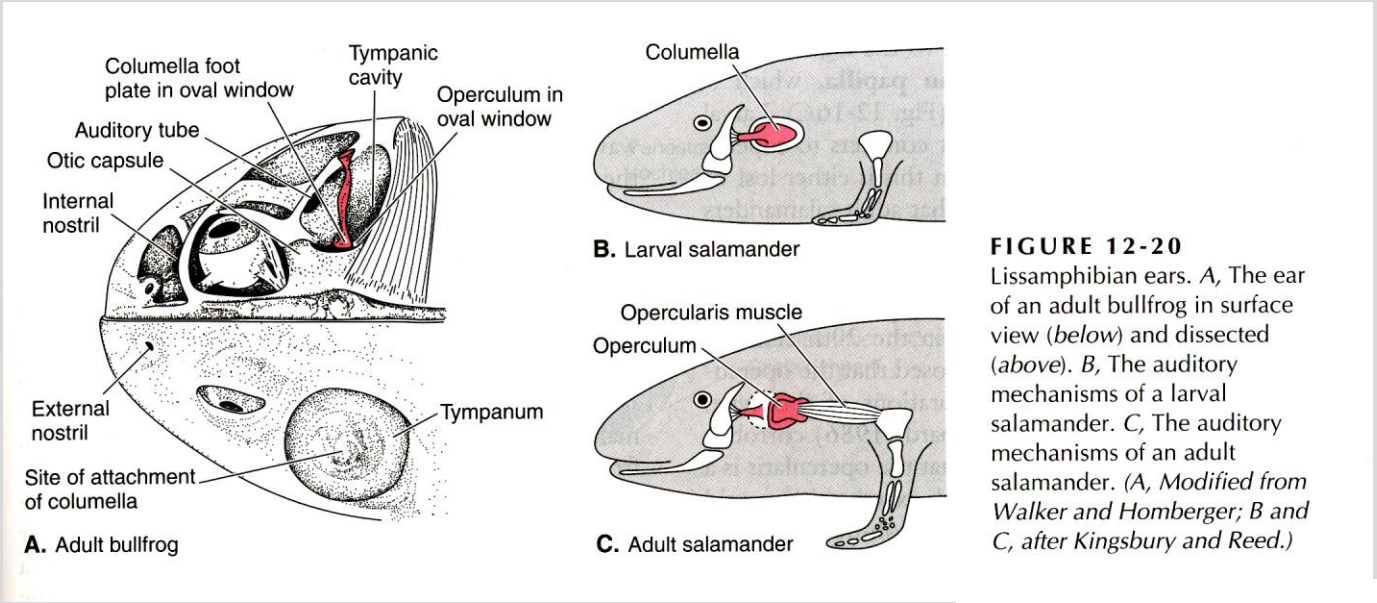

FIGURE 12-20
Lissamphibian ears. *A,* The ear of an adult bullfrog in surface view (*below*) and dissected (*above*). *B,* The auditory mechanisms of a larval salamander. *C,* The auditory mechanisms of an adult salamander. *(A, Modified from Walker and Homberger; B and C, after Kingsbury and Reed.)*

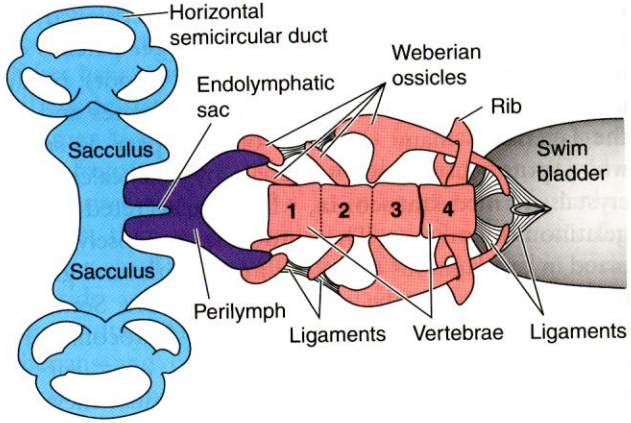

FIGURE 12-17
A dorsal view of the Weberian apparatus of an ostariophysan. *(After Popper.)*

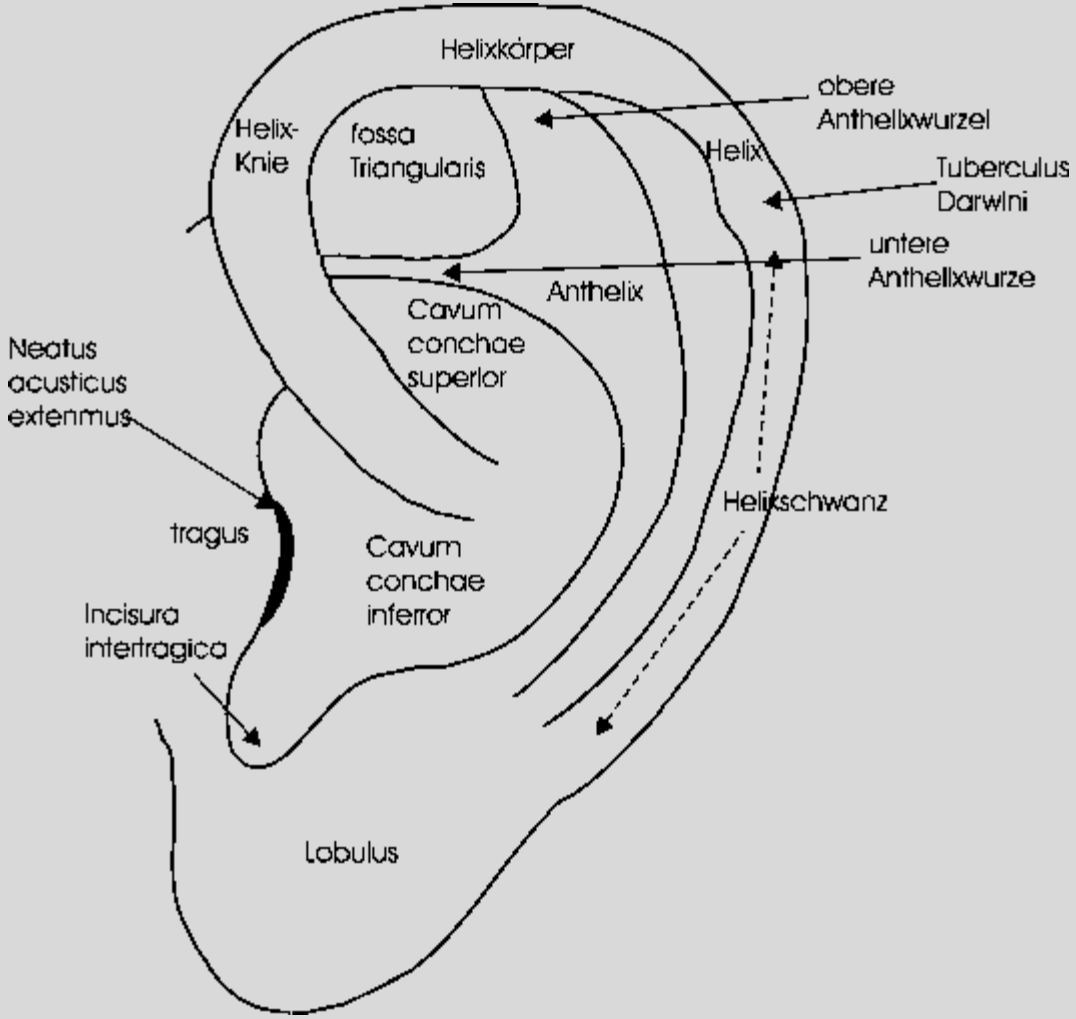
Helixkörper
obere
Anthelixwurzel
Helix-
Knie
fossa
Triangularis
Helix
Tuberculus
Darwini
untere
Anthelixwurze
Anthelix
Cavum
conchae
superior
Neatus
acusticus
externus
Helixschwanz
tragus
Cavum
conchae
inferior
Incisura
intertragica
Lobulus

nerikanische Hasen

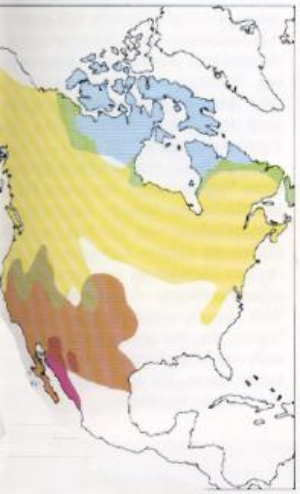

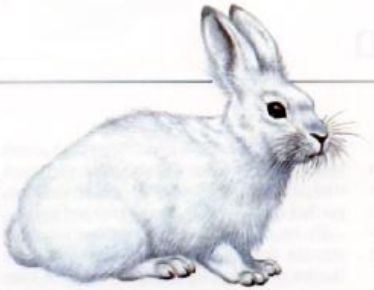

Schneehase (Lepus arcticus)

Vom nördlichsten bis zum südlichsten Teil Nordamerikas begegnen wir einer Abfolge verschiedener Hasenarten. Je weiter nördlich eine Art lebt, desto kürzer sind ihre Ohren und Läufe. Lange Gliedmaßen und Ohren lassen den Körper mehr Wärme verlieren und sind damit in kalten Gebieten von Nachteil.

Schneeschuhhase (Lepus americanus)

Kalifornischer Eselhase (Lepus californicus)

Antilopenhase (Lepus alleni)

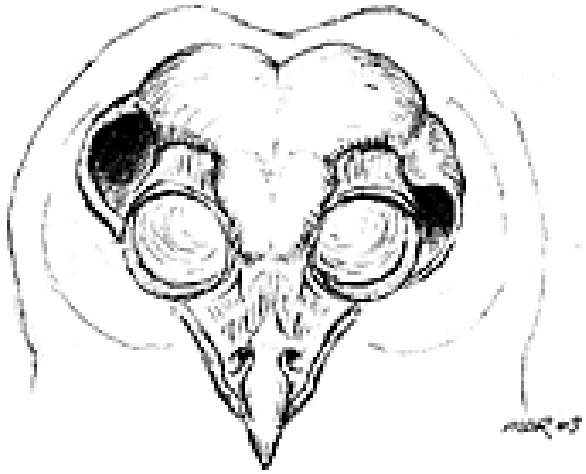

(B)

(C)

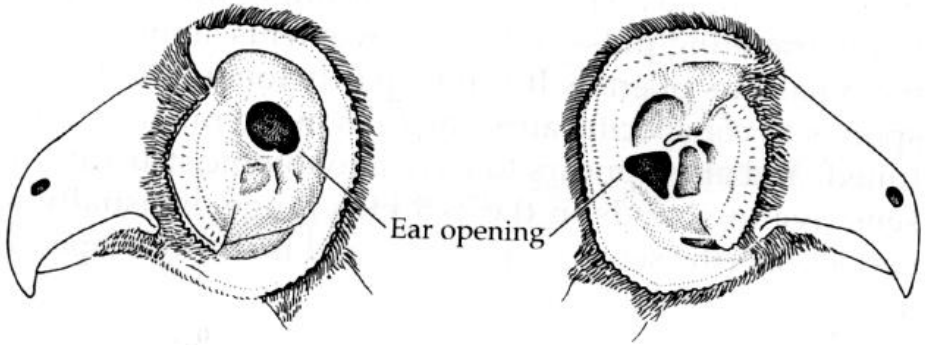

(D)

Přesnost lokalizace: 1° horizontal a vertikal

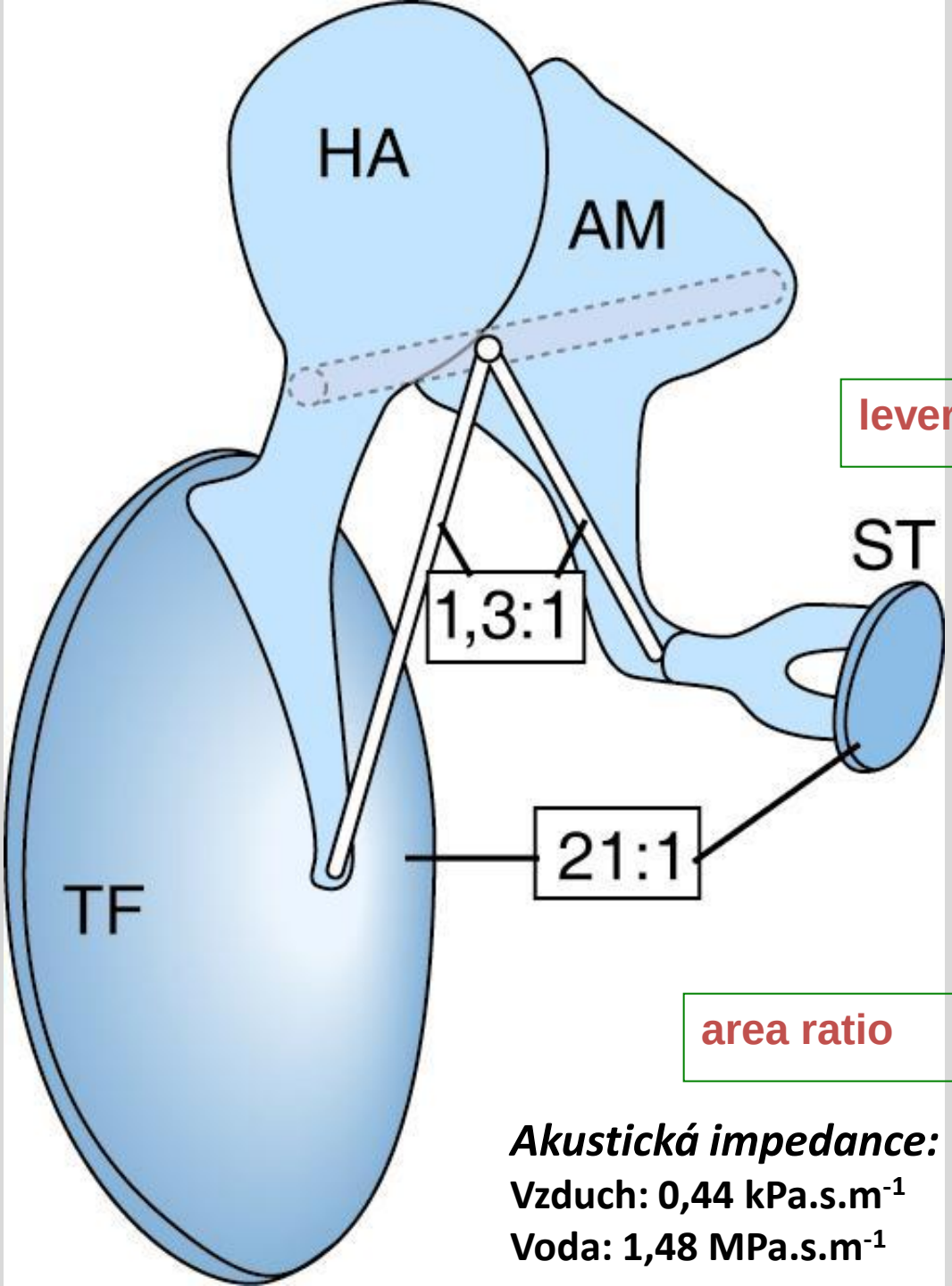

lever ratio

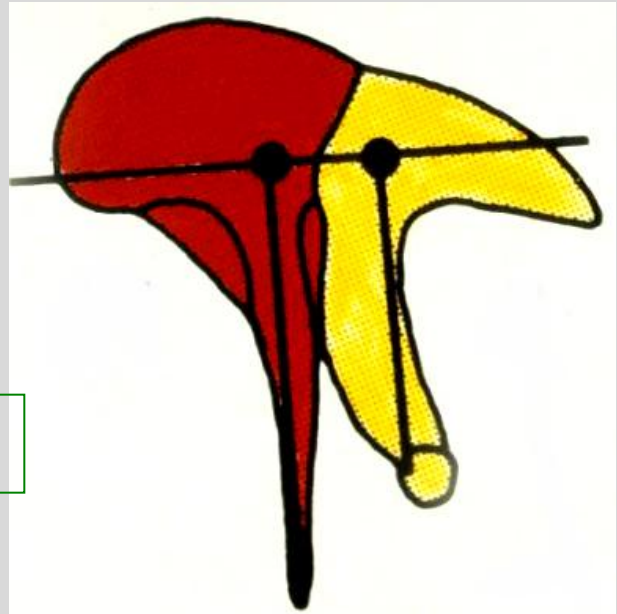

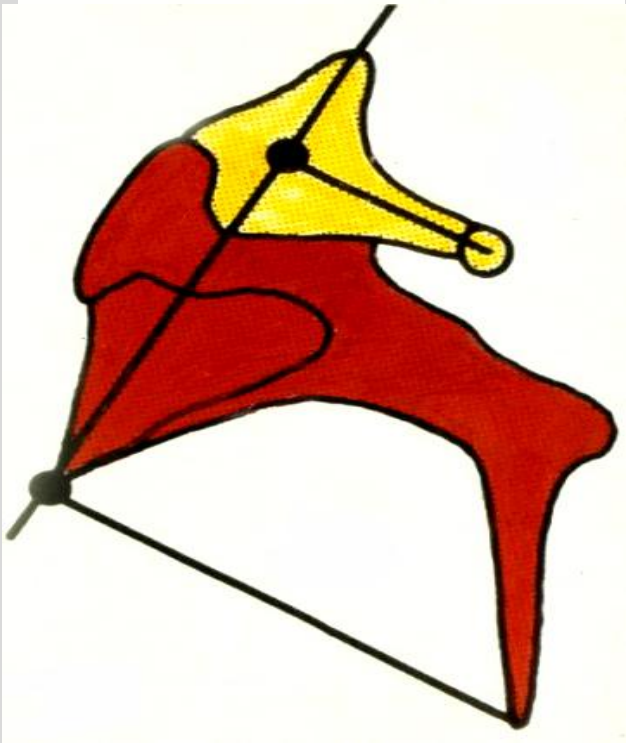

area ratio

Akustická impedance:

Vzduch: 0,44 kPa.s.m^{-1}

Voda: 1,48 MPa.s.m^{-1}

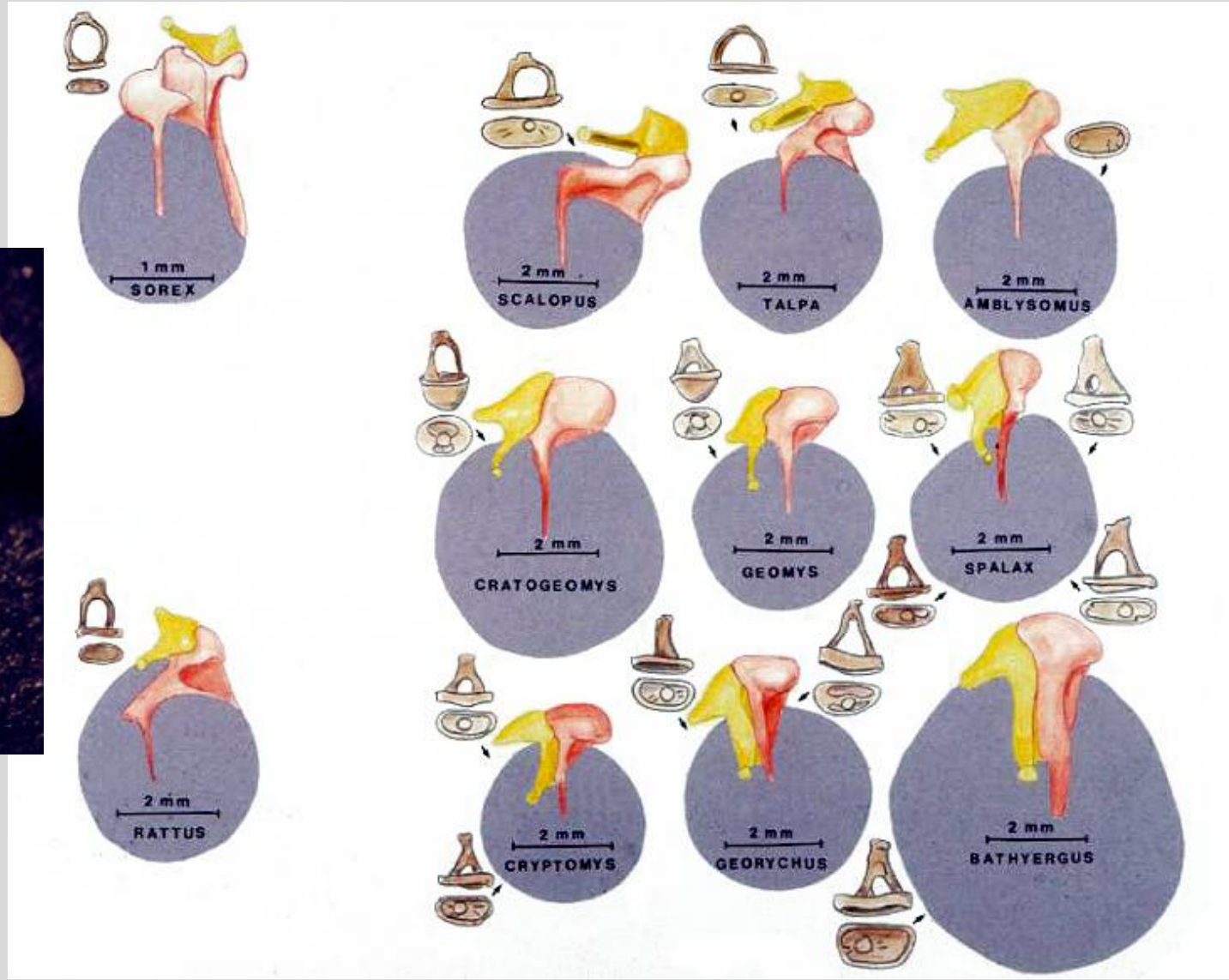
1 mm
SOREX
2 mm
SCALOPUS
2 mm
TALPA
2 mm
AMBLYSOMUS
2 mm
CRATOGEOMYS
2 mm
GEOMYS
2 mm
SPALAX
2 mm
RATTUS
2 mm
CRYPTOMYS
2 mm
GEORYCHUS
2 mm
BATHYERGUS

Vnitřní ucho obratlovců

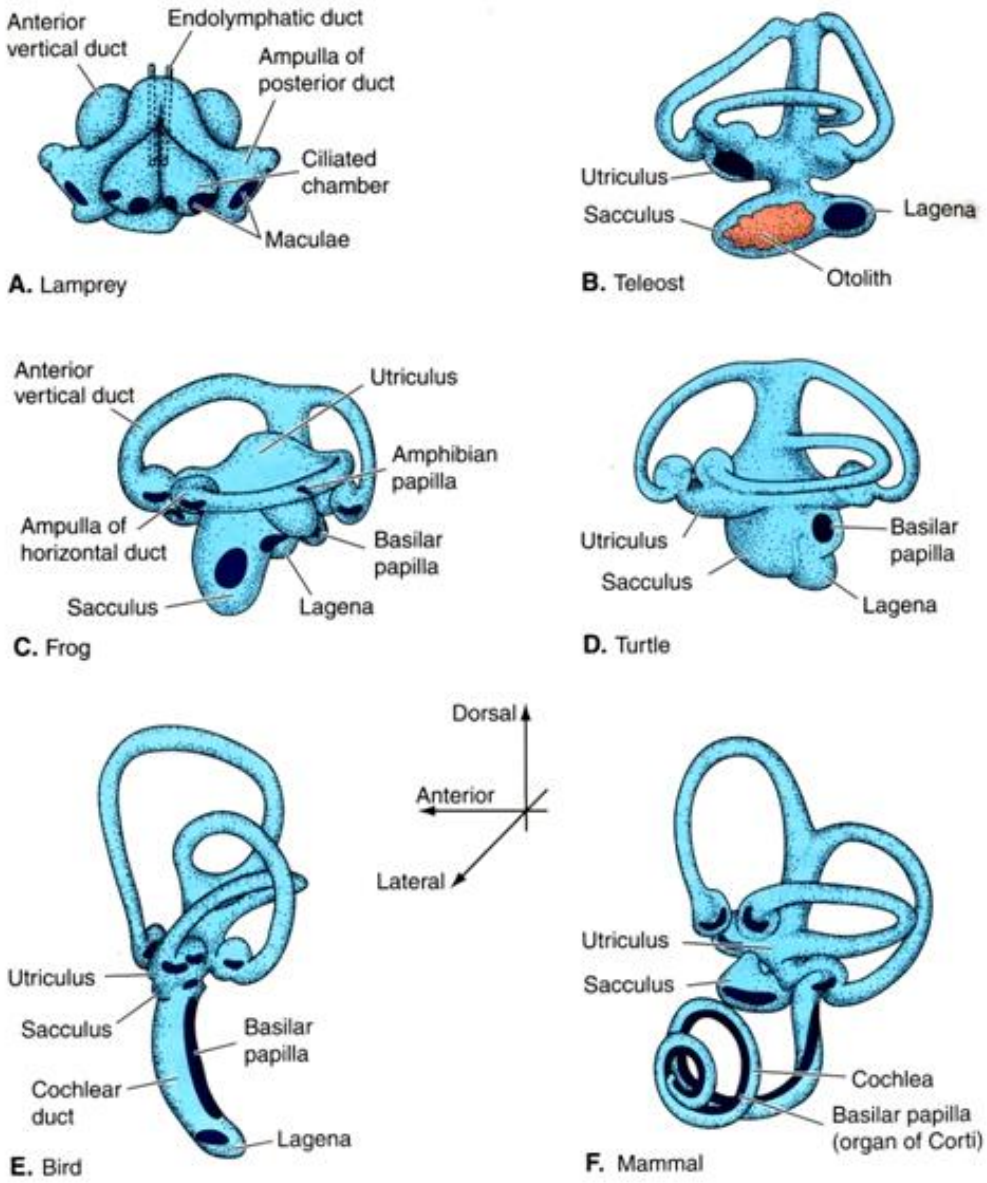

FIGURE 12-16
Lateral views of the labyrinth of representative vertebrates. *A,* A lamprey. *B,* A teleost. *C,* A frog. *D,* A turtle. *E,* A bird. *F,* A mammal. *(A and C, After Retzius.)*

Vnitřní ucho

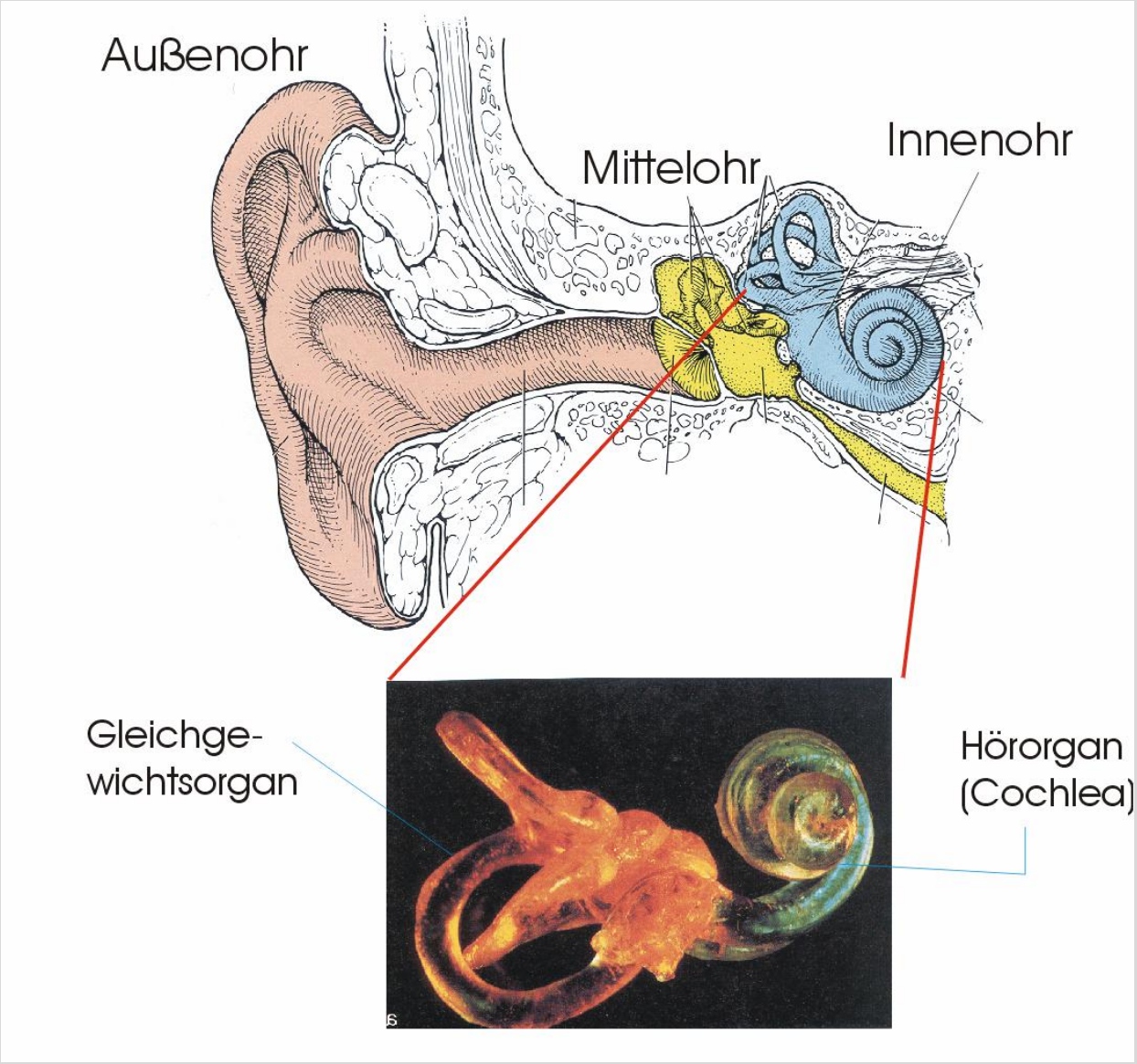

Vnitřní ucho

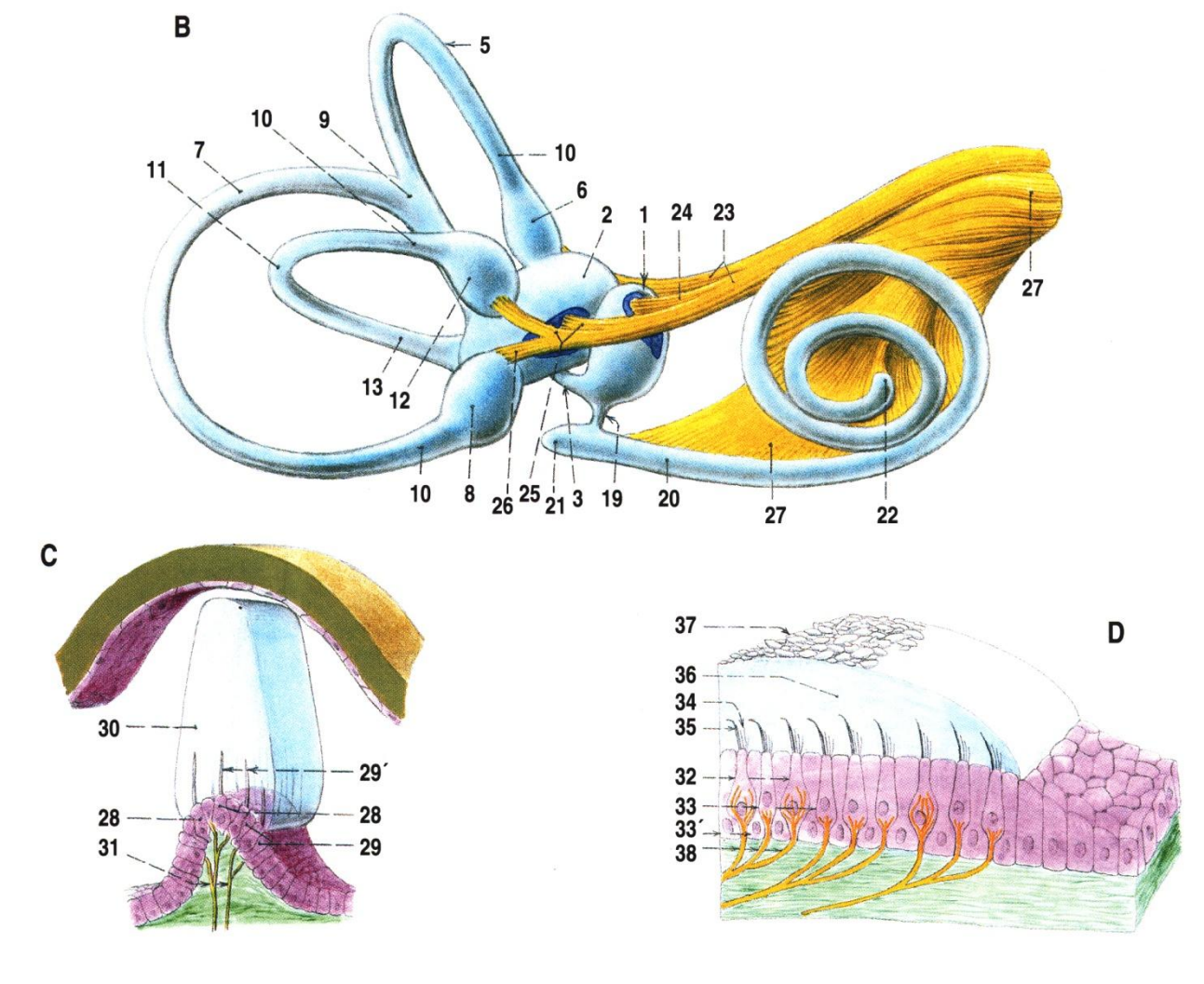

Cochlea

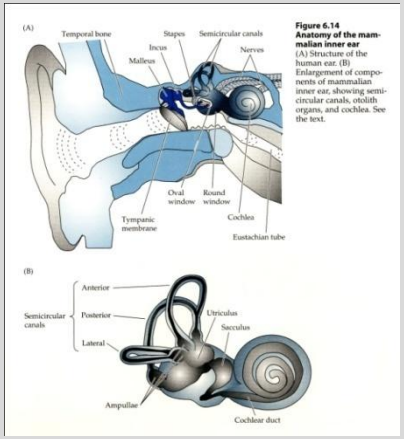

Figure 6.14
Anatomy of the mammalian inner ear
(A) Structure of the human ear. (B) Enlargement of components of mammalian inner ear, showing semicircular canals, otolith organs, and cochlea. See the text.

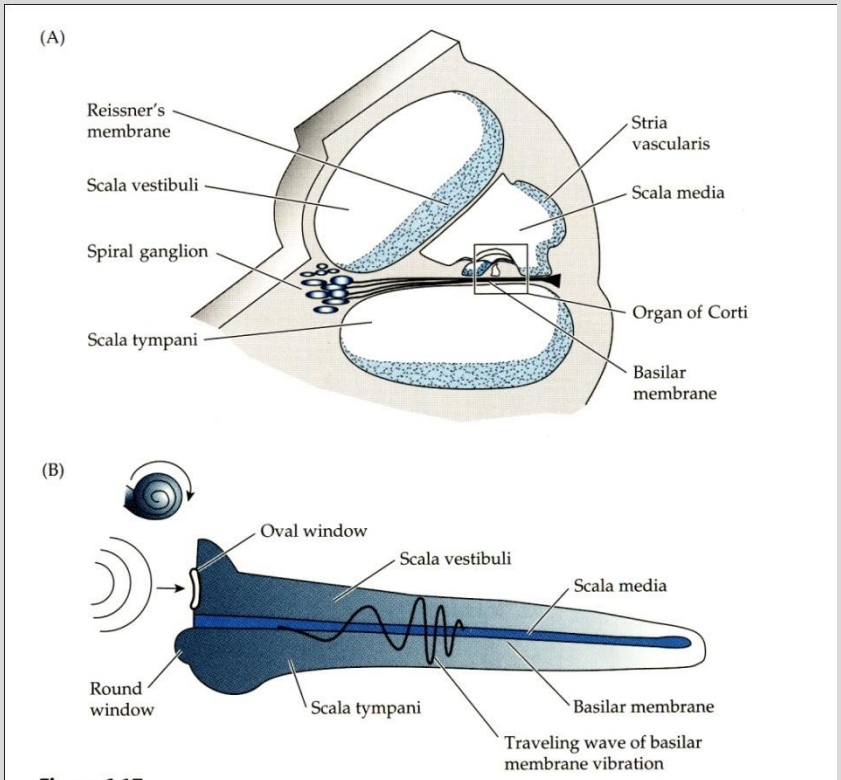

Figure 6.17
The mammalian cochlea (A) Cross section of the cochlea. (B) The cochlea imagined as uncoiled to illustrate motion of the basilar membrane. Pressure on the oval window is communicated through the fluids of the scala vestibuli and scala tympani to the round window, producing a traveling wave of basilar membrane oscillation. (A after Pickles, 1988; B after Nobili et al., 1998.)

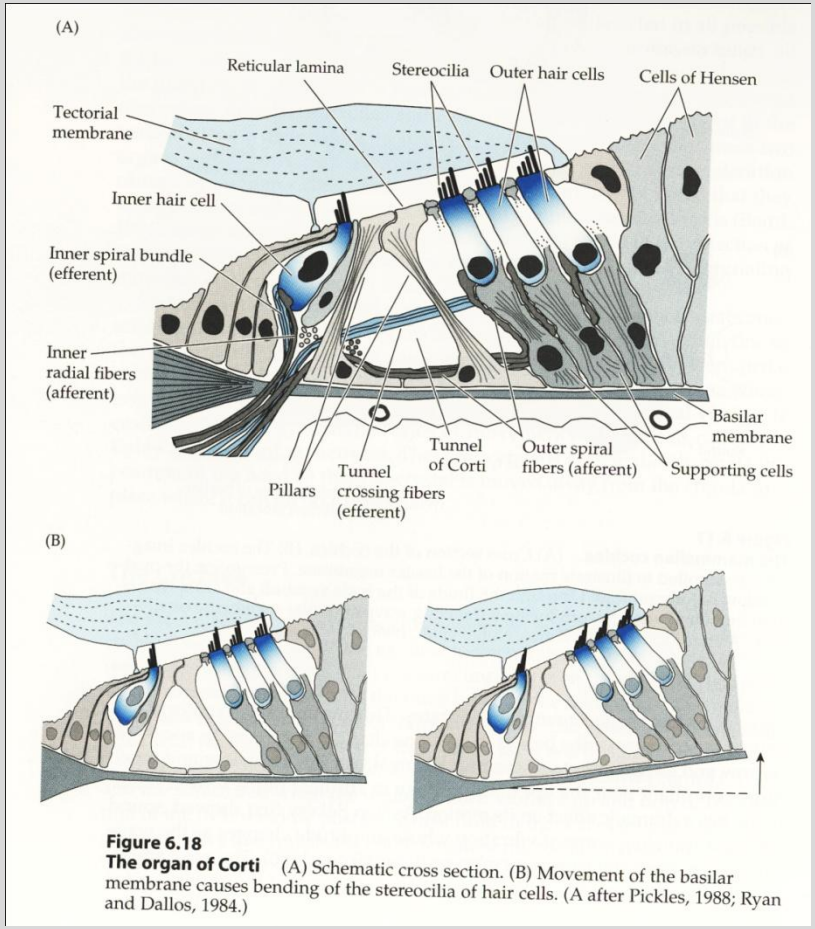

Figure 6.18
The organ of Corti (A) Schematic cross section. (B) Movement of the basilar membrane causes bending of the stereocilia of hair cells. (A after Pickles, 1988; Ryan and Dallos, 1984.)

Cochlea savců

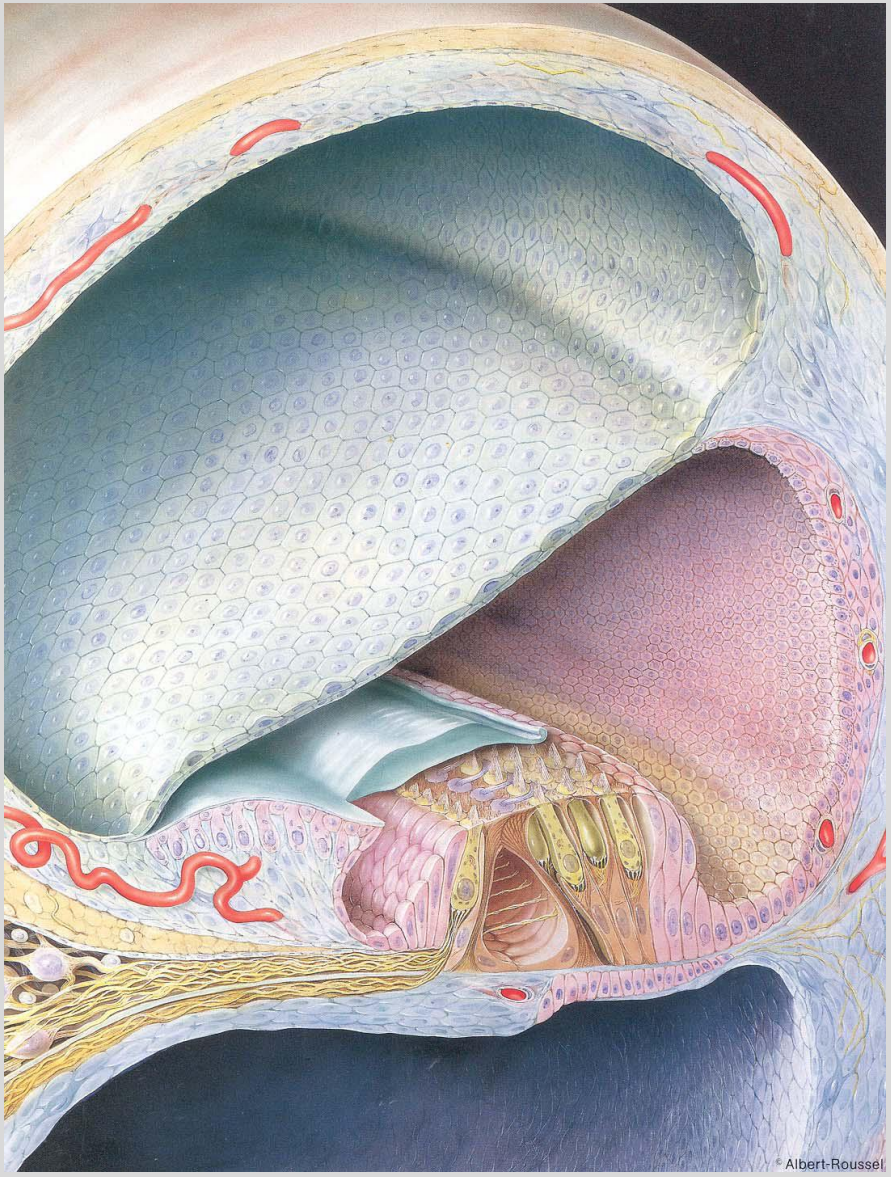

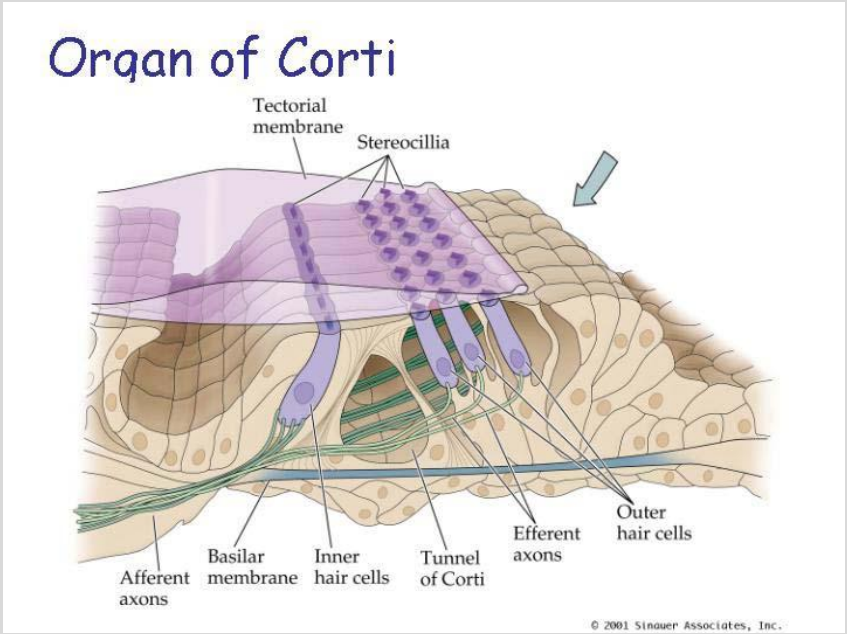

Cochlea savců

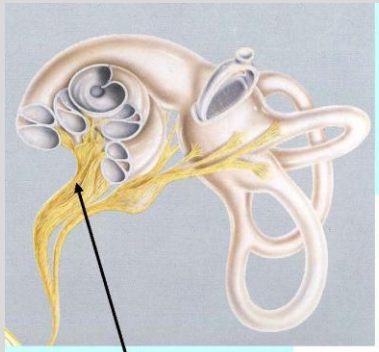

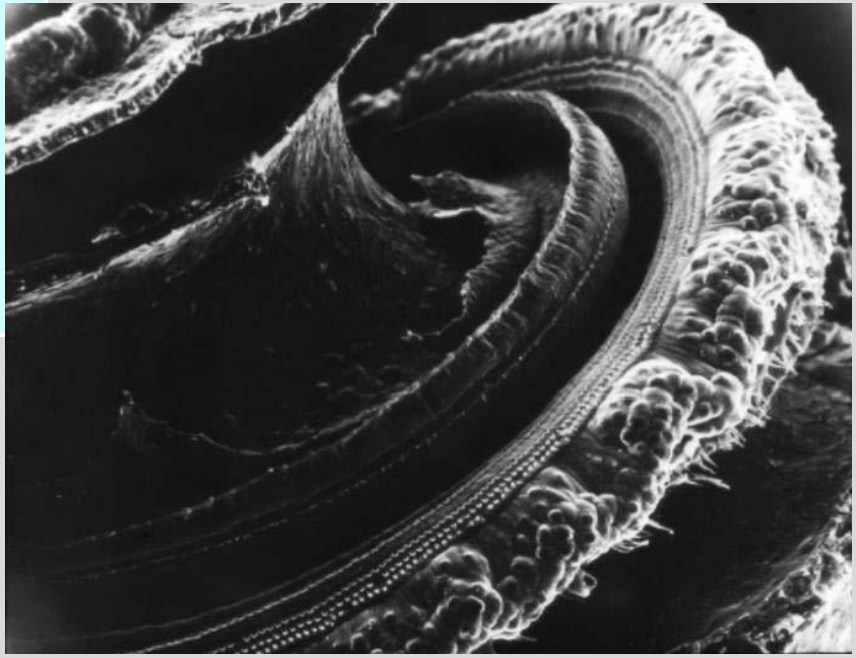

Tonotopické uspořádání

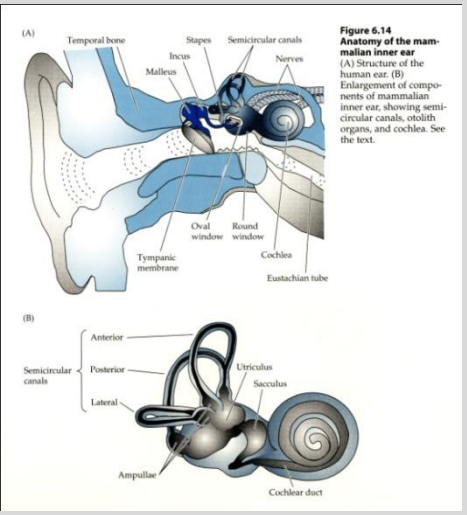

Figure 6.14
Anatomy of the mammalian inner ear
(A) Structure of the human ear. (B) Enlargement of components of mammalian inner ear, showing semicircular canals, otolith organs, and cochlea. See the text.

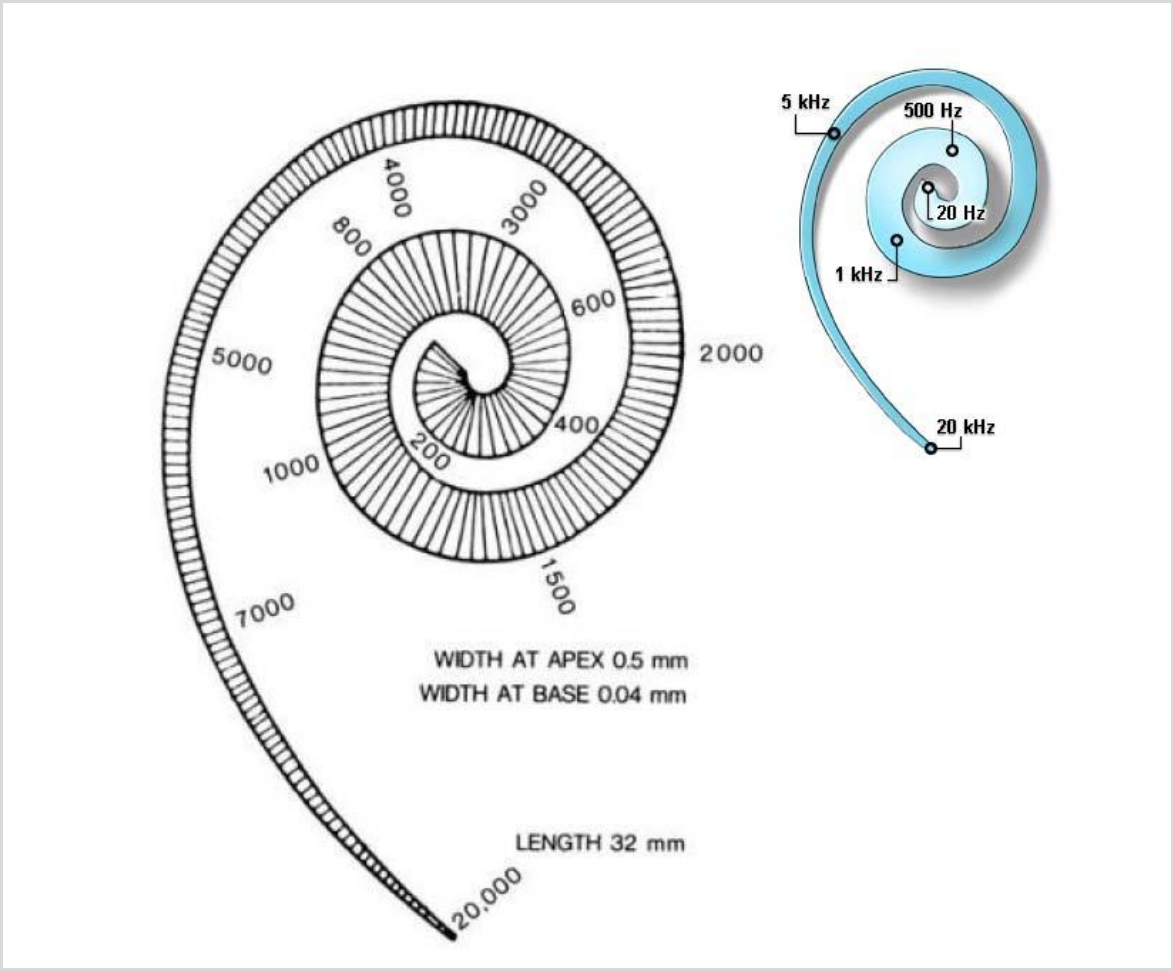

Cochlea savců

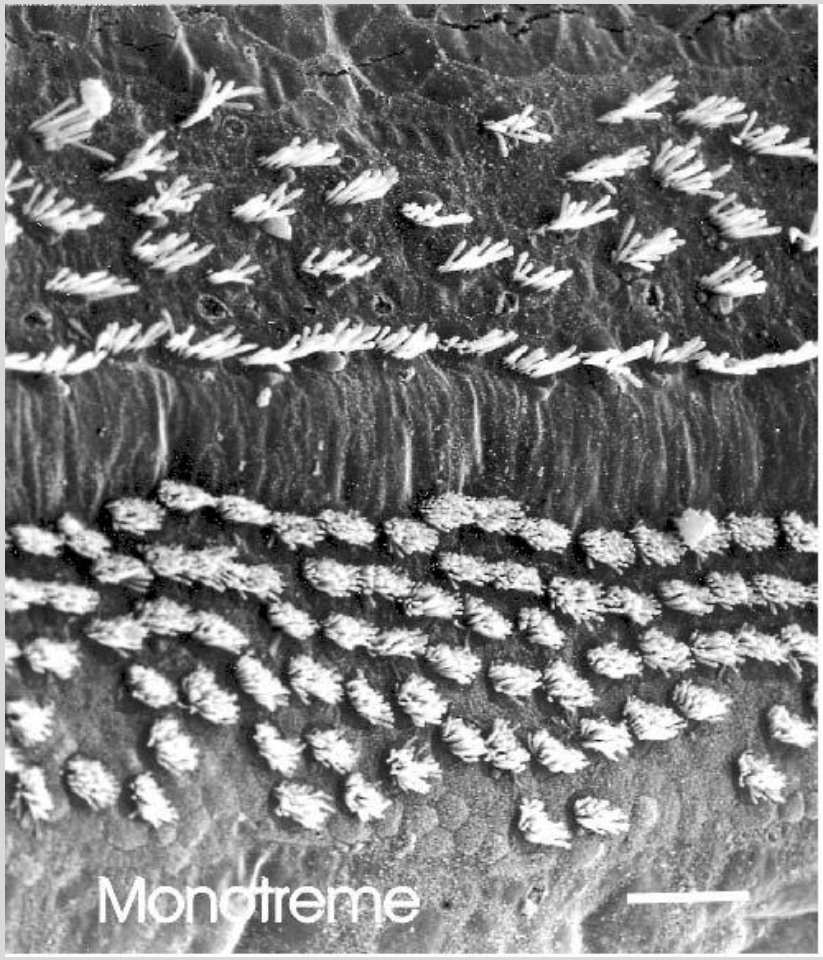

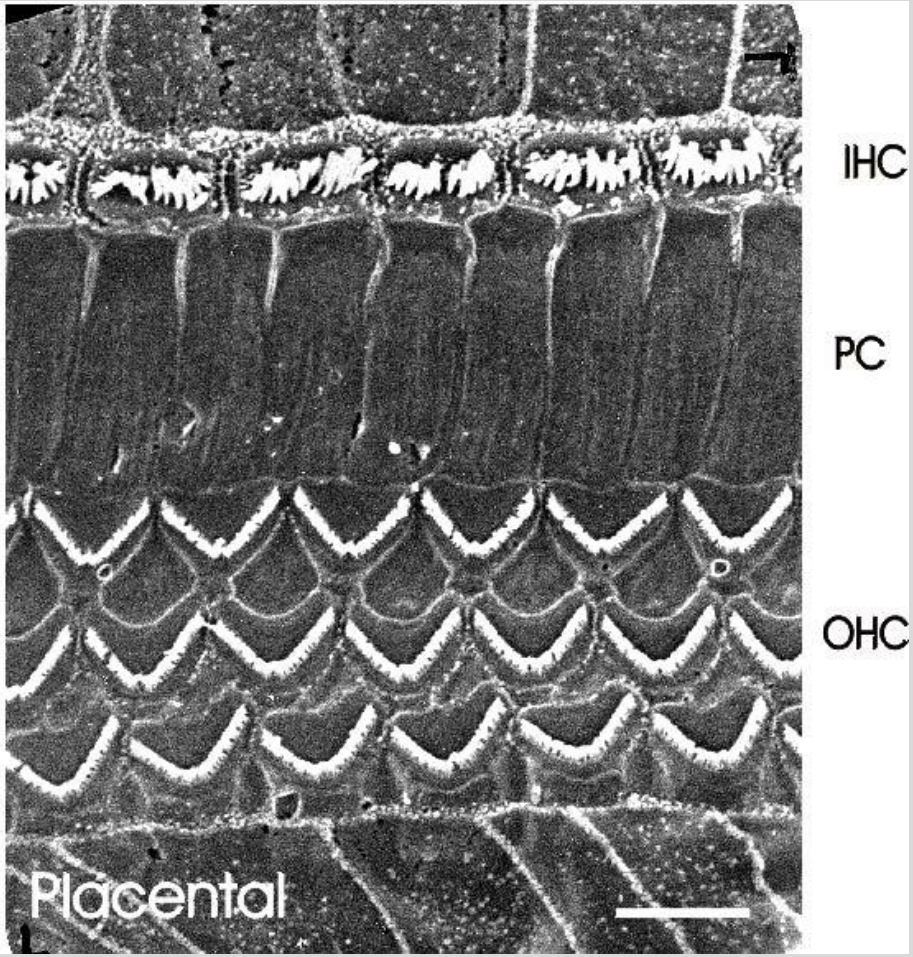

Vestibulární systém

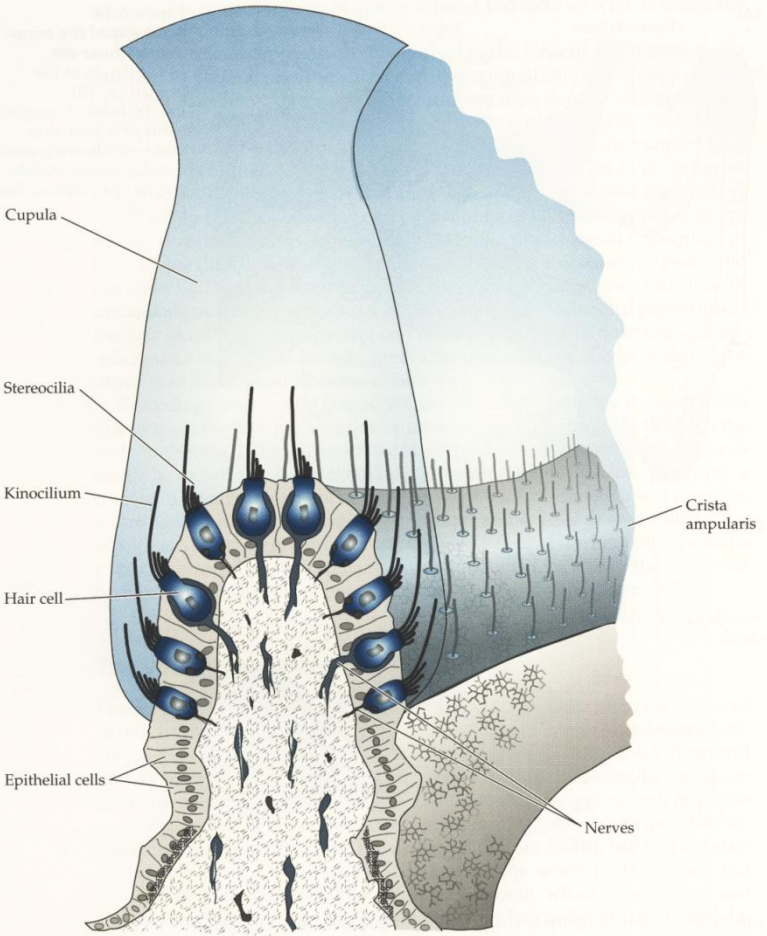

Figure 6.15
Hair cells of the mammalian semicircular canal in the crista ampularis of the ampulla Stereocilia of hair cells are embedded in gelatinous cupula and are stimulated when cupula is moved by movement of fluid in the semicircular canal. (After Wersäll and Bagger-Sjöbäck, 1974.)

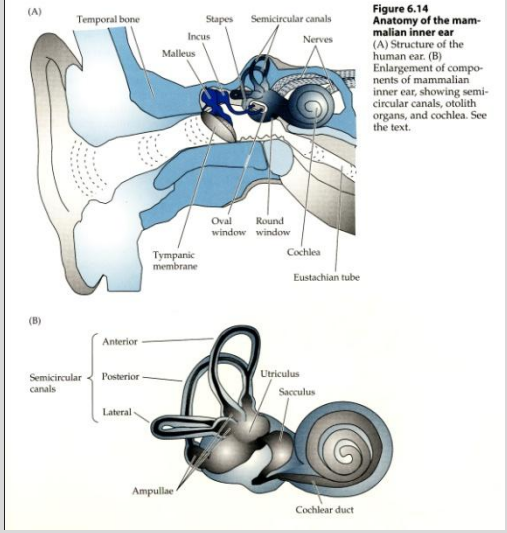

Figure 6.14
Anatomy of the mammalian inner ear (A) Structure of the human ear. (B) Enlargement of components of mammalian inner ear, showing semicircular canals, otolith organs, and cochlea. See the text.

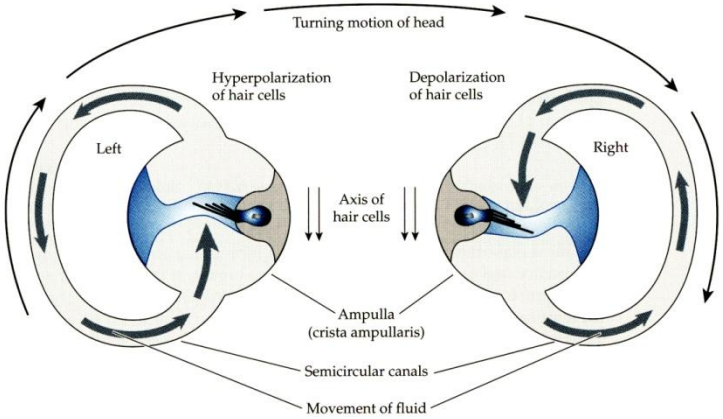

Figure 6.16
Stimulation of hair cells of the semicircular canals by head movement Turning the head laterally to the right produces inertial fluid movement in the horizontally oriented semicircular canals on either side of the head, so that hair cells on the right are depolarized, and those on the left are hyperpolarized.

Specializované termoreceptory – vnímání infračerveného světla

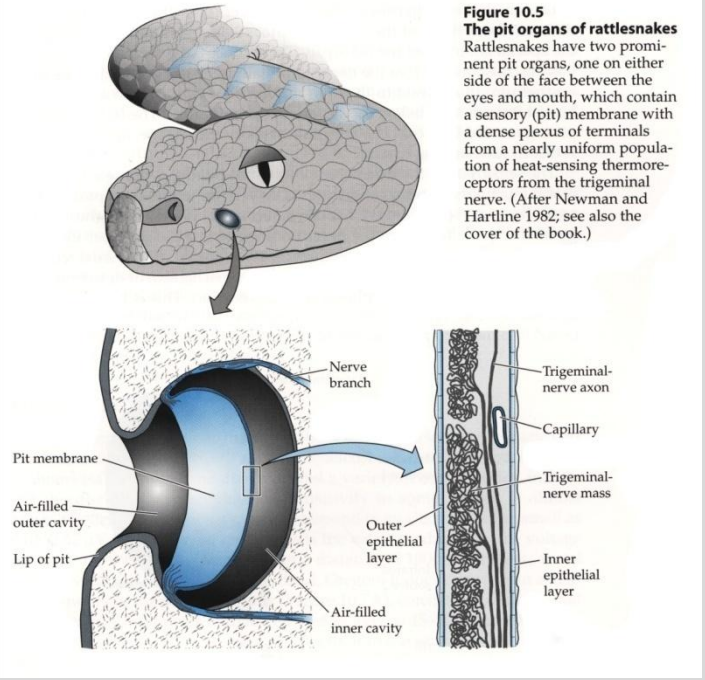

Figure 10.5
The pit organs of rattlesnakes Rattlesnakes have two prominent pit organs, one on either side of the face between the eyes and mouth, which contain a sensory (pit) membrane with a dense plexus of terminals from a nearly uniform population of heat-sensing thermoreceptors from the trigeminal nerve. (After Newman and Hartline 1982; see also the cover of the book.)

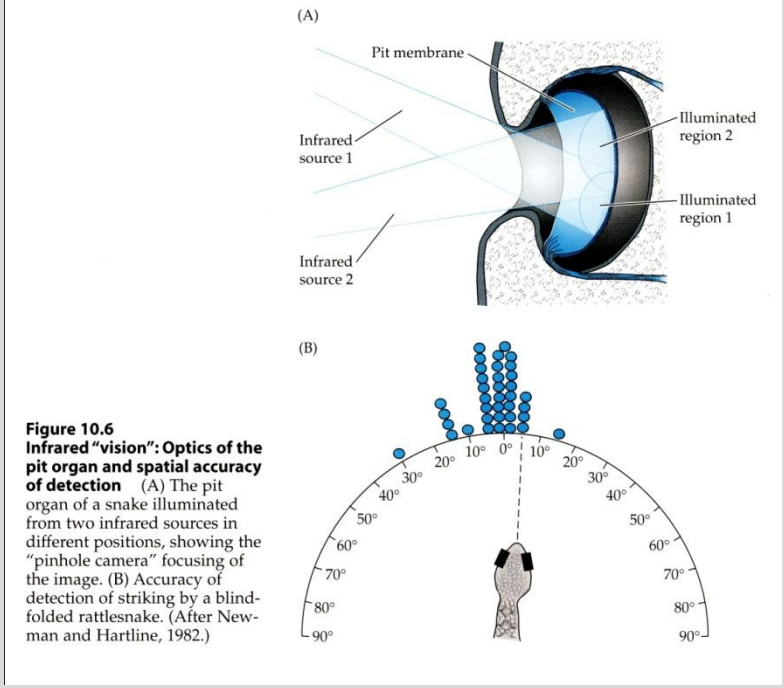

Figure 10.6
Infrared "vision": Optics of the pit organ and spatial accuracy of detection (A) The pit organ of a snake illuminated from two infrared sources in different positions, showing the "pinhole camera" focusing of the image. (B) Accuracy of detection of striking by a blindfolded rattlesnake. (After Newman and Hartline, 1982.)

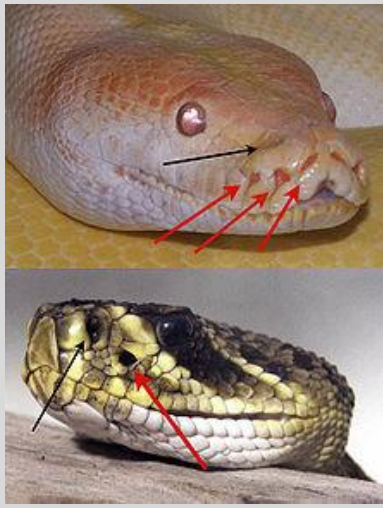

Crotalinae – chřestýšovití
Boidae – hroznýšovití
Phytonidae – krajtovití

Figure 10.4
Extracellular recording of action potentials from heat-sensitive fibers of facial pits in the python *Morelia spilotes* Responses to warming produced by the light of a flashlight (A) and cooling produced by placing a cold object in front of the facial pits (B). Contrast is reversed. Time course of stimuli indicated by blue bars. (From Warren and Proske, 1968.)

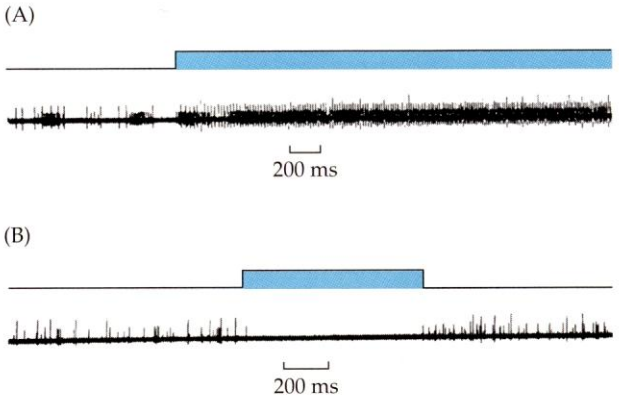

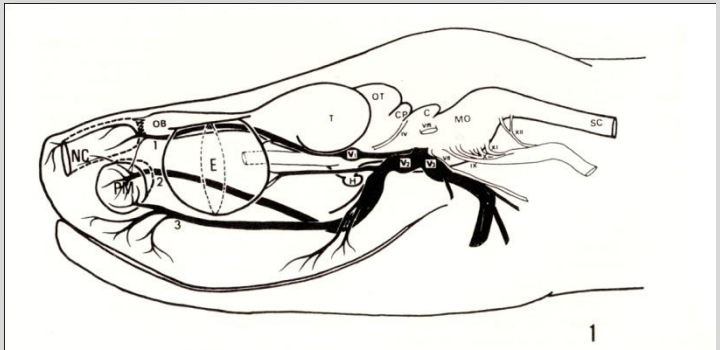

Fig. 1. Schematic drawing of the head of *Agkistrodon blomhoffi brevicaudus*, showing the distribution of the trigeminal nerve branches and ganglia. C, cerebellum; CP, colliculus posterior; E, eye; H, hypophysis; MO, medulla oblongata; NC, nasal chamber; OB, olfactory bulb; OT, optic tectum; PM, pit membrane; SC, spinal cord; T, telencephalon; 1, ophthalmic nerve; 2, deep branch of maxillary nerve; 3, superficial branch of maxillary nerve; IV, trochlear nerve; V_1, ophthalmic ganglion; V_2 and V_3, maxillo-mandibular ganglion; VII, facial nerve; IX, glossopharyngeal nerve; X, vagus nerve; XI, accessory nerve; XII, hypoglossal nerve.

Elektroreceptory postranní čáry

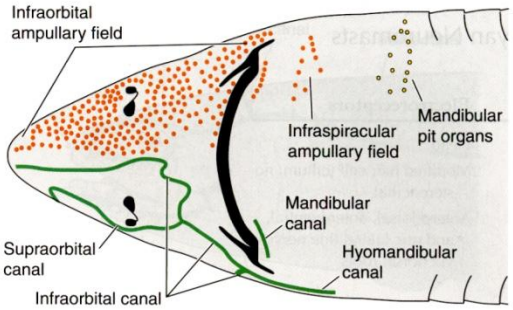

A. Ventral view of a shark head

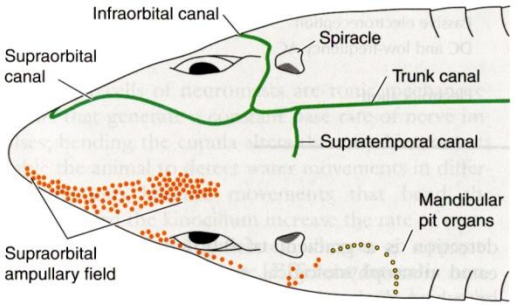

B. Dorsal view of a shark head

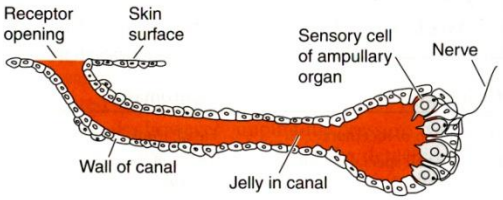

C. Anatomy of an individual ampullary organ of a shark

FIGURE 12-11
Electroreceptive organs of sharks and coelacanths. *A,* Ventral view showing the distribution of the lateral line and ampullary organs on the head of a shark. *B,* Dorsal view of the lateral line and ampullary organs on the head of a shark. *C,* Anatomy of an individual ampullary organ

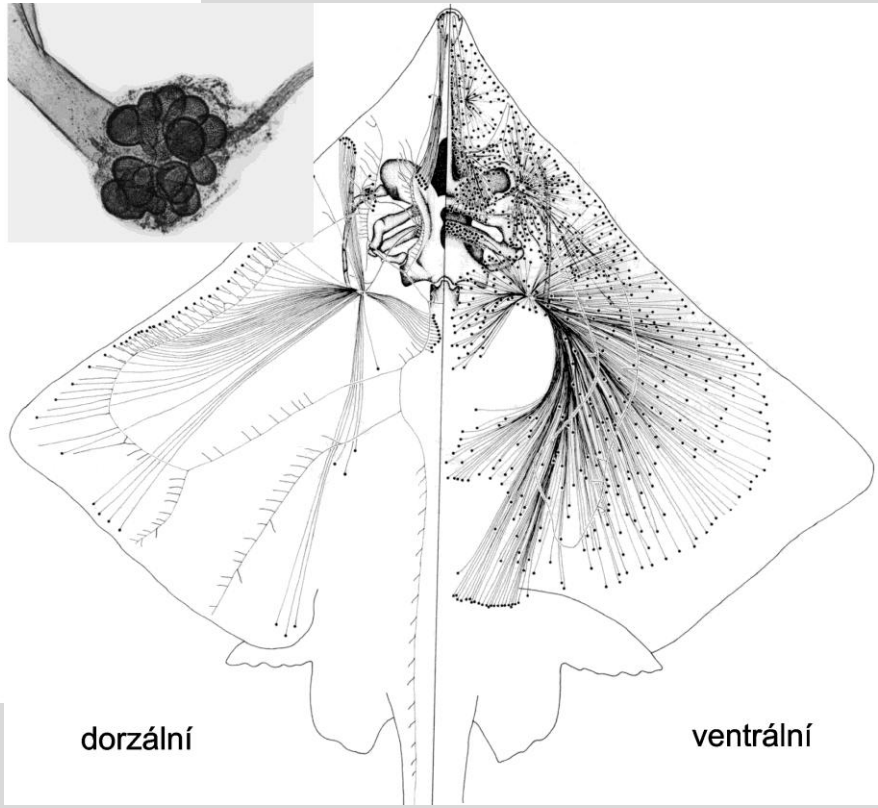

Evoluce elektrorecepce

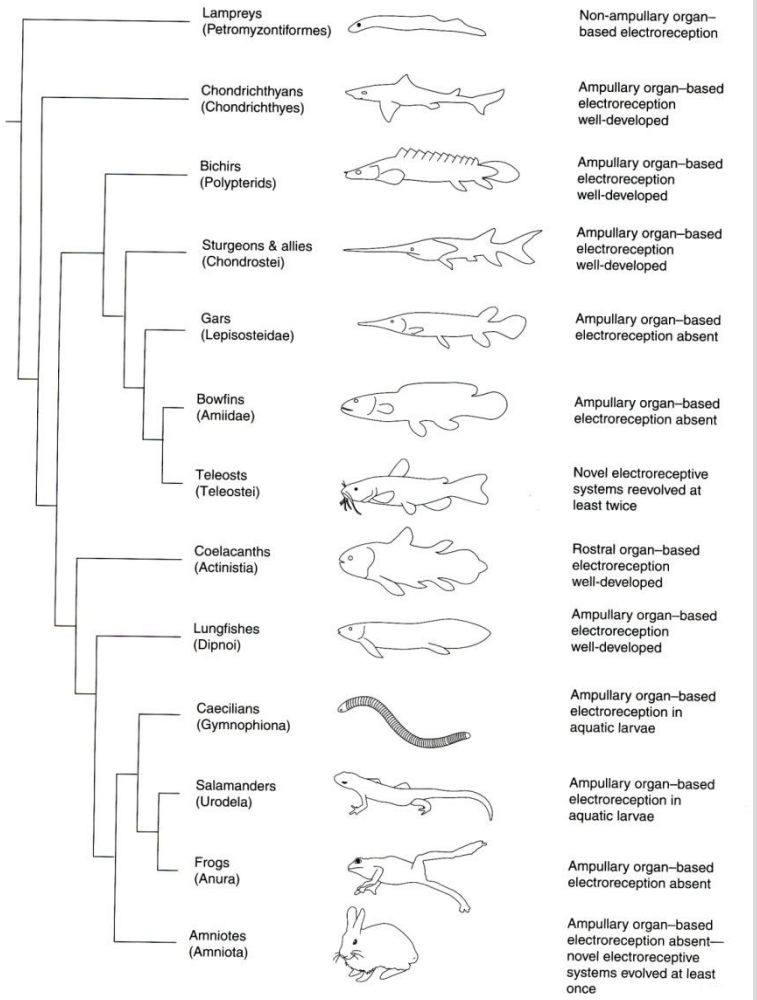

FIGURE 12-13
Cladogram of electroreception. Ampullary electroreception was independently lost in neopterygians (the group of actinopterygian fishes that includes gars, bowfins, and teleosts), frogs, and amniotes. Electroreception re-evolved at least twice in teleosts and at least once in amniotes.

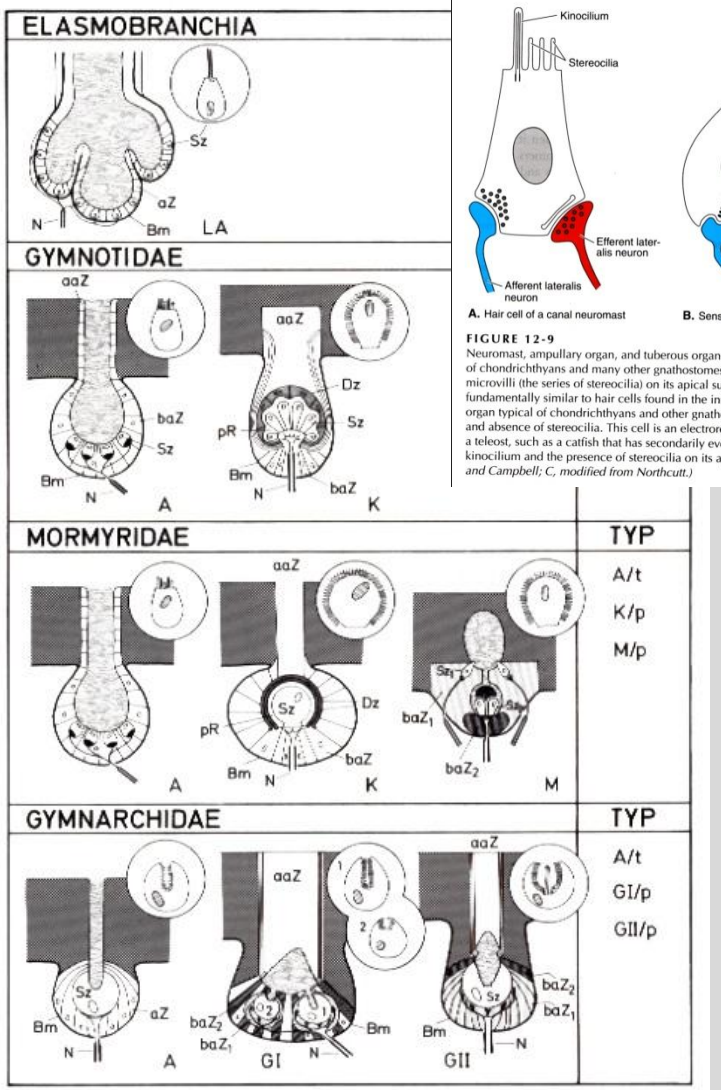

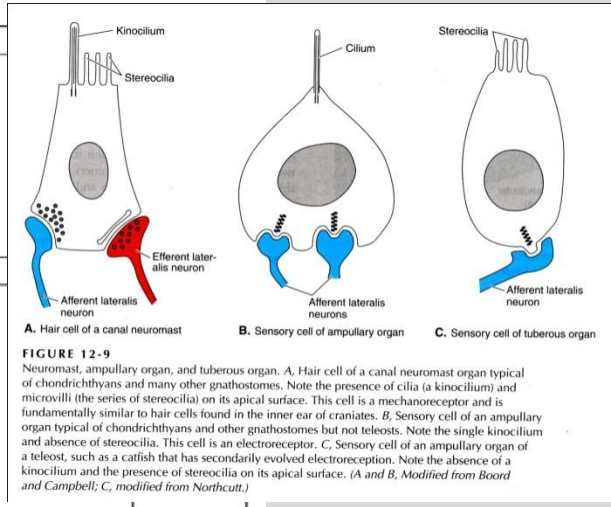

FIGURE 12-9
Neuromast, ampullary organ, and tuberous organ. *A*, Hair cell of a canal neuromast organ typical of chondrichthyans and many other gnathostomes. Note the presence of cilia (a kinocilium) and microvilli (the series of stereocilia) on its apical surface. This cell is a mechanoreceptor and is fundamentally similar to hair cells found in the inner ear of craniates. *B*, Sensory cell of an ampullary organ typical of chondrichthyans and other gnathostomes but not teleosts. Note the single kinocilium and absence of stereocilia. This cell is an electroreceptor. *C*, Sensory cell of an ampullary organ of a teleost, such as a catfish that has secondarily evolved electroreception. Note the absence of a kinocilium and the presence of stereocilia on its apical surface. *(A and B, Modified from Boord and Campbell; C, modified from Northcutt.)*

Elektrorecepce ptakořitných (Monotremata)

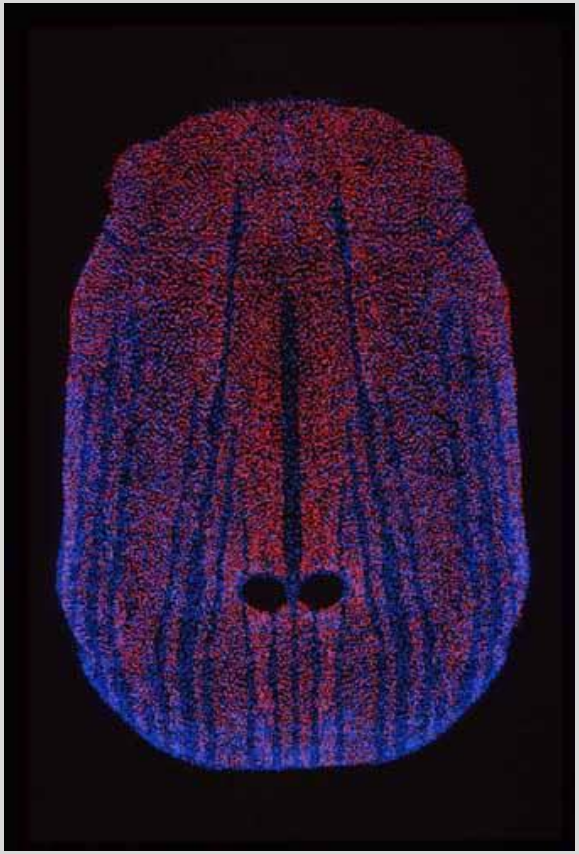

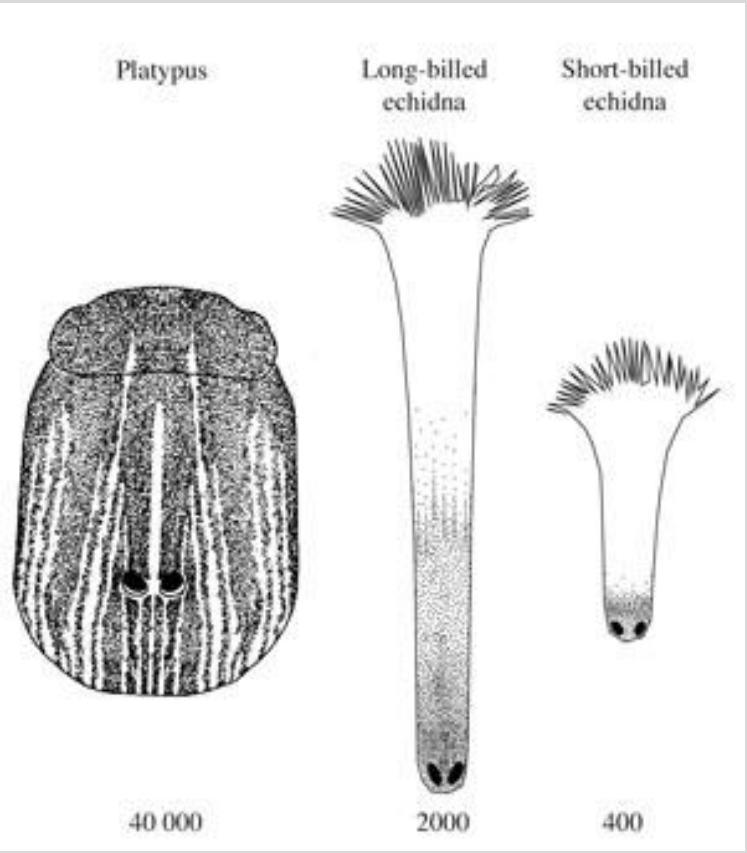

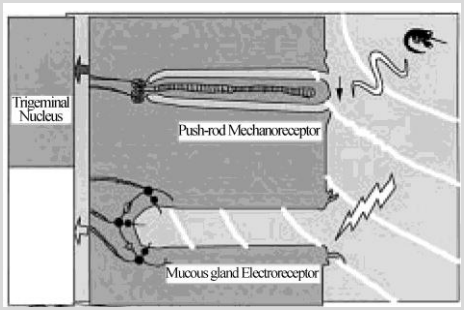

Nature 319: 401-402 (1986)

Phil.Trans. R. Soc. Lond. B (1998) 353, 1171-186

Elektrorecepce delfínů

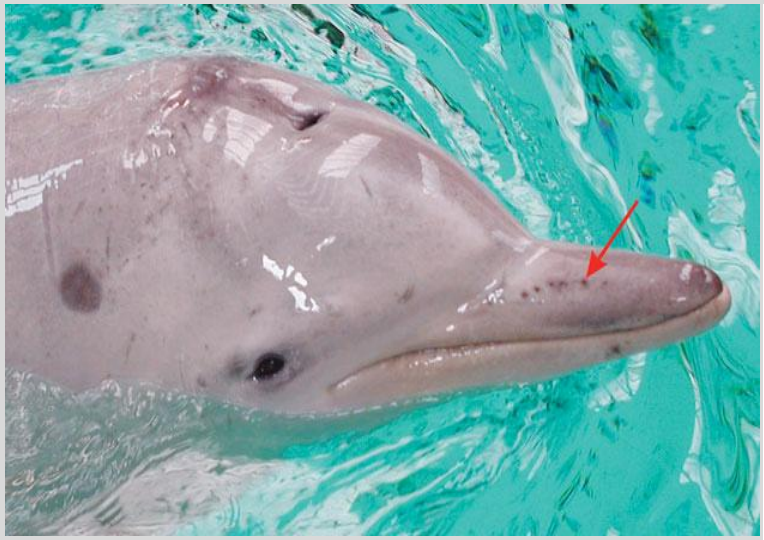

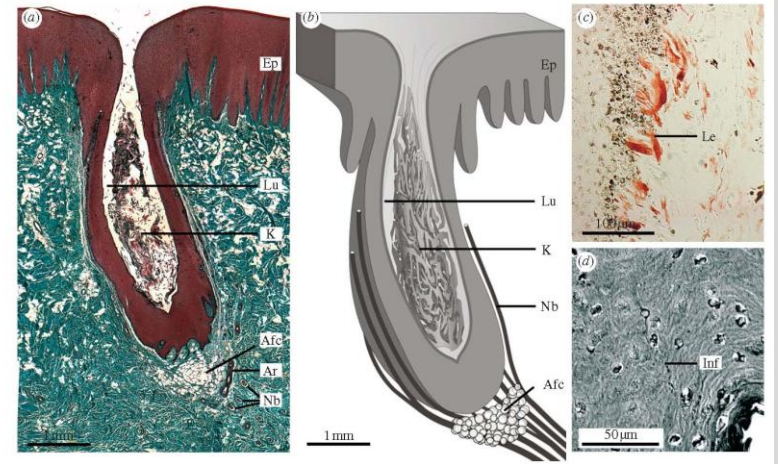

Figure 3. Histology of the vibrissal crypts in the Guiana dolphin. (*a*) Longitudinal section through a representative vibrissal crypt stained with Masson–Goldner trichrome. (*b*) Schematic drawing. The vibrissal crypt consists of an ampulla-shaped invagination of the epidermal integument lacking most characteristic morphological features of mammalian follicle-sinus complexes (F-SCs). (*c*) Vibrissal crypt innervation with lanceolate endings. (*d*) Intraepithelial nerve fibre reaches close to the lumen. Ep, epidermis; Lu, Lumen; K, meshwork of corneocytes and keratinous fibres; Afc, agglomeration of fat cells (probably the former hair papilla); Ar, artery; Nb, nerve bundles of the deep vibrissal nerve; Le, lanceolate endings; Inf, intraepithelial nerve fibre.

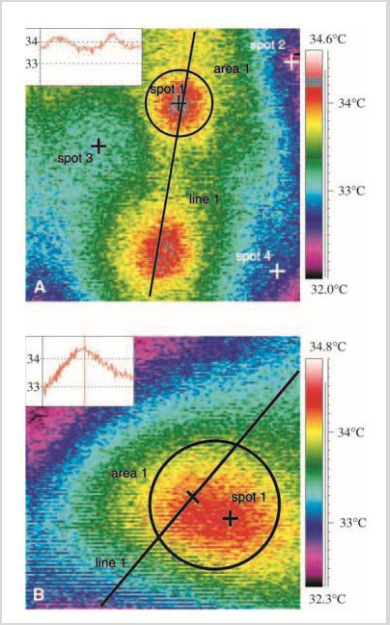

Czech-Damal et al (2011) Proc. R. Soc. B. in the press

Elektrorecepce delfínů

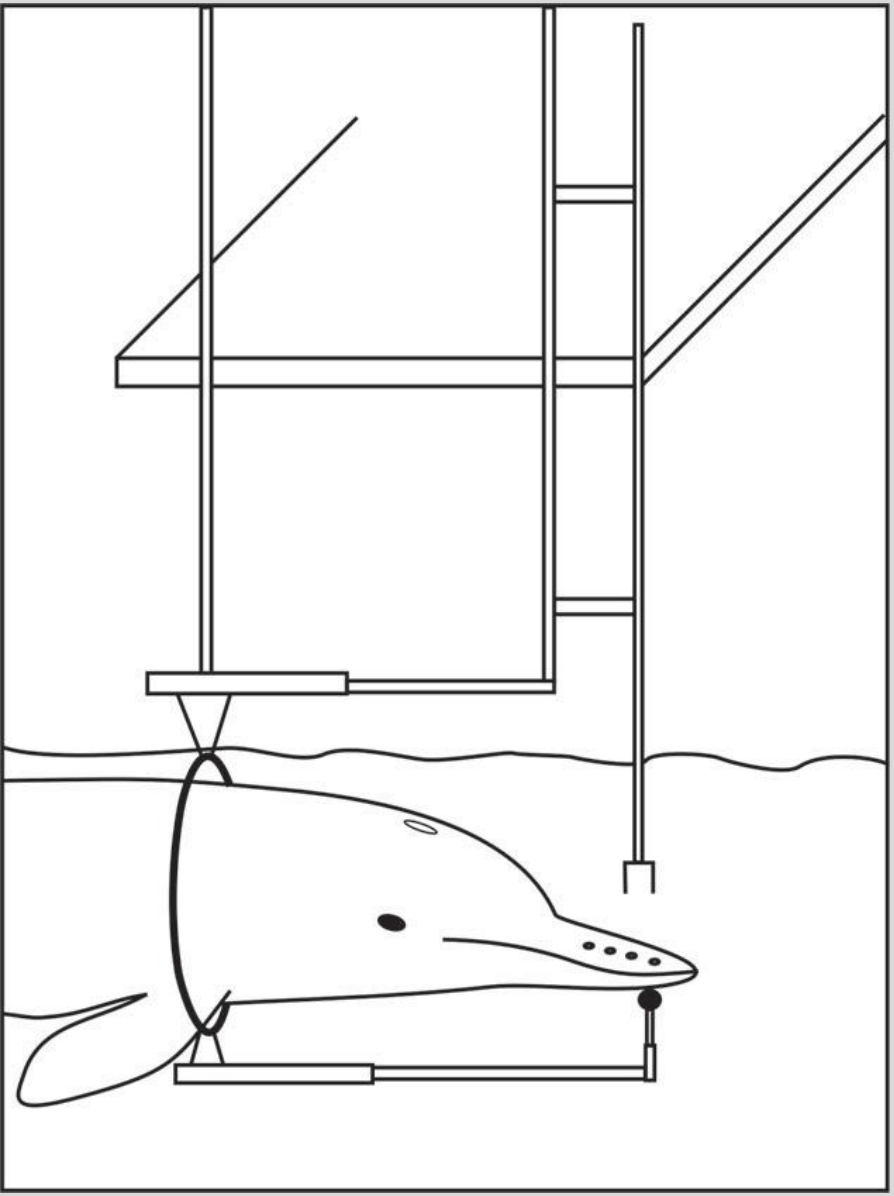

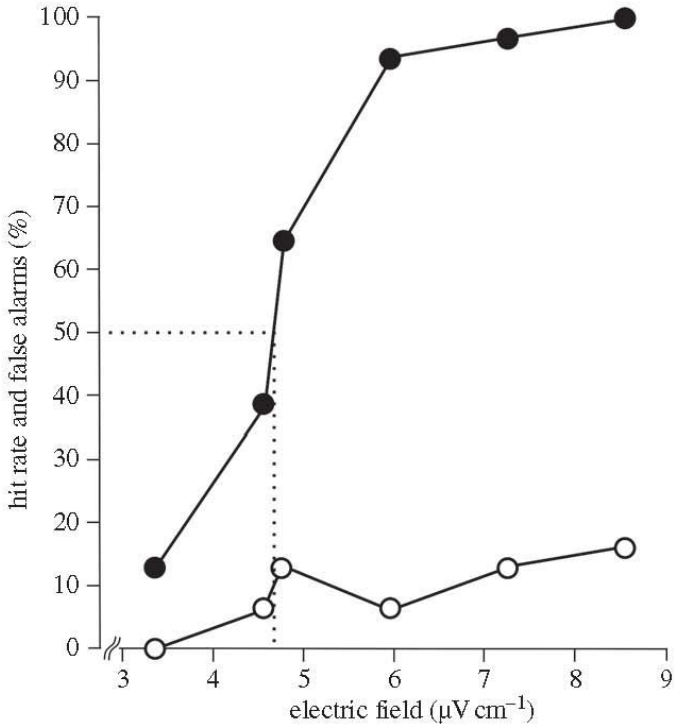

Figure 4. Experimental results from the psychophysical study on the electrosensitivity in the Guiana dolphin. Abscissa: the electric field strength at the location of the nearest vibrissal crypt, calculated from the current through the stimulus electrodes. Ordinate: percentage of correct choice during stimulus-present trials (hit rate) or, respectively, percentage of go responses during stimulus-absent trials (false alarm rate). Black circles: hit rate (i.e. the animal left the station correctly in response to an electric stimulus). White circles: false alarms (i.e. the animal left the station erroneously when no signal was present). At 50 per cent hit rate, the dolphin's absolute detection threshold for the electrical signals is defined (4.6 $\mu V\,cm^{-1}$).

Czech-Damal et al (2011) Proc. R. Soc. B. in the press

Magnetotaxis: Magnetotactic Bacteria

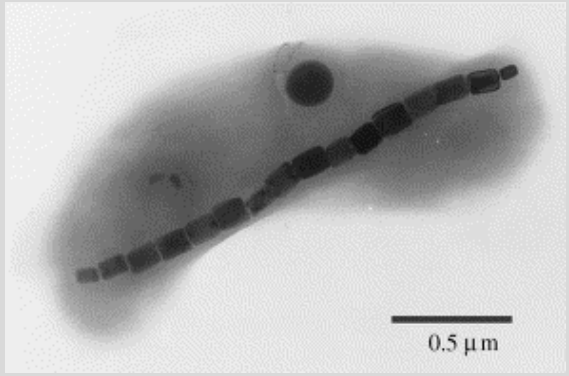

Magnetospirillum magnetotacticum

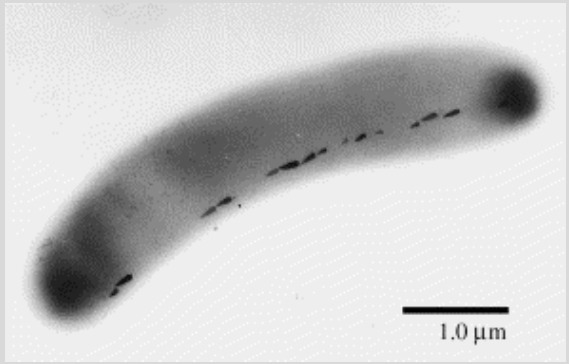

Magnetovibrio sp.

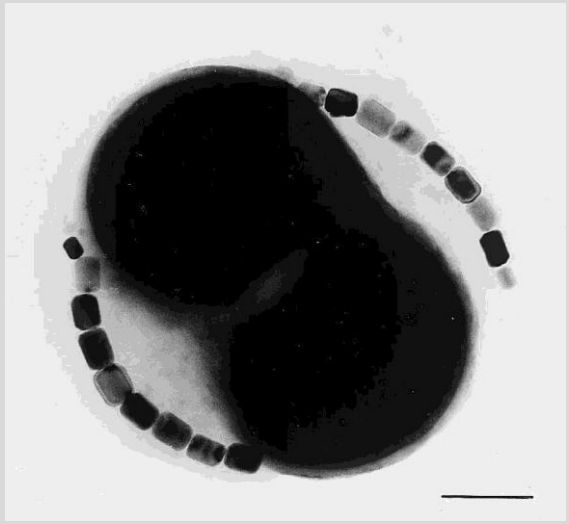

Magnetococcus sp.

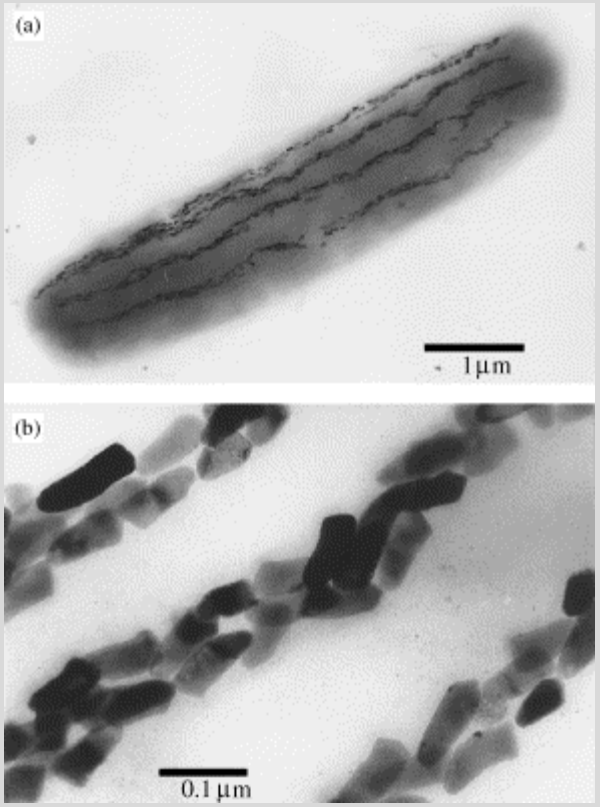

Magnetobacterium bavaricum

Hanzlik et al. (2002) J. Magnetism Magnet. Mater. 248: 258-267

Rainbow Trout

Oncorhynchus mykiss

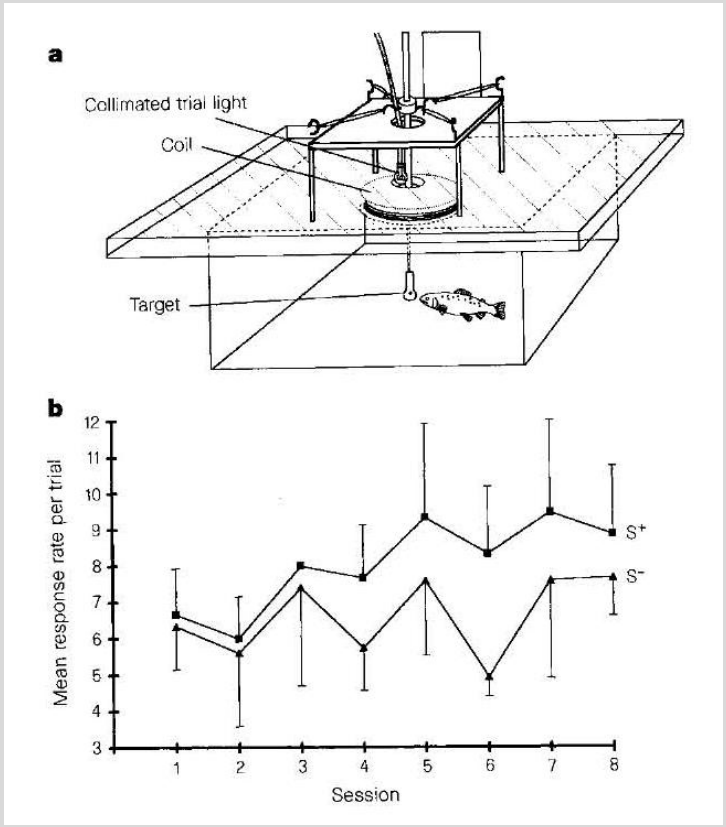

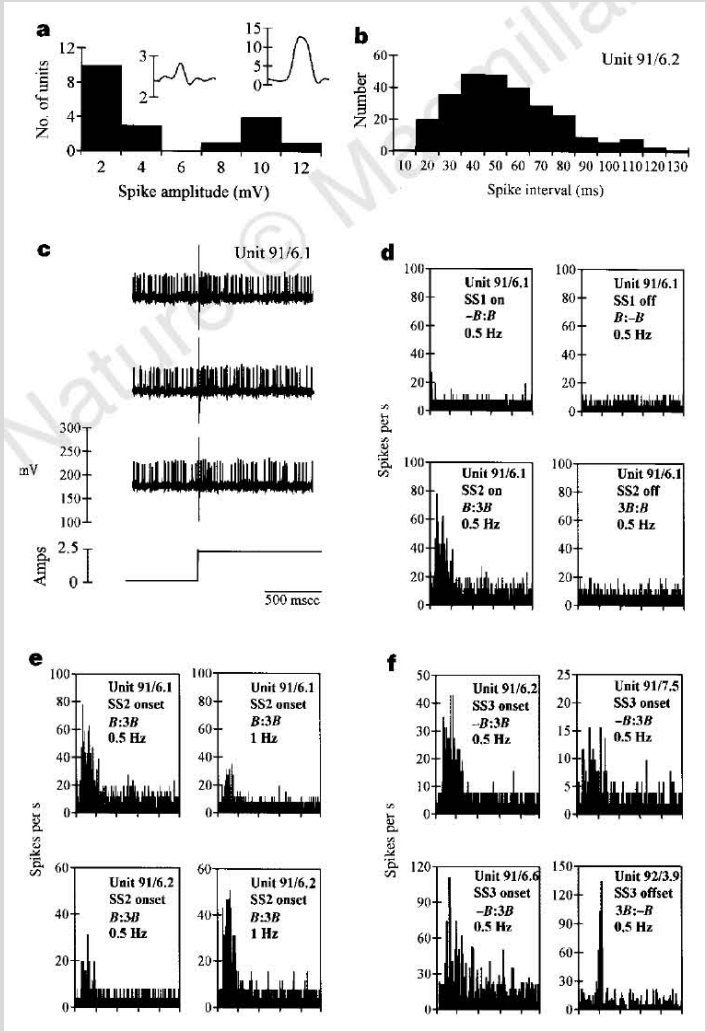

n. trigeminus r. ophthalmicus superficialis

Walker et al (1997) Nature 390:371-376

Rainbow Trout
Oncorhynchus mykiss

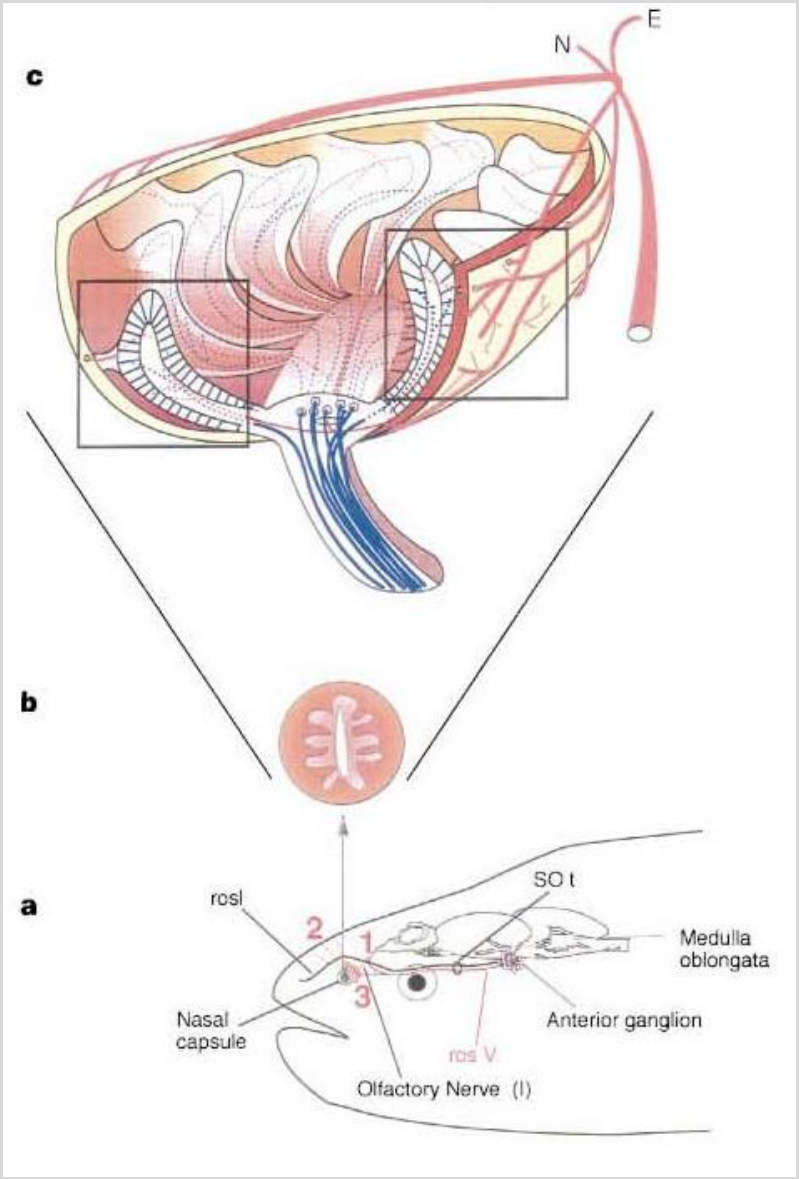

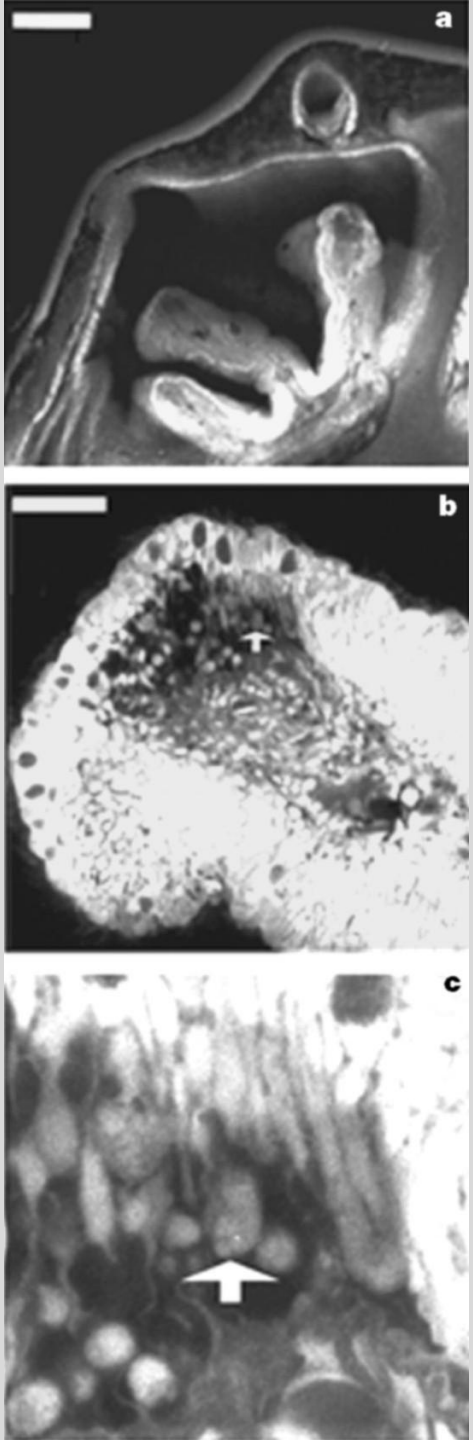

Walker et al (1997)
Nature 390:371-376

Rainbow Trout
Oncorhynchus mykiss

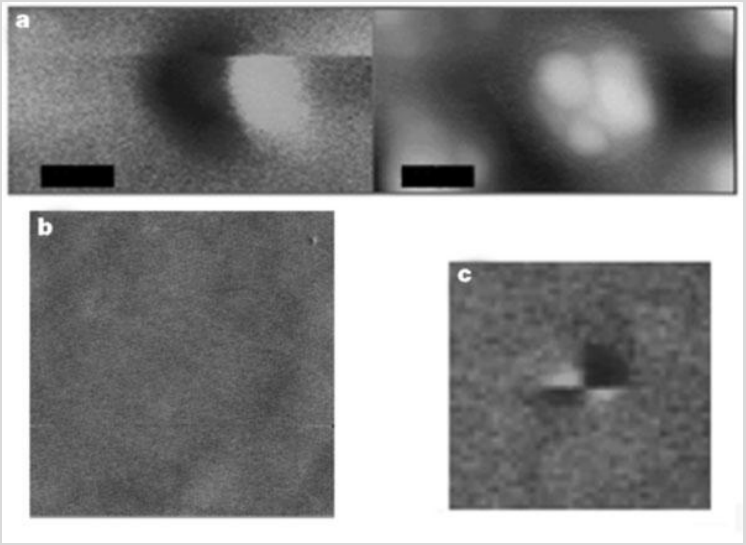

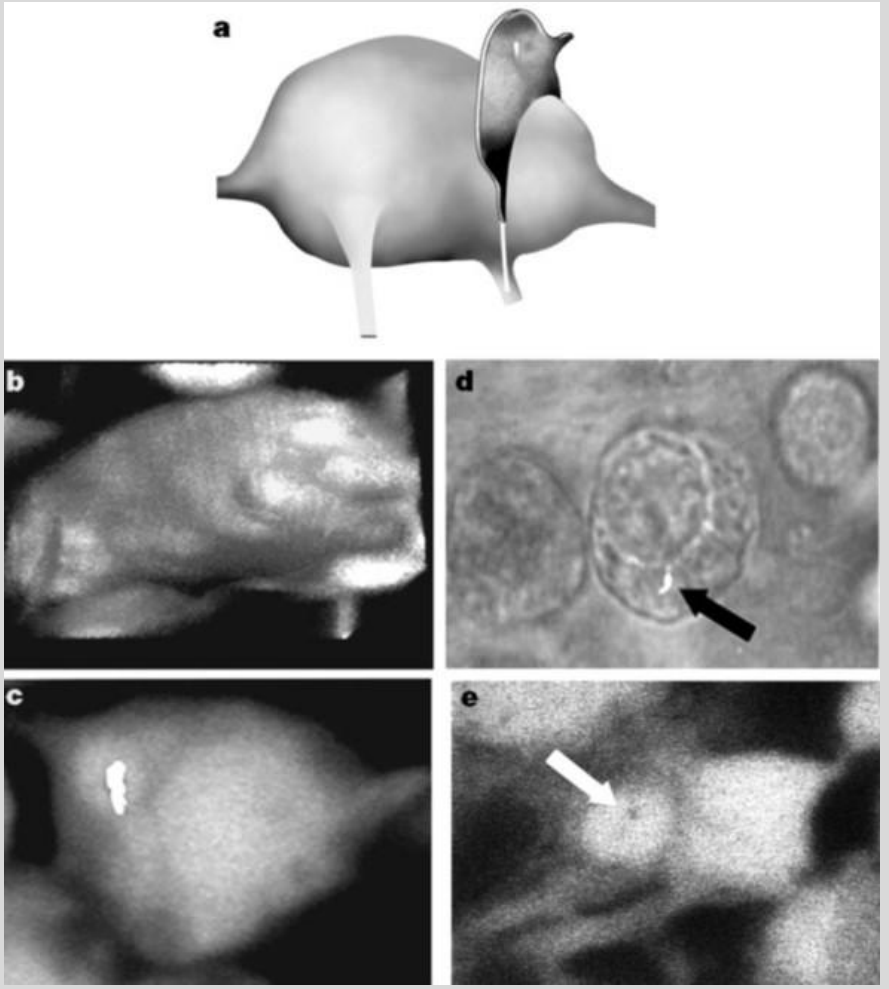

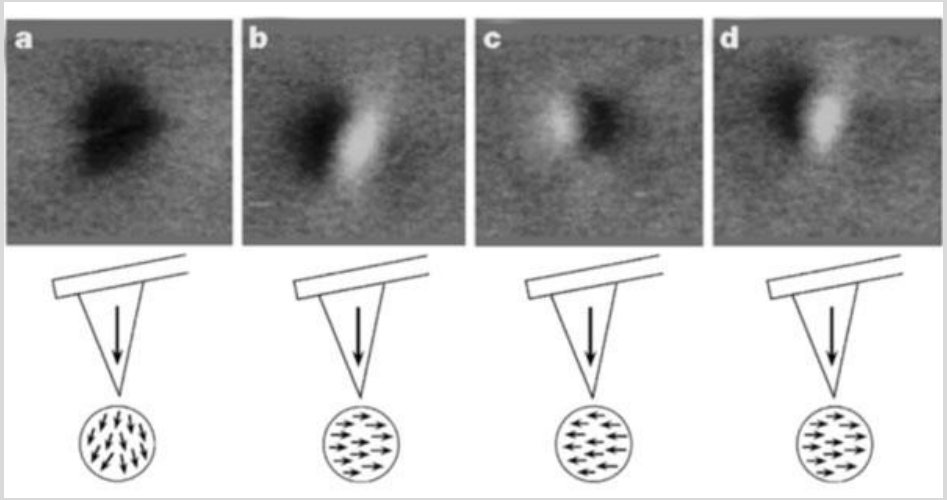

Diebel et al. (2000) Nature 406: 299-302

Pigeon (Columba livia)

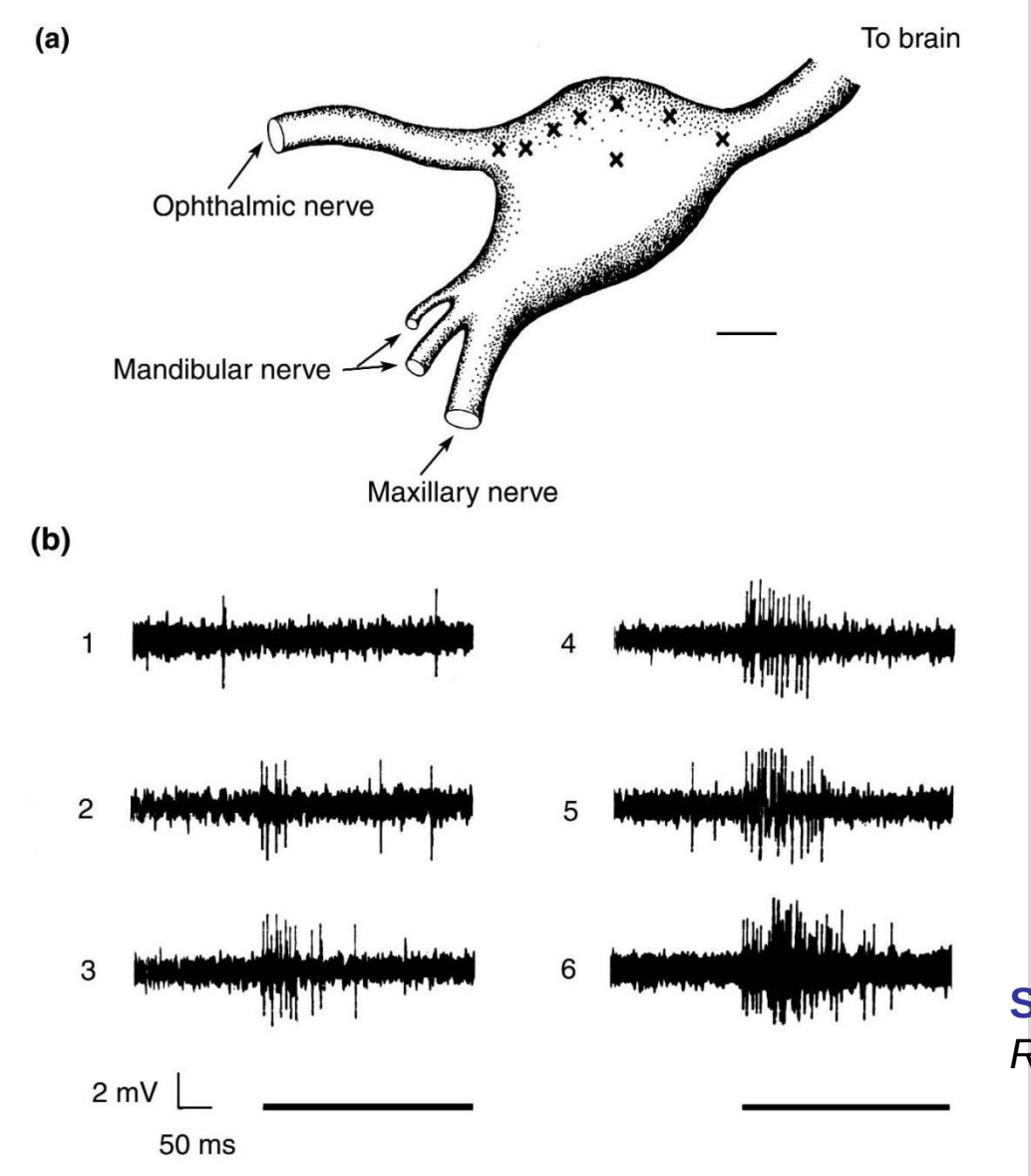

Semm P, Beason RC (1990) *Brain Res Bull* 25:735–740

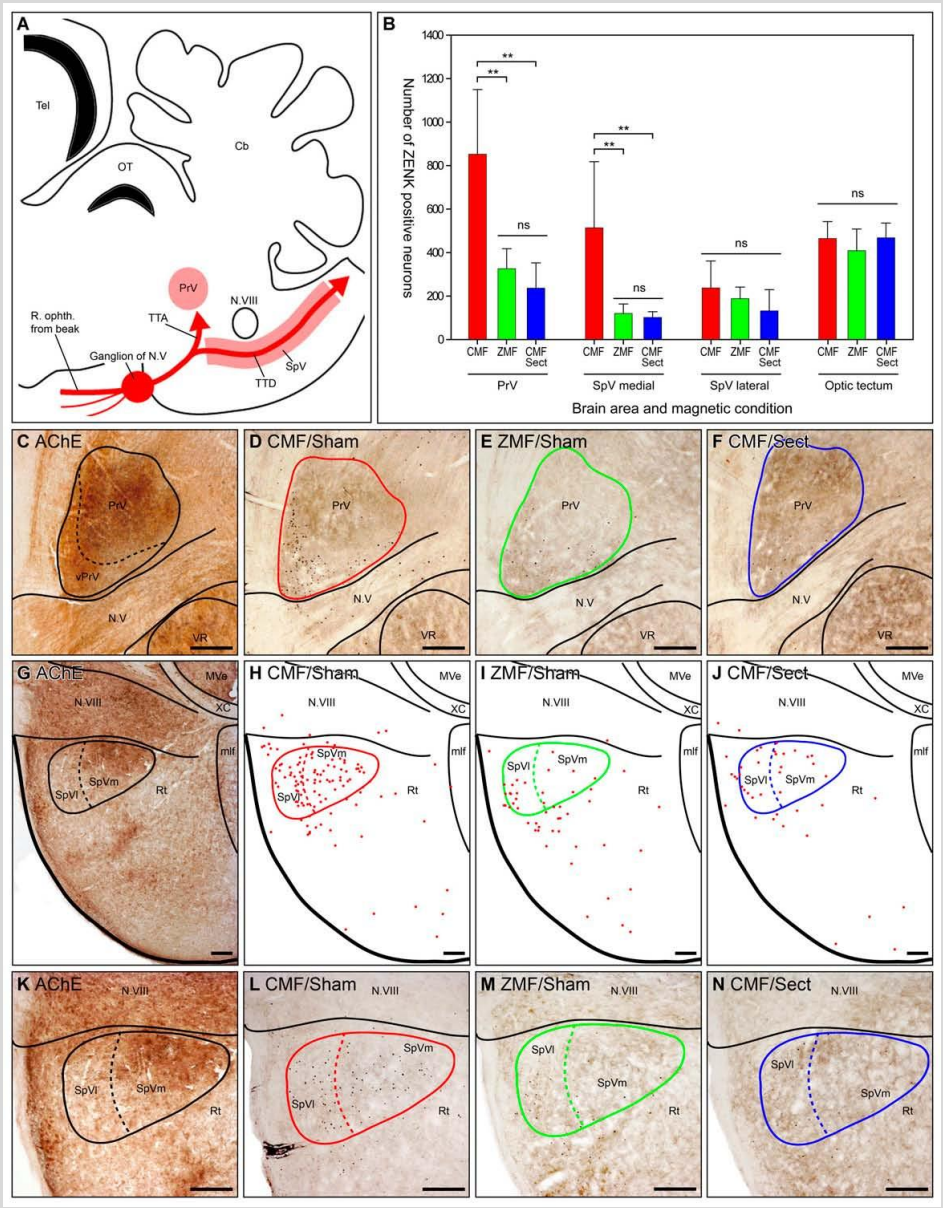

Heyers et al (2010) PNAS 107: 9394-9399

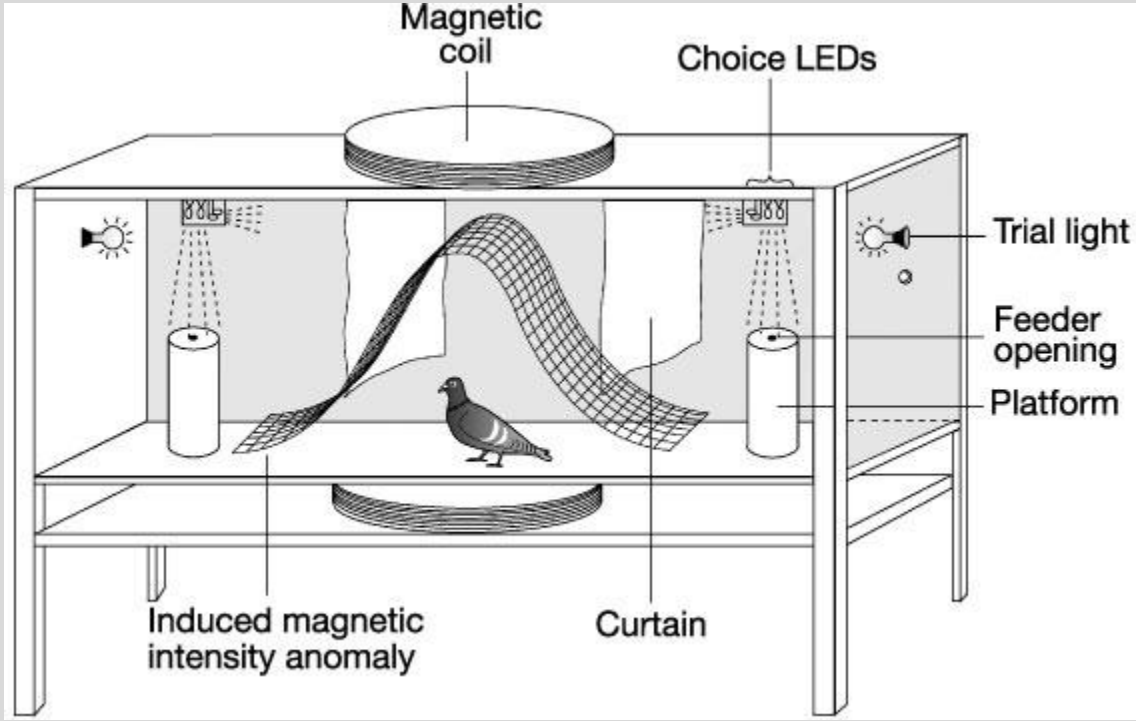

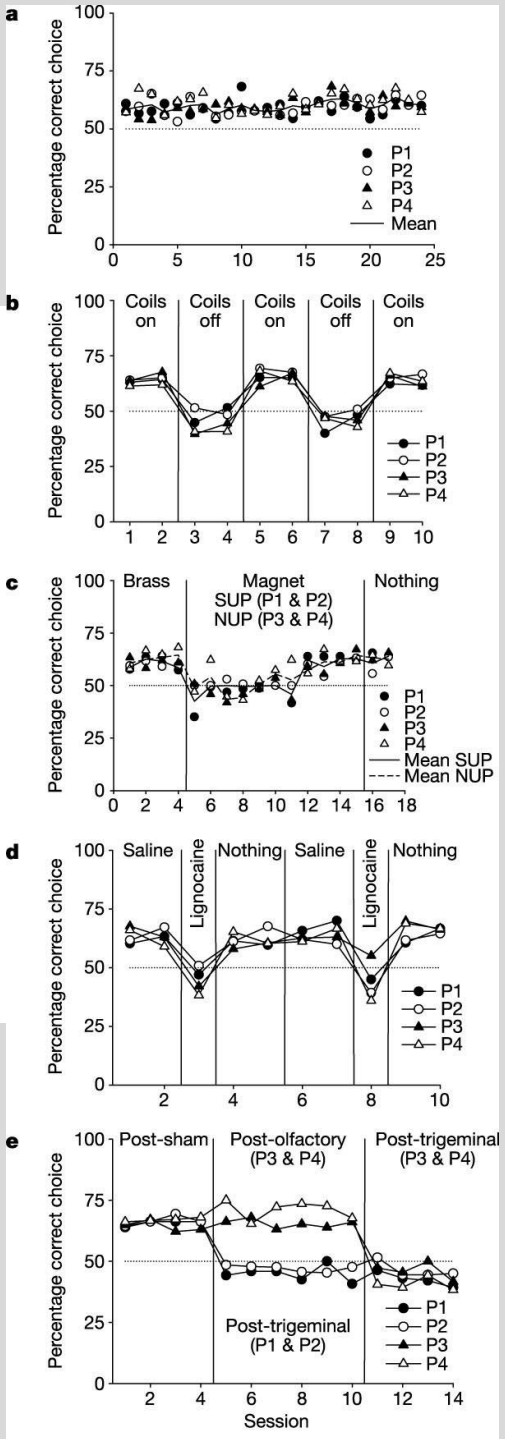

Mora et al (2004) Nature 432:508-511

"Radical pair"- model

(after Ritz et al. 2000)

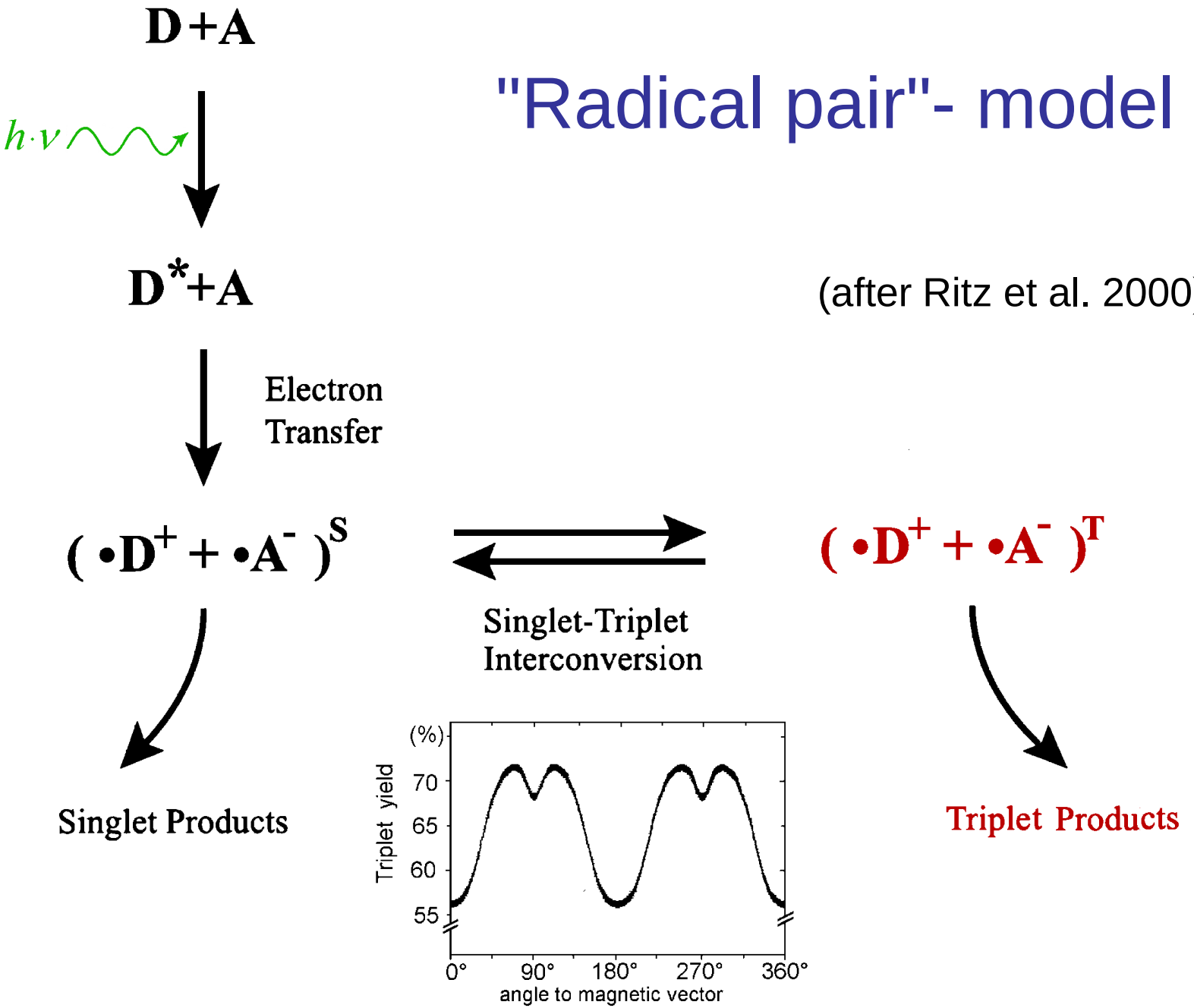

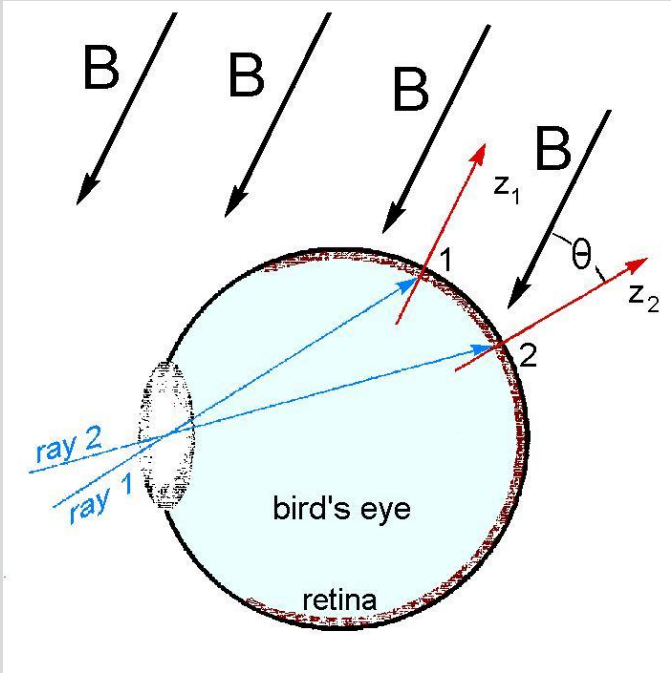

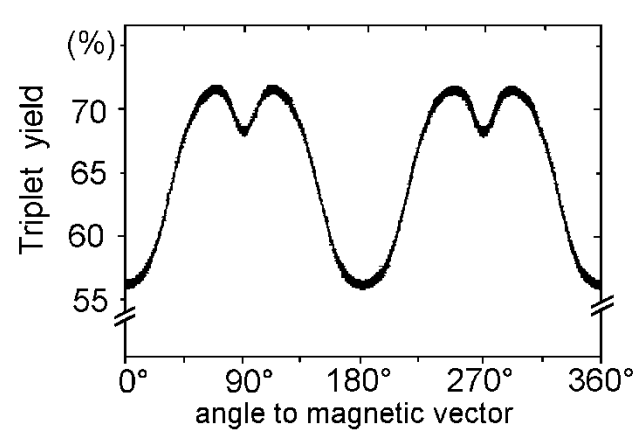

Assumed pattern modulation by the geomagnetic field in a bird flying in different directions:

(from Ritz et al. 2000)

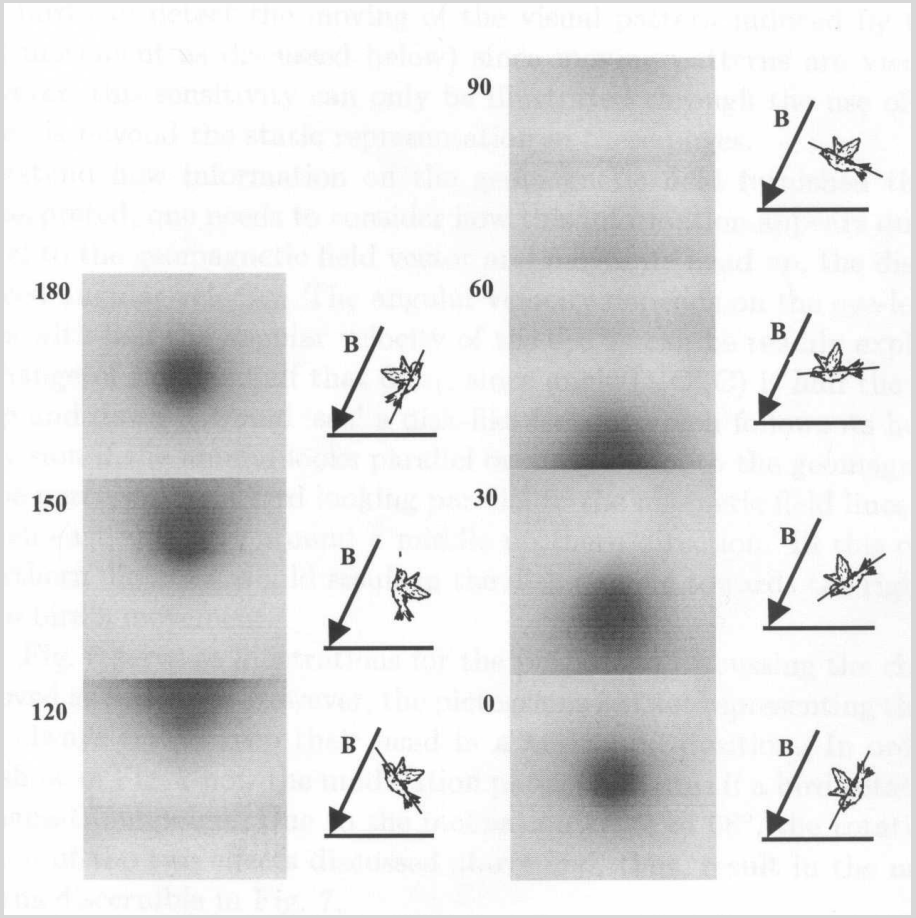

Axial response resulting in an inclination compass

Orientation of European Robins tested in spring under different wavelengths at low intensity:

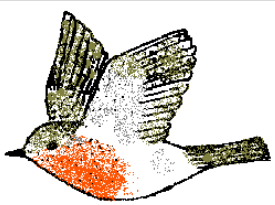

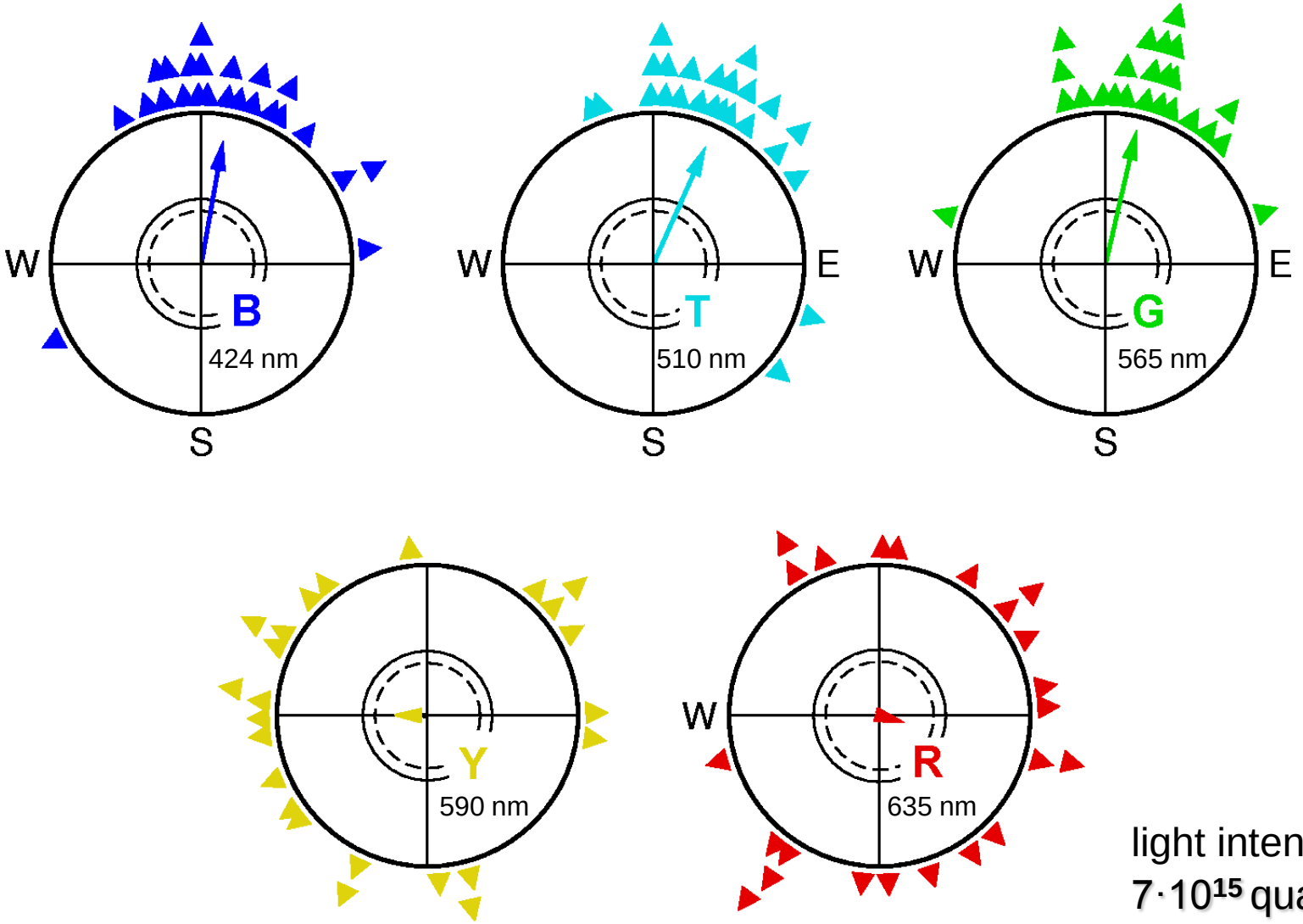

light intensity:
$7 \cdot 10^{15}$ quanta/s m²

Lateralization of magnetic compass orientation

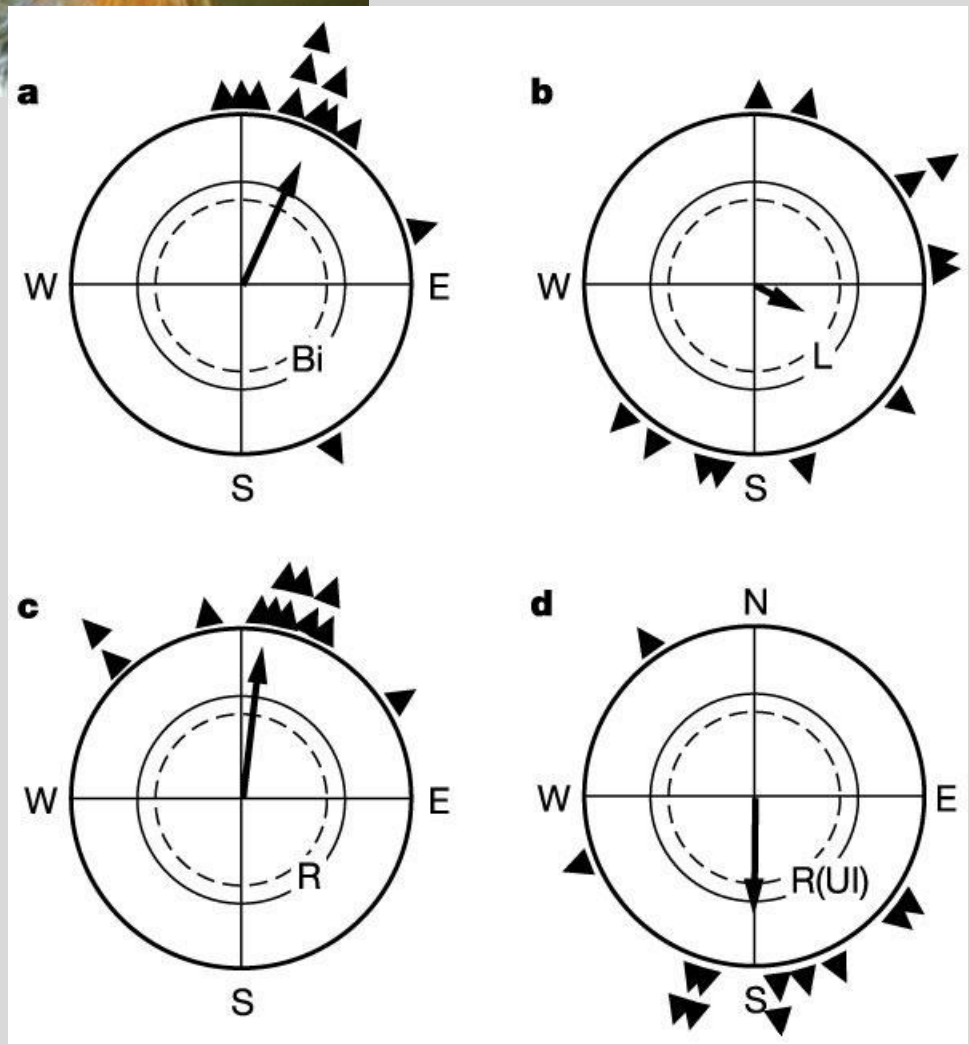

Wiltschko et al. (2002) Nature 419:467-469

Magnetoreception of Directional Information in Birds Requires Nondegraded Vision

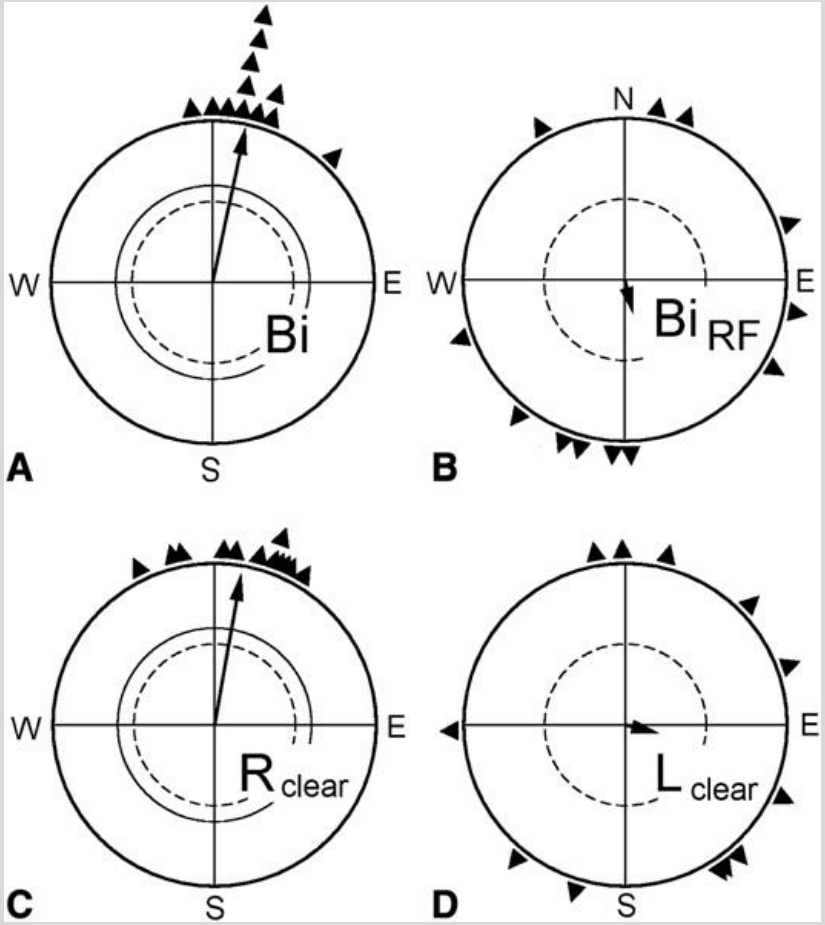

Stapput et al. (2010) Curr Biol 20: 1259-1262

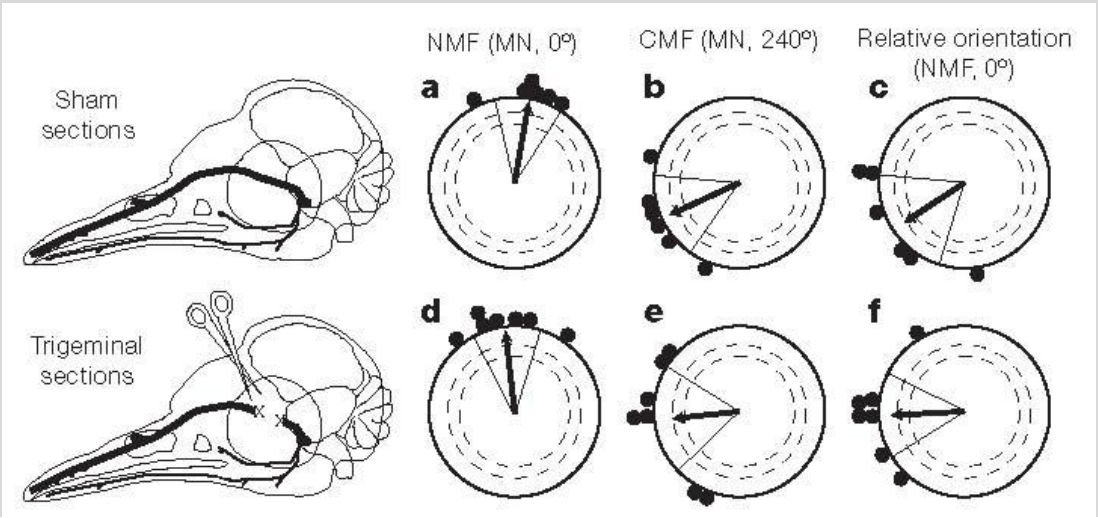

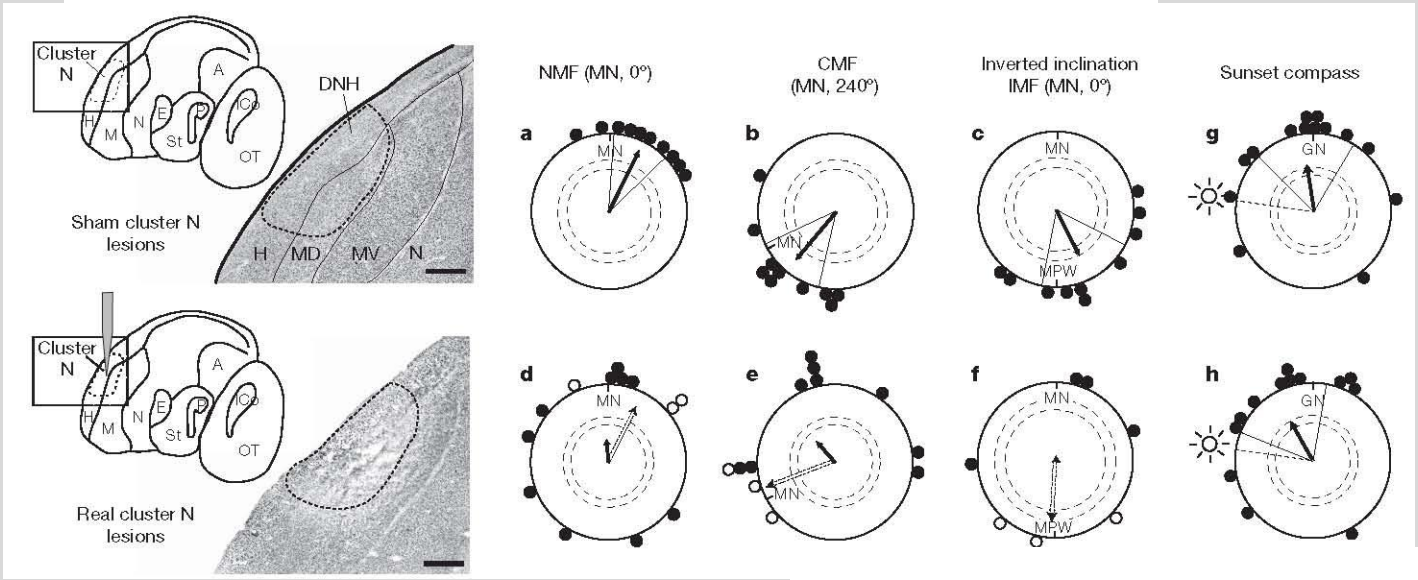

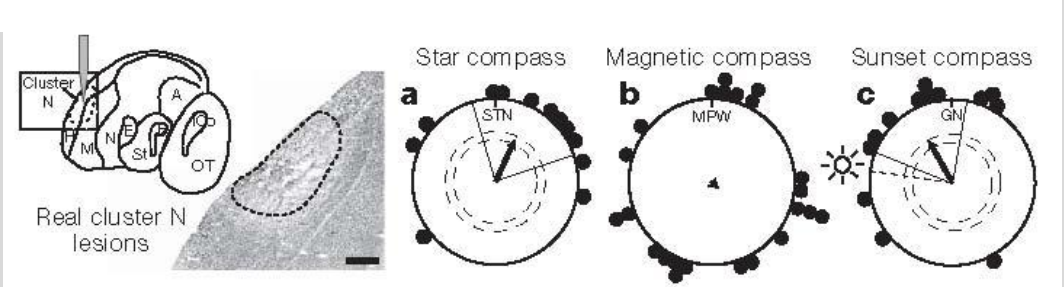

Zapka et al. (2009) Nature 461: 1274 –1278

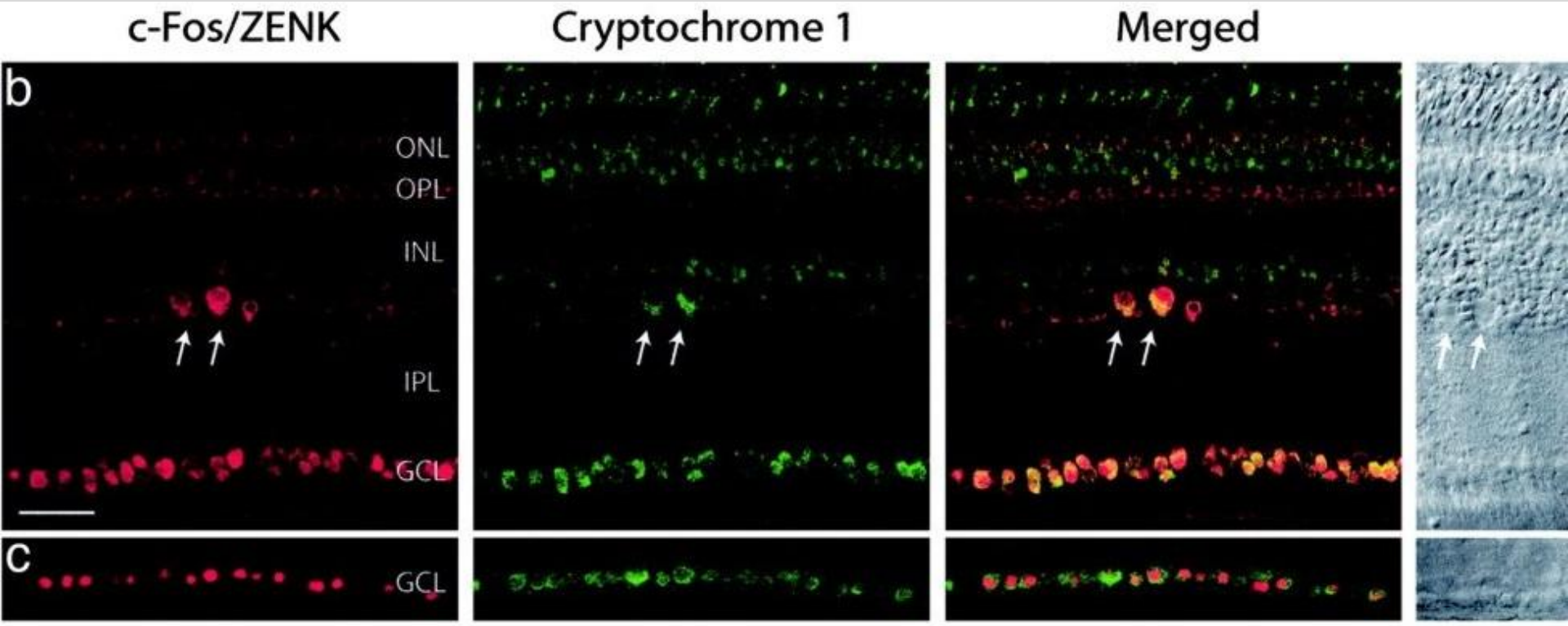

Mouritsen at al. (2004) PNAS 101: 14294-14299

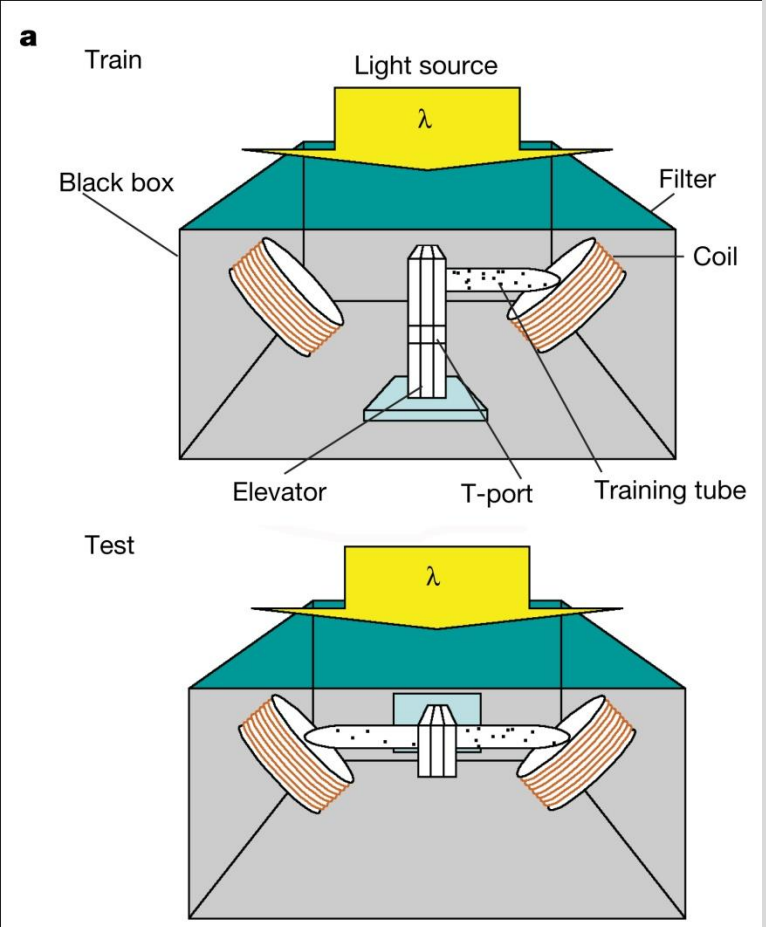

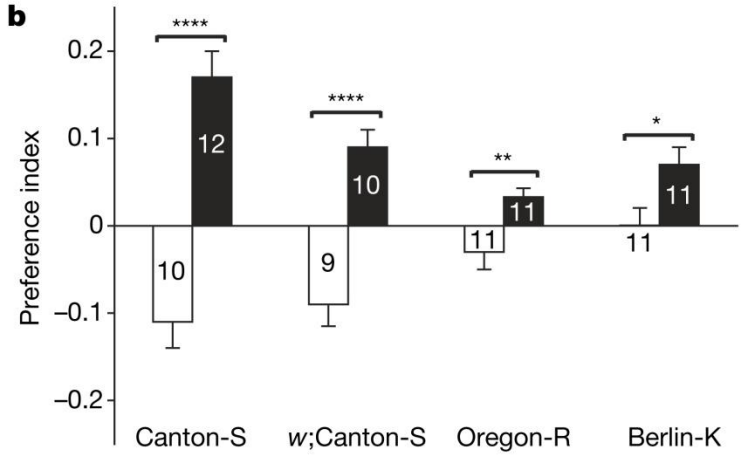

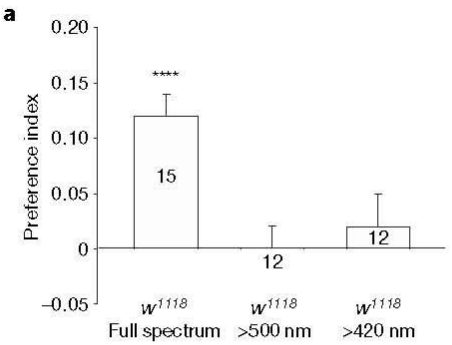

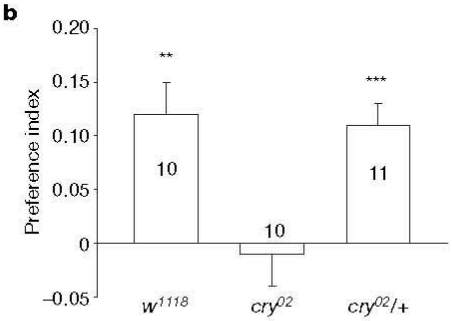

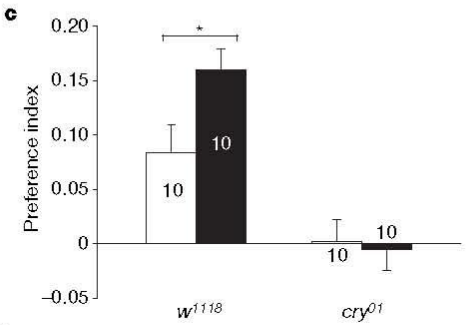

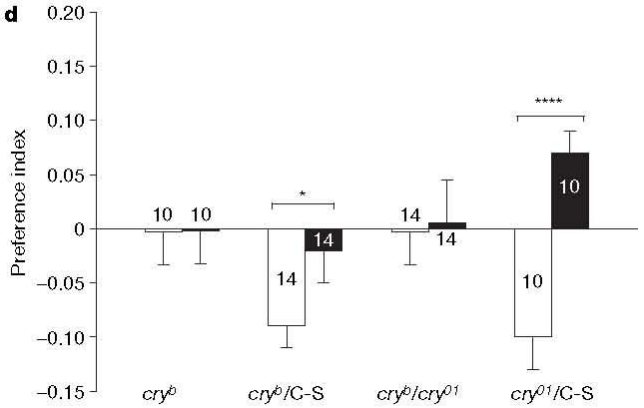

Gegear et al. (2008) Nature 454: 1014–1019

Gegear et al. (2010) Nature 463: 804–809

Počty funkčních genů a pseudogenů kódujících chemoreceptory u obratlovců a hmyzu

OR – čichové receptory

V1R a V2R – vomeronasální receptory

T1R a T2R – chuťové receptory

TAAR – „trace amine associated receptors“

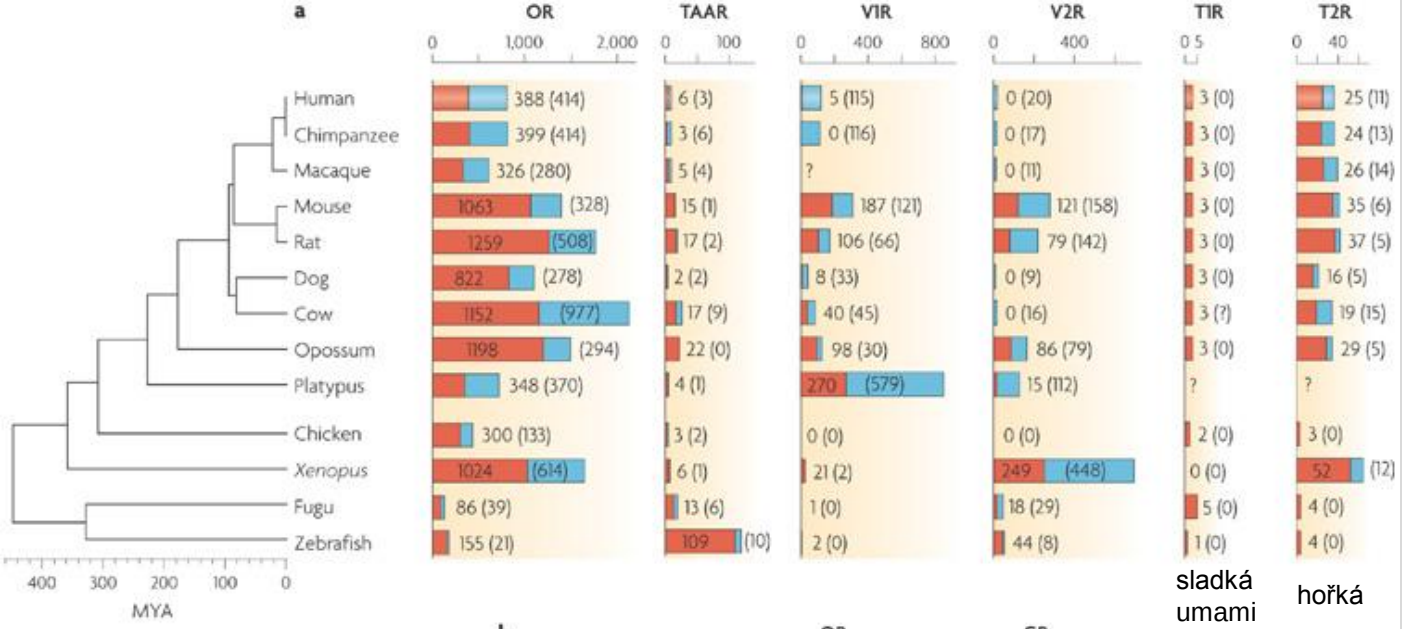

sladká umami

hořká

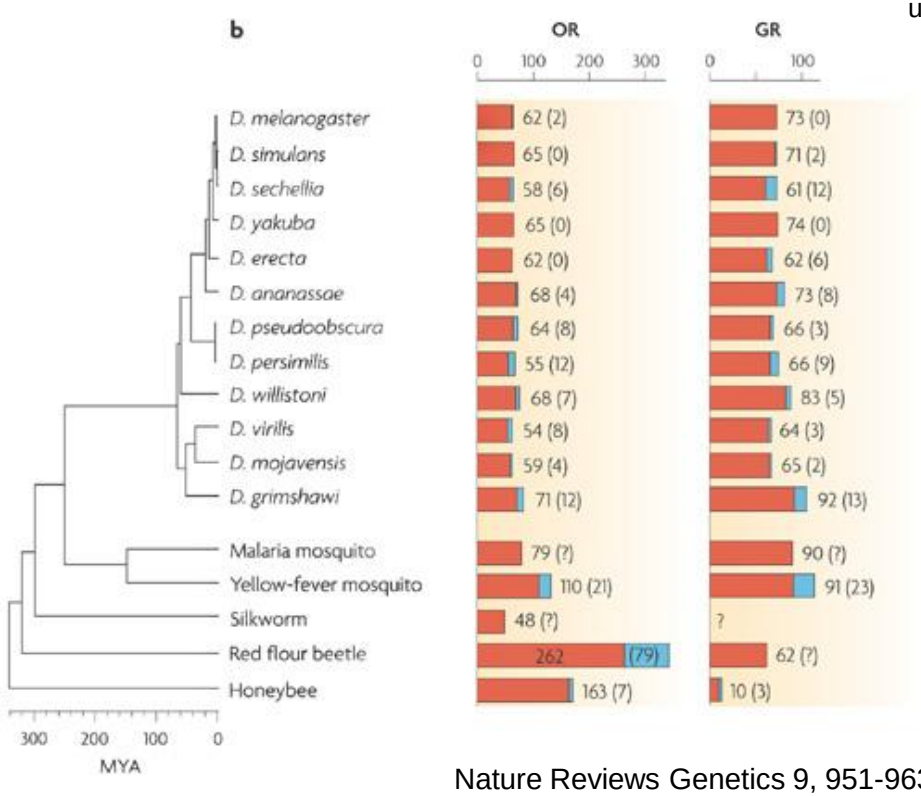

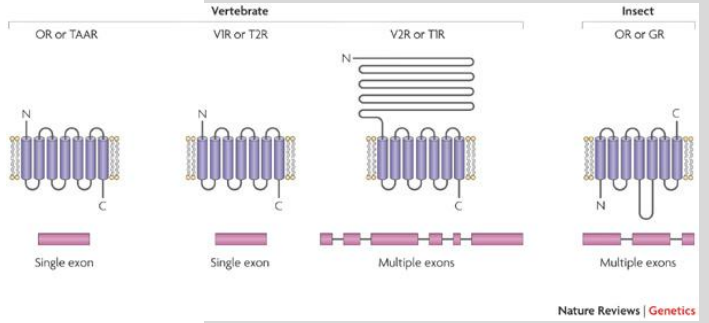

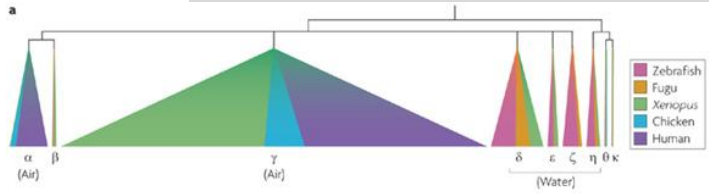

čichové receptory:
α (~OR1) a ϒ (~OR1) -
enormní rozvoj u čtvernožců

Nature Reviews Genetics 9, 951-963 (2008)

Čichové sensily hmyzu

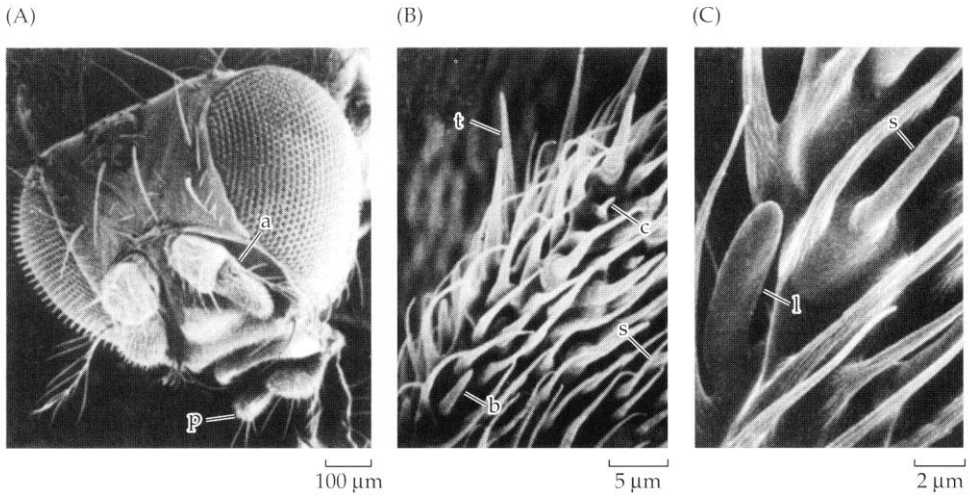

Figure 7.5
Insect olfaction: the olfactory bristles (or sensilla) of *Drosophila* (A) Olfactory bristles in *Drosophila* in the funiculus of the antenna (a) and maxillary palp (p). (B) Surface of funiculus, showing three classes of sensilla: basiconic (b), coeloconic (c), and trichoid (t). Also shown are hairs that have no nerve innervation and serve no sensory function, called spinules (s). (C) Two types of basiconic sensilla, the large (l) and the small (s). (A from de Bruyne et al., 2001; B, C from Riesgo-Escovar et al., 1997.)

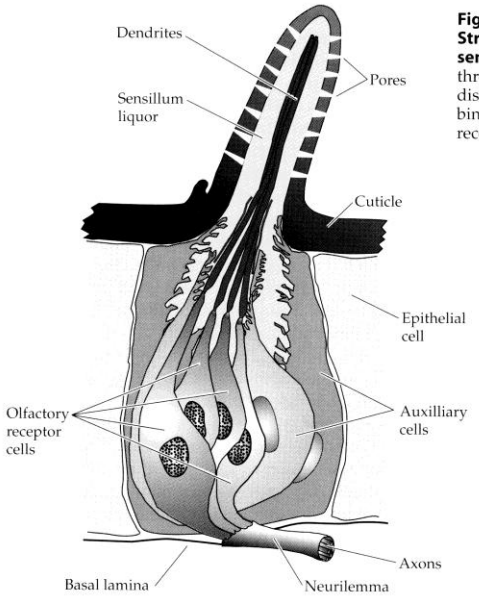

Figure 7.6
Structure of an insect olfactory sensillum Odors enter the sensillum through pores in the wall of the bristle, dissolve in the sensillum liquor, and bind to the dendrites of the olfactory receptor neurons.

Čichový epitel

Čichové buňky (bipolární neurony)
Podpůrné buňky
Bazální buňky (kmenové)
Mukózní (Bowmanovy) žlázy

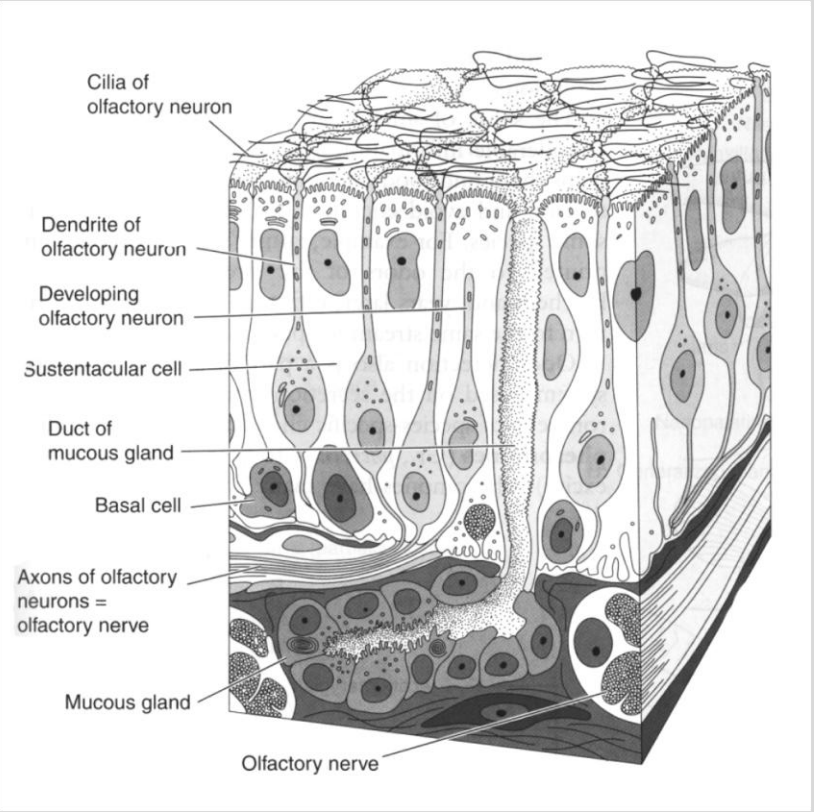

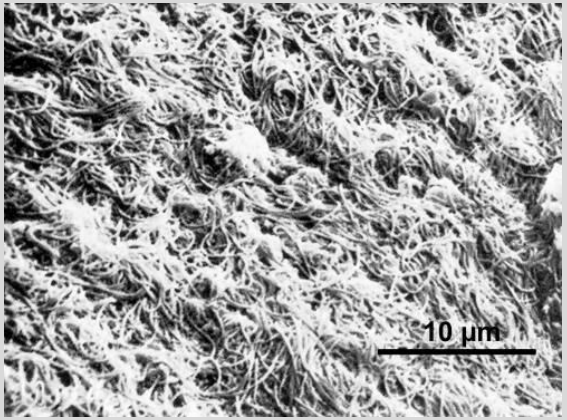

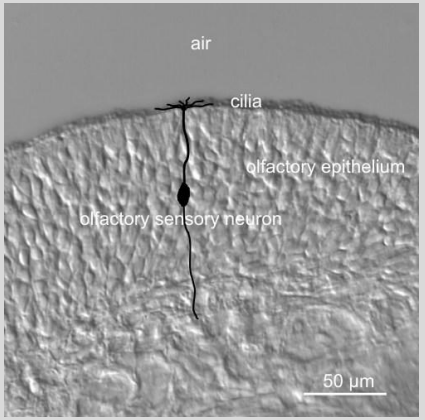

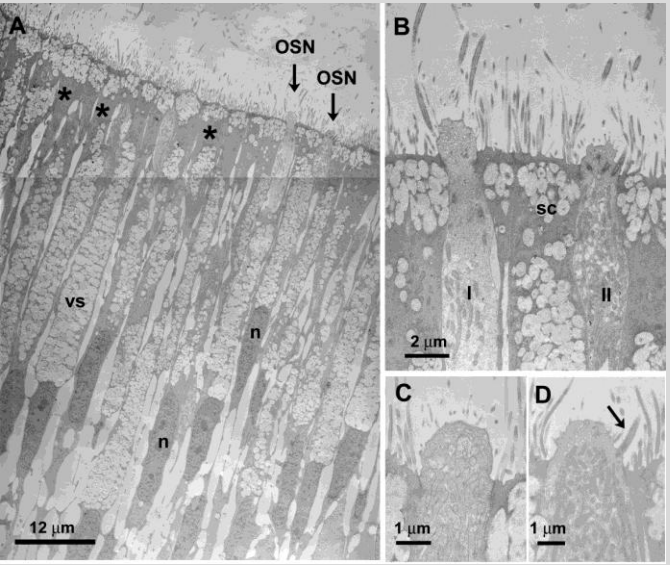

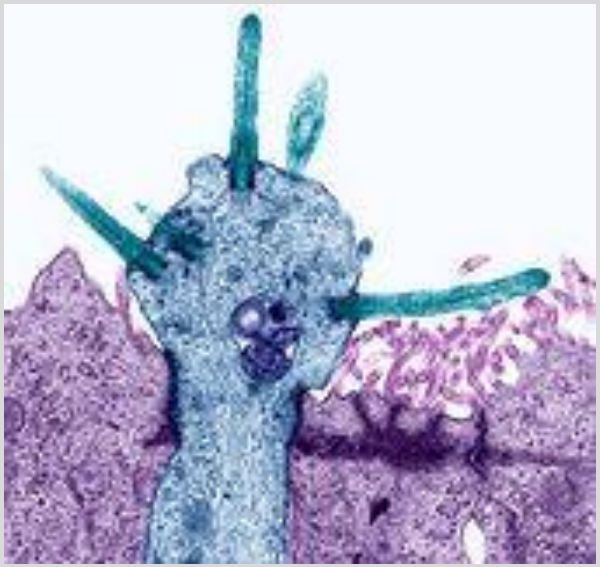

Nozdry a čichové dutiny – vodní obratlovci

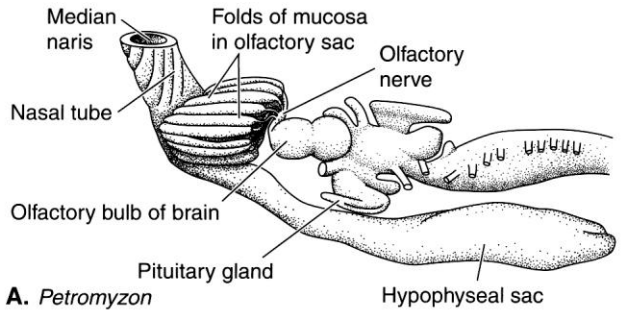

A. *Petromyzon*

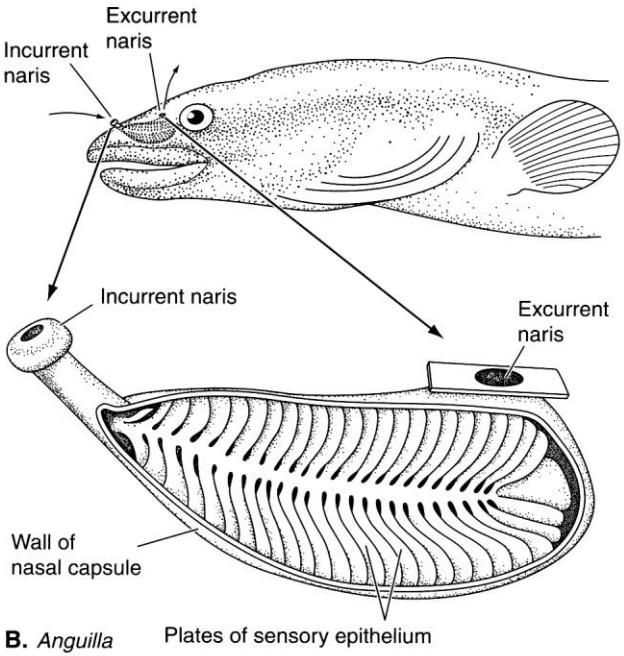

B. *Anguilla*

FIGURE 12-2
Olfactory organs of fishes. *A,* Olfactory organ of a lamprey. *B,* Olfactory organ of an eel. *(After Kleerekoper.)*

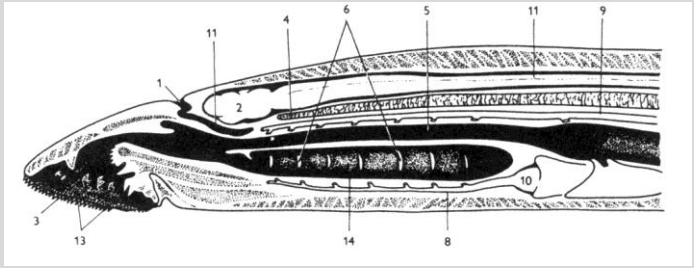

Mihule-nepárová nozdra

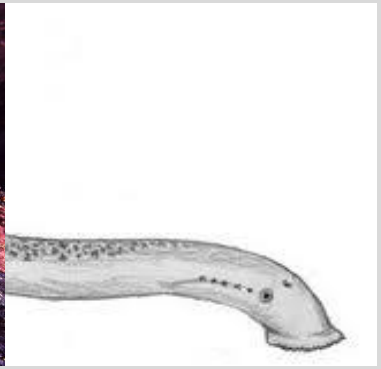

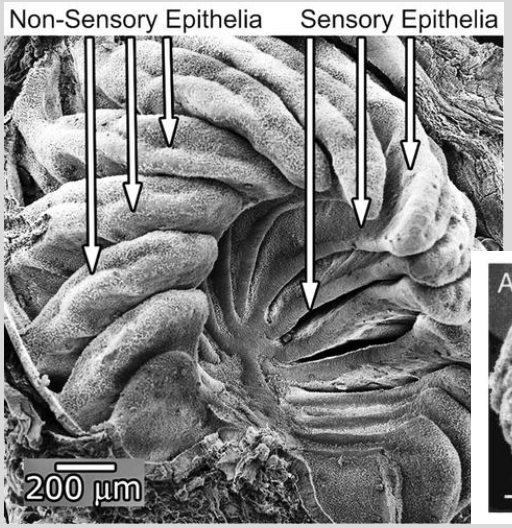

čichová rozeta ryb

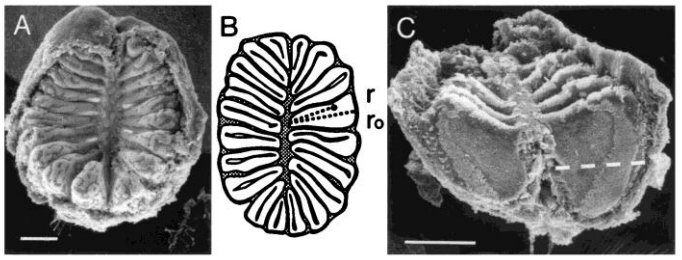

Nozdry a čichové dutiny – Tetrapoda

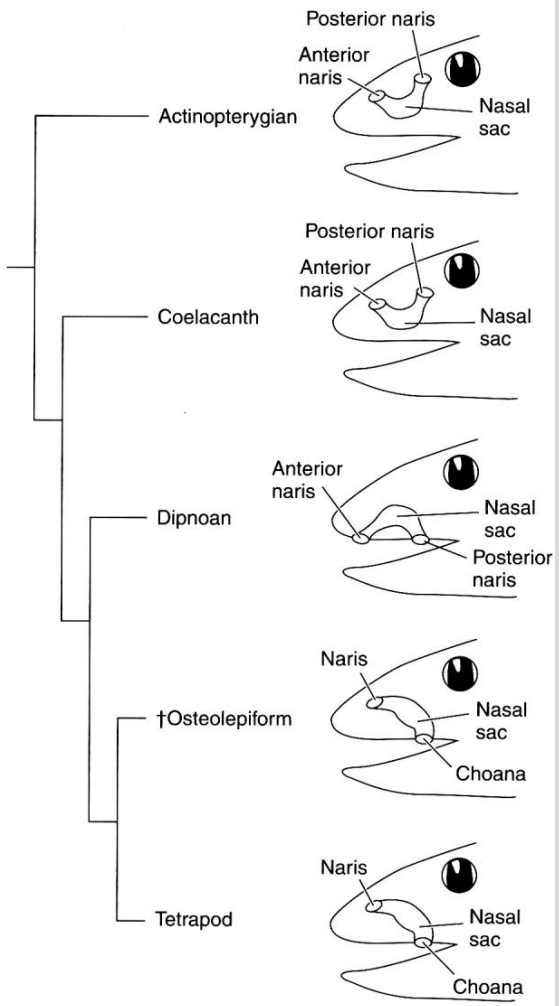

FIGURE 12-3
Evolution of nasal passages and the choana. †Osteolepiforms and tetrapods have a choana, which is a connection of the nasal passages to the oral cavity.

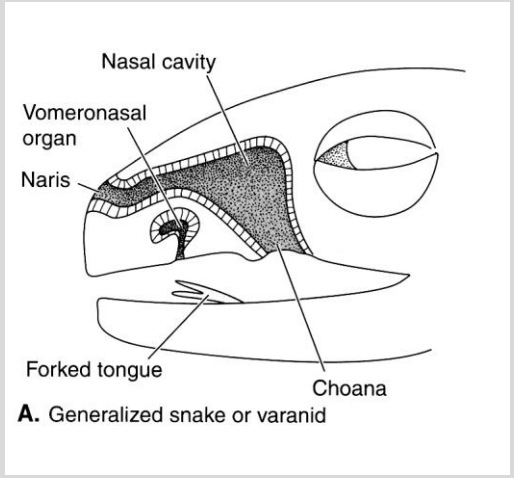

A. Generalized snake or varanid

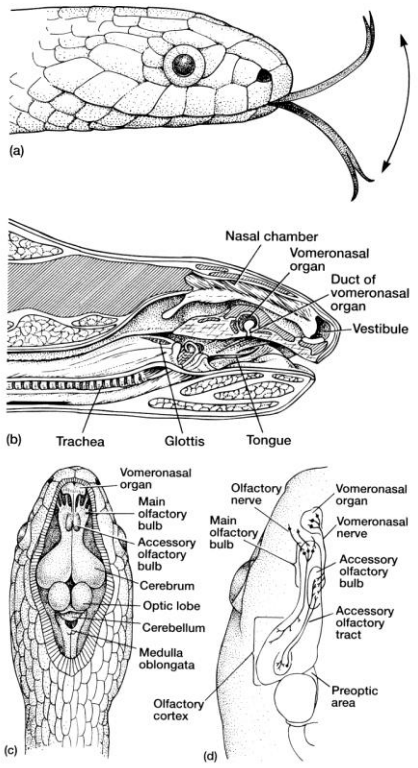

FIGURE 17.14 **Tongue flicking in snakes.** (a) Snakes, like lizards, extend their tongues to sweep air in front of them. The tongue collects and then transports airborne particles into the mouth. Probably along with other oral membranes, the tongue wipes these particles onto the vomeronasal organ on the roof of the mouth. (b) Sagittal section of the head of a boa constrictor. The vomeronasal organ is a blind pocket with a lumen that opens directly into the mouth via a duct. The tip of the retracted tongue projects from its sheath beneath the trachea. (c) Skull and overlying tissue have been cut away to reveal a dorsal view of the snake brain. (d) Neuroanatomy of a snake's olfactory organs. The main olfactory bulb receives input from the olfactory epithelium. The accessory olfactory bulb, via a separate tract, receives information from the vomeronasal organ. Vomeronasal and olfactory systems are separate chemoreceptive organs whose fibers travel separately within the olfactory tract. Thereafter, sensory information tends to be brought together in the olfactory cortex of the telencephalon.

After Kubie et al; Halpern and Kubie.

Nozdry a čichové dutiny – savci

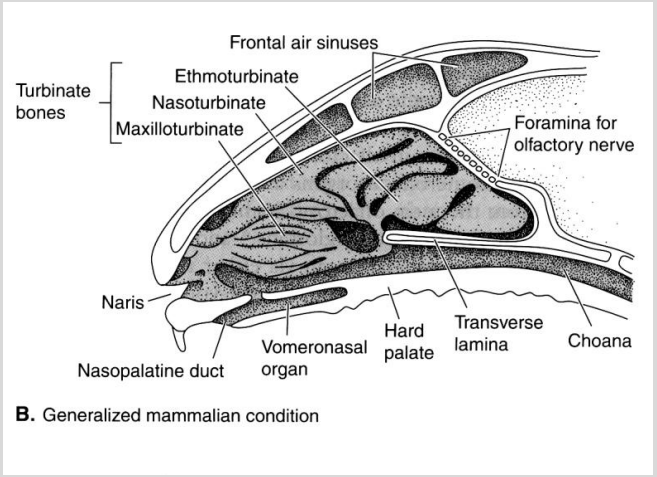

B. Generalized mammalian condition

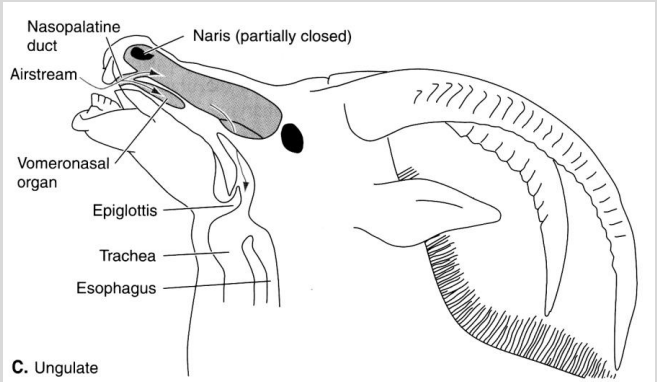

C. Ungulate

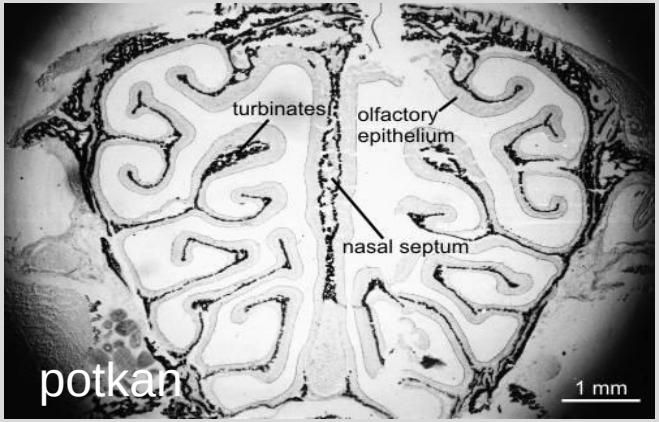

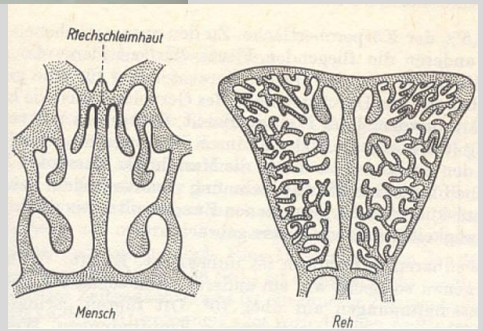

Regionální specializace čichových receptorů

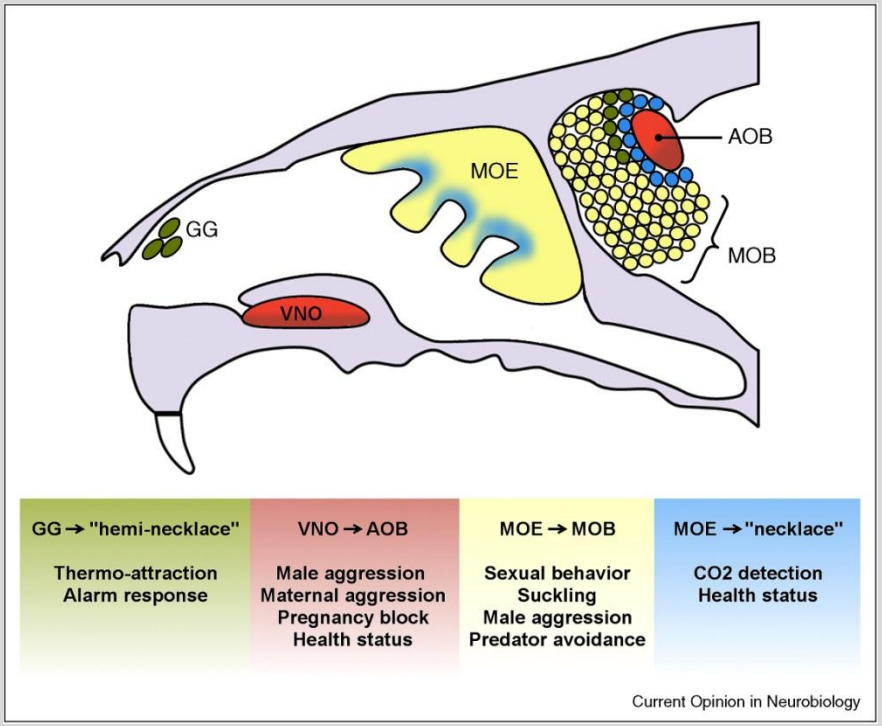

Current Opinion in Neurobiology 20, 274-280 (2010)

Čichový epitel – dorzální zóna – vrozené reakce

Ventrální zóna – naučené reakce

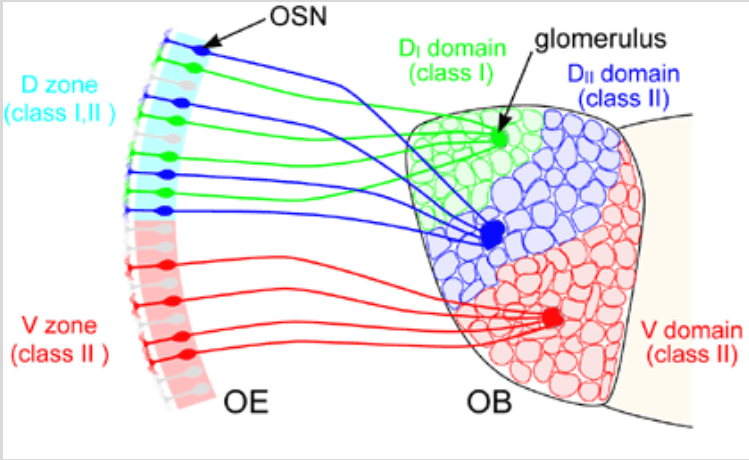

NATURE 450, 503-508 (2007)

Konvergence čichové informace

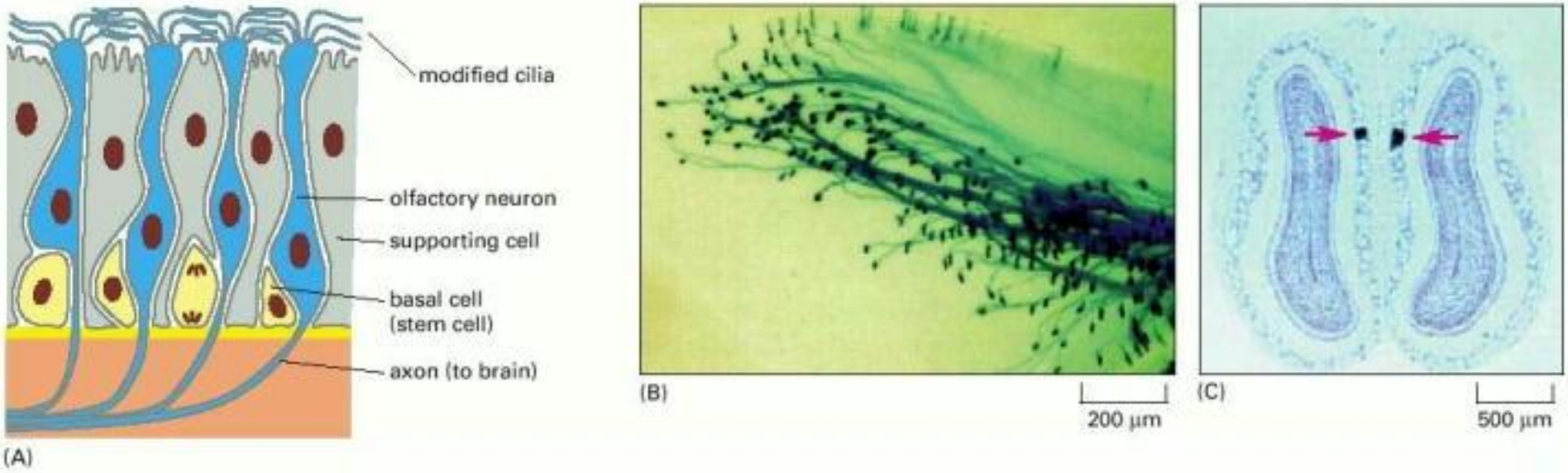

(A) Olfactory epithelium consists of supporting cells, basal cells, and olfactory sensory neurons. The basal cells are the stem cells for production of the olfactory neurons. Six to eight modified cilia project from the apex of the olfactory neuron and contain the odorant receptors. (B) This micrograph shows olfactory neurons in the nose of a genetically modified mouse in which the gene encoding LacZ has been inserted into an odorant receptor locus, so that all the cells that would normally express that particular receptor now make the enzyme LacZ in addition. The LacZ is detected through the blue product of the enzymatic reaction that it catalyzes. The cell bodies *(dark blue)* of the marked olfactory neurons, lying scattered in the olfactory epithelium, send their axons *(light blue)* toward the brain (out of the picture to the *right).* (C) A cross section of the *left* and *right* olfactory bulbs, stained for LacZ. Axons of all the olfactory neurons expressing the same odorant receptor converge on the same glomeruli *(red arrows)* symmetrically placed within the bulbs on the *right* and *left* sides of the brain. Other glomeruli (unstained) receive their inputs from olfactory neurons expressing other odorant receptors. (B and C, from P. Mombaerts et al., *Cell* 87:675–686, 1996. © Elsevier.)

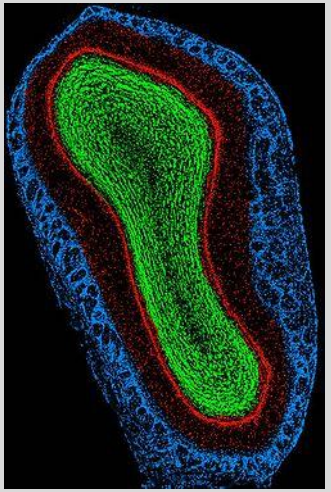

Recepce odorantů a feromonů oddělena na periferii i na úrovni CNS

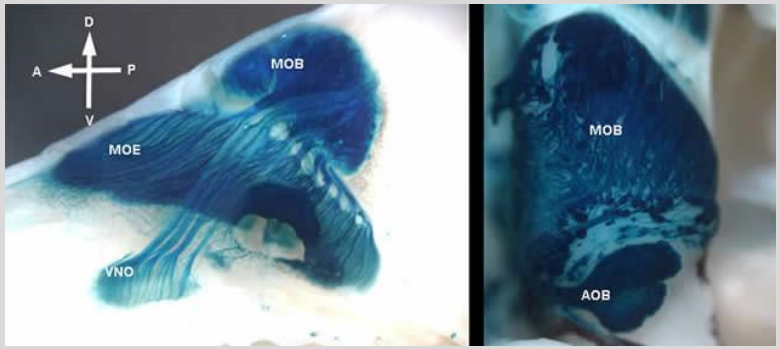

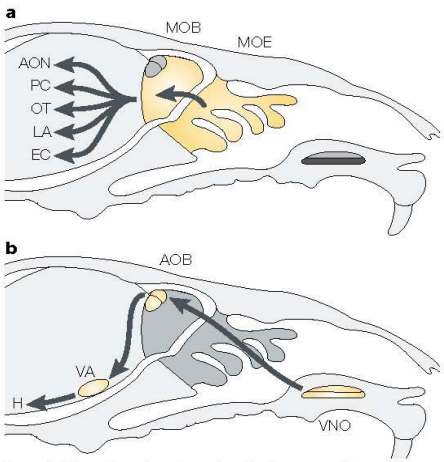

Figure 1 | **Functional and anatomical segregation of the two mammalian olfactory systems. a** | Olfactory sensory neurons in the main olfactory epithelium (MOE) are specialized for detecting small volatile odorants. The olfactory information is transmitted from the MOE to the main olfactory bulb (MOB), then to distinct brain nuclei that form the primary olfactory cortex and that include the anterior olfactory nucleus (AON), the piriform cortex (PC), the olfactory tubercle (OT), the entorhinal cortex (EC) and the lateral part of the cortical amygdala (LA). **b** | Information provided by pheromone signals is primarily processed by a distinct neural circuit. Pheromones are mostly detected by sensory neurons in the vomeronasal organ (VNO), a bilateral tubular structure in the anterior region of the nasal cavity. VNO axons project to the accessory olfactory bulb (AOB), which in turn transmits sensory information to the vomeronasal amygdala (VA) and then to specific nuclei of the hypothalamus (H), which are involved in regulating genetically pre-programmed physiological and reproductive responses.

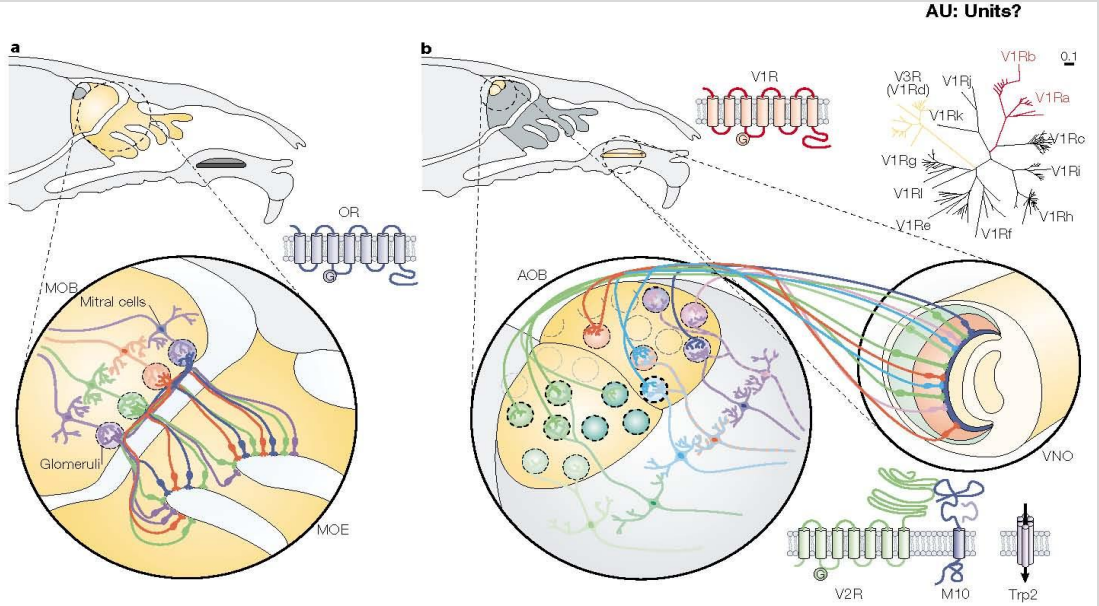

Figure 3 | **Cellular logic of sensory processing in the main and accessory olfactory systems. a** | In the main olfactory system, olfactory receptor neurons expressing a given olfactory receptor (OR) project to two bilaterally symmetrical, spatially conserved glomeruli in the main olfactory bulb (MOB), creating a topopographic map of olfactory receptor activation in the MOB. MOE, main olfactory epithelium. **b** | In the vomeronasal organ (VNO) two categories of sensory neurons can be distinguished anatomically and molecularly. VNO neurons in the apical half of the neuroepithelium (pink, red and turquoise) co-express the G-protein subunit $G\alpha_o$ and a single receptor from the V1R class of pheromone receptors. The V1Rs are subdivided into 12 families, including the two families of receptors V1Rab and V3R (red and yellow in the upper right evolutionary tree). Vomeronasal receptor neurons in the basal vomeronasal epithelium (green) co-express the G-protein subunit $G_{\alpha i2}$ and a single receptor from the structurally distinct V2R family of vomeronasal receptors. V2Rs interact with a non-classical major histocompatibility complex (MHC) class 1b molecule (M10) and the accessory molecule β2-microglobulin (β2m) to form a functional receptor complex. The activity of V1R- and V2R-expressing neurons requires expression of Trp2, a channel that is localized in the dendritic tips of the neurons (purple), and is a crucial component of the vomeronasal signalling cascade. Neurons expressing V1R and V2R receptors project to the anterior and posterior AOB, respectively, where they form multiple glomeruli in spatially conserved domains.

NATURE REVIEWS NEUROSCIENCE 4, 551-562, 2003

Gruenebergovo ganglion

✓ **detekce poplašných feromonů**

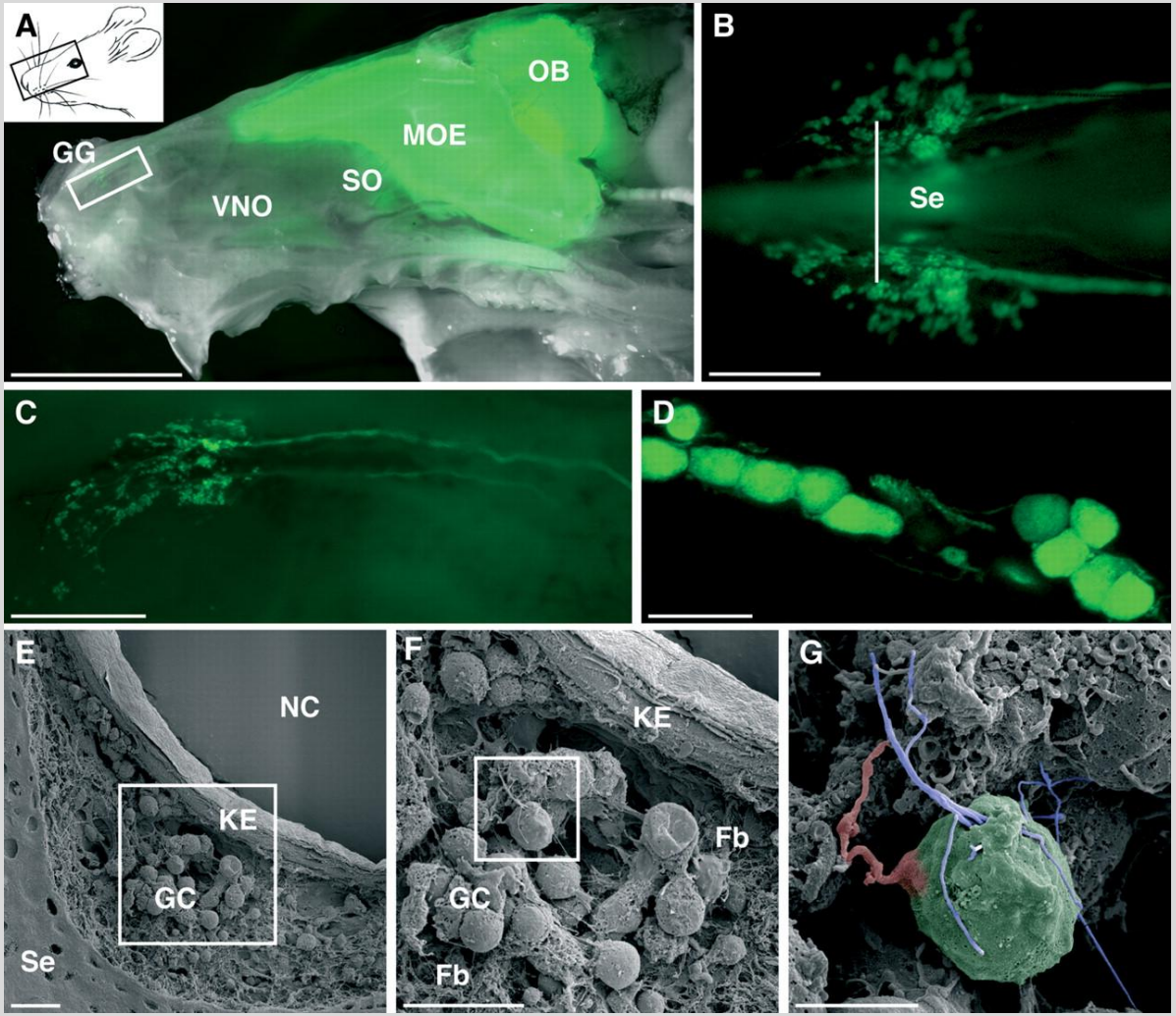

cca 1 mm
300-500 buněk

Fig. 1. Ciliary processes are present on the mouse GG cells.

J Brechbühl et al. Science 2008;321:1092-1095

Science
AAAS

Chuťové pohárky - jazyk

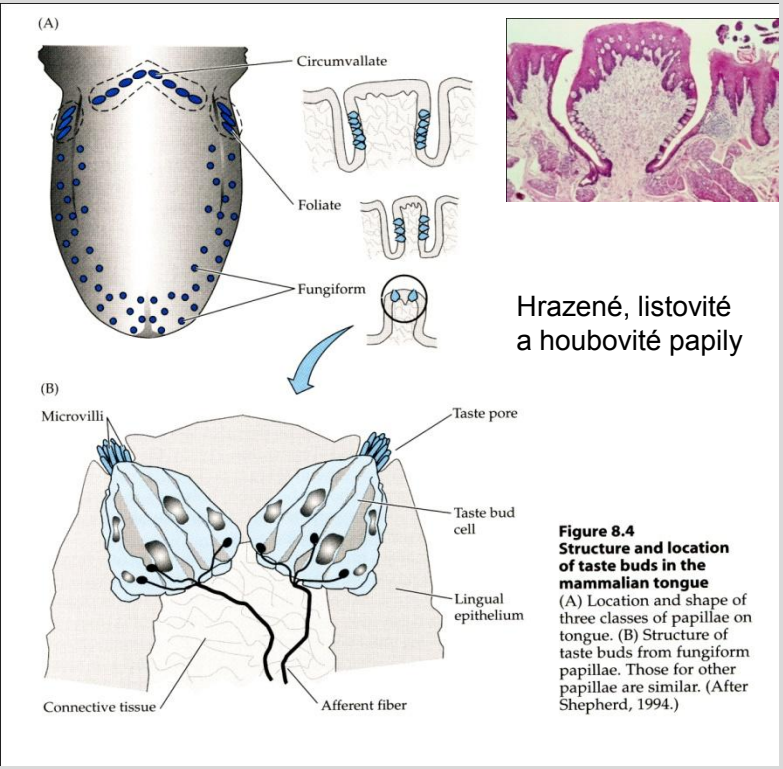

Hrazené, listovité a houbovité papily

Figure 8.4 Structure and location of taste buds in the mammalian tongue
(A) Location and shape of three classes of papillae on tongue. (B) Structure of taste buds from fungiform papillae. Those for other papillae are similar. (After Shepherd, 1994.)

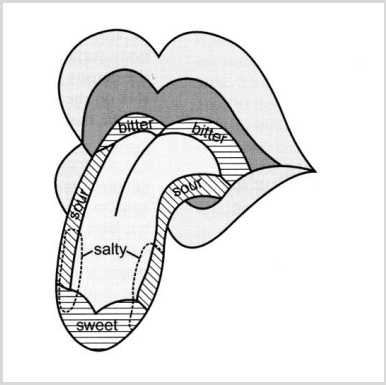

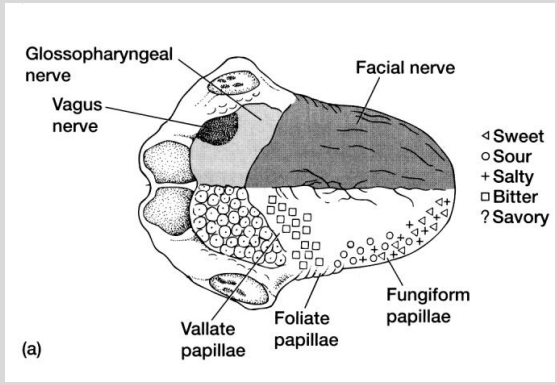

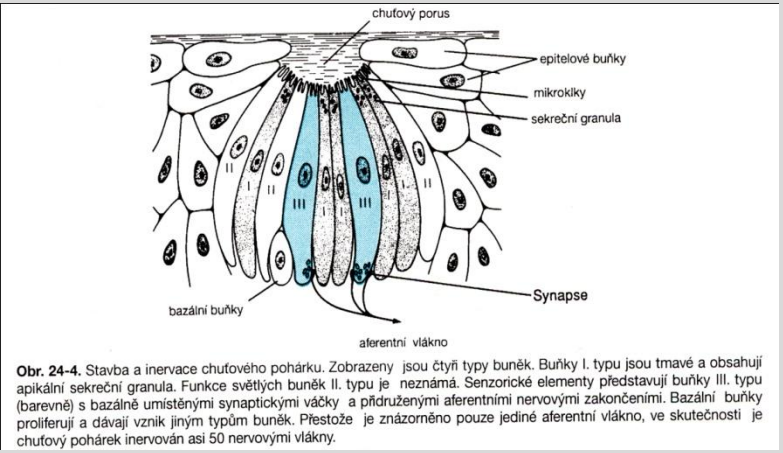

Obr. 24-4. Stavba a inervace chuťového pohárku. Zobrazeny jsou čtyři typy buněk. Buňky I. typu jsou tmavé a obsahují apikální sekreční granula. Funkce světlých buněk II. typu je neznámá. Senzorické elementy představují buňky III. typu (barevně) s bazálně umístěnými synaptickými váčky a přidruženými aferentními nervovými zakončeními. Bazální buňky proliferují a dávají vznik jiným typům buněk. Přestože je znázorněno pouze jediné aferentní vlákno, ve skutečnosti je chuťový pohárek inervován asi 50 nervovými vlákny.

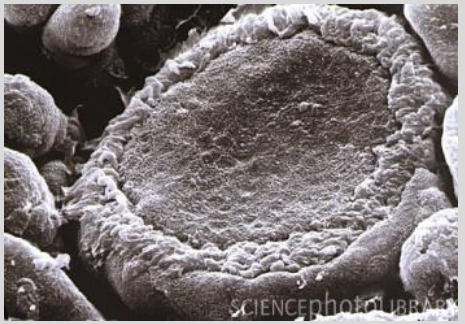

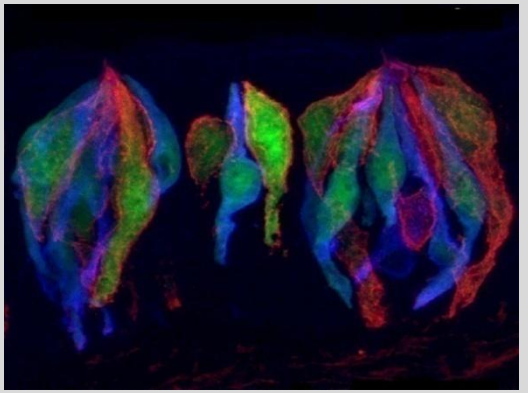

Chuťové papily

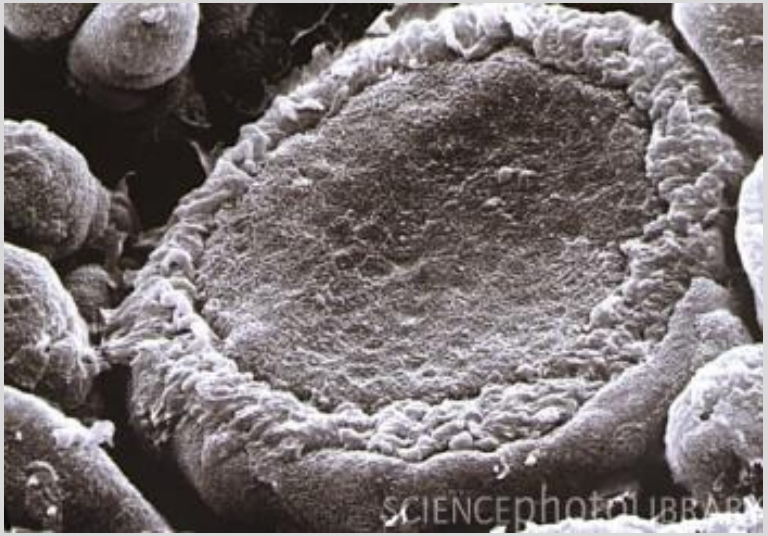

Chuťové pohárky ryb – často po celém těle

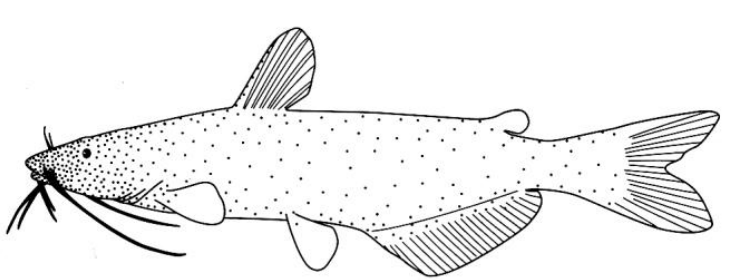

B. Taste buds on catfish skin

Distribuce chuťových pohárků na těle sumečka

The catfish is built for taste. On their head they have 7 taste buds per square millimeter. On their barbells (whiskers) they have 25 taste buds per square millimeter, On their lips they have 10 taste buds per square millimeter. On their mouth the catfish has 5 to 25 taste buds per square millimeter. On their gills they have 7 taste buds per square millimeter with some areas as high as 50 taste buds per square millimeter. Over all the catfish has 20,000 internal taste buds, and externally they have 175,000 taste buds. The bottom line this fish species is flat built for taste!

„vagový lalok“ kaprovitých ryb

15 vrstev, tvoří cca 20% objemu mozku

✓ 11 dorsálních vrstev je sensorických – vstup z chuťových pupeny – homologie s nc. solitarius

✓ vrstvy 14 + 15 motorické – inervují svaly ústní dutiny – homologie s nc. ambiguus